DISSERTATION

submitted to the
Combined Faculties for the Natural Sciences
and for Mathematics
of the Ruperto-Carola-University Heidelberg, Germany,
for the degree of
Doctor of Natural Sciences

presented by
Markus Andreas Moosmeier, M.Sc.
born in Landshut, Germany
Date of oral examination: 2009/07/23

DEVELOPMENT OF UNIVERSAL TRANSMEMBRANE TRANSPORTER SYSTEMS

Referees: Professor Dr. Stephan Urban
Professor Dr. Hanswalter Zentgraf

To my parents and Andrea,
for their endless love and encouragement.

“In the beginning, I looked around
and could not find quite the protein I dreamed of.
So I decided to build it myself.”
Freely adapted from Dr. Ing. h.c. Ferdinand Porsche

Table of Contents

Summary

The delivery of molecules into cells poses a major problem that has to be solved for the development of therapeutic agents acting on intracellular targets. Cargos which cannot penetrate cellular membranes by themselves due to their biophysical properties can achieve cell membrane permeability by fusion to protein transduction domains (PTDs). Since the design and generation of PTD-fused proteins can result in reduced expression and purification levels and/or in altered biophysical properties of cargos, two transporter systems for the transmembrane delivery of non-modified and modified cargos were developed.

The first model system aimed at the internalization of a protein binder which can bind to, and subsequently sequester, an intracellular target molecule. Streptavidin (SA) was employed as a model protein binder and was internalized into mammalian cells via its ligand *Strep*-tag II, fused to a PTD. Inside the cells, the non-covalently bound PTD-*Strep*-tag II was displaced by biotin which exhibits a higher affinity to the SA binding pocket than *Strep*-tag II. Successful displacement of PTD-*Strep*-tag II was monitored by measuring the thermal tetramer stability of SA which is increased upon biotin binding. These results indicate that it is principally possible to intracellularly sequester target molecules with higher affinities for a protein binder than the PTD-ligand utilized for its internalization. Under therapeutic aspects, it could be envisioned to use such systems for the intracellular sequestration, and consequently, functional inactivation of pathologically relevant factors.

A second transmembrane delivery system was developed for introducing cargos which themselves exert intrinsic biochemical activities, rather than acting as “passive” protein binders. Since covalent PTD fusion can influence cargo function, care was taken to introduce the cargos by non-covalent linkage to a transporter. PTD-fused SA and *Strep*-Tactin (ST) derivatives, termed Transvidins and Transtactins, were engineered as model transporters for biotin- and/or *Strep*-tag II-linked compounds. The expression of both transporters as insoluble inclusion bodies in bacteria prevented the common problems of both reduced expression levels and purification yields which have been observed for other PTD-fused proteins. Biochemical characterization of Transvidin and Transtactin variants bearing different PTDs revealed high thermal stabilities and robust secondary structures, indicating that SA and ST were extremely rigid protein scaffolds. Internalization studies demonstrated that both transporters facilitated simple, safe, and efficient transport of biotinylated and *Strep*-tag II-linked organics, peptides, proteins, and multicomponent complexes into cultured human cells. Transvidin- and Transtactin-introduced cargos were functionally active, as shown for the model protein horseradish peroxidase. These results demonstrate that Transvidin and Transtactin transporters provide universal and efficient delivery systems for biotinylated and *Strep*-tag II-fused cargos.

Zusammenfassung

Der Transport von Molekülen durch die Zellmembran stellt für die Entwicklung von intrazellulär aktiven Therapeutika eine große technische Herausforderung dar. Moleküle, z. B. Proteine, die aufgrund ihrer biophysikalischen Eigenschaften *per se* nicht in der Lage sind die Zellmembran zu durchdringen, können diese Fähigkeit durch ihre Kopplung an Proteintransduktionsdomänen (PTDs) erlangen. Die Fusion von PTDs kann jedoch zu reduzierten Ausbeuten während der Produktion und Reinigung, sowie zu veränderten biophysikalischen Eigenschaften von Proteinen führen. Daher wurden zwei neue Transportersysteme entwickelt, um nicht-modifizierte sowie modifizierte Moleküle durch die Zellmembran zu schleusen.

Das erste Modellsystem wurde generiert, um Bindungsproteine einzuschleusen, die intrazelluläre Zielmoleküle spezifisch sequestrieren können. Als Modell für ein solches Bindungsprotein diente Streptavidin (SA), das mit Hilfe einer an den SA-Bindungsliganden *Strep*-tag II gekoppelten PTD in Säugerzellen eingeschleust wurde. Im Zytoplasma wurde der PTD-*Strep*-tag II-Ligand durch Biotin ersetzt, das im Vergleich zu *Strep*-tag II eine höhere Affinität für die SA-Bindetasche besitzt. Der erfolgreiche Austausch von PTD-*Strep*-tag II durch Biotin wurde durch Bestimmung der thermischen Tetramerstabilität von SA nachgewiesen, die nach Bindung von Biotin ansteigt. Diese Ergebnisse zeigen, dass es prinzipiell möglich ist, intrazelluläre Moleküle spezifisch zu sequestrieren, die eine höhere Affinität zum Bindungsprotein aufweisen als der für die Internalisierung benutzte Ligand. Unter therapeutischen Gesichtspunkten ist es vorstellbar, entsprechende Systeme für die intrazelluläre Sequestrierung und funktionelle Inaktivierung pathologisch relevanter Faktoren einzusetzen.

Ein zweites Transportsystem wurde entwickelt, um Moleküle in Zellen einzuschleusen, die im Gegensatz zu den eher „passiv“ wirksamen Bindungsproteinen eigene biochemische Aktivitäten aufweisen. Da eine kovalente Fusion von PTDs die funktionellen Eigenschaften von Molekülen beeinflussen kann, wurde ein besonderes Augenmerk darauf gelegt, Moleküle durch nicht-kovalente Kopplung an einen Transporter einzuschleusen. Hierfür wurden PTD-fusionierte SA- und *Strep*-Tactin- (ST-) Derivate, sog. „Transvidine“ und „Transtactine“, als Transporter für Biotin- und/oder *Strep*-tag II-gekoppelte Moleküle entwickelt. Durch Produktion der Transvidine und Transtactine als unlösliche bakterielle Einschlusskörper konnte das Problem der geringen Ausbeute während der Produktion und Reinigung umgangen werden, das für andere PTD-gekoppelte Proteine beobachtet wurde. Die biophysikalische Charakterisierung der Transvidin- und Transtactin-Transporter ergab hohe thermische Stabilitäten und stabile Sekundärstrukturen. Dies zeigte, dass sowohl SA als auch ST überaus rigide Proteingerüste darstellen. Zellkulturstudien zeigten, dass beide Transportersysteme Biotin- und/oder *Strep*-tag II-gekoppelte niedermolekulare Moleküle, Peptide, Proteine sowie multifaktorielle Komplexe einfach, sicher und effizient in humane Zellen internalisierten. Anhand des Modellproteins Meerrettichperoxidase wurde außerdem demonstriert, dass Proteine durch Transvidine und Transtactine in funktionell aktiver Form eingeschleust werden können. Diese Ergebnisse zeigen, dass Transvidine und Transtactine als universelle und effiziente Transportersysteme für die Internalisierung von Biotin- und *Strep*-tag II-gekoppelten Molekülen in Säugerzellen dienen können.

Acknowledgment

The following dissertation was accomplished in the work group “Molecular Therapy of Virus-Associated Cancers” at the German Cancer Research Center in Heidelberg, Germany, with scientific guidance by Professor Dr. Felix Hoppe-Seyler. This thesis marks the end of a triannual journey on which I got accompanied by many people whom I would like to thank for their scientific and personal support.

I would like to express my gratitude to Professor Dr. Felix Hoppe-Seyler for giving me the opportunity to implement my ideas of universal transmembrane transporter systems in the innovative and ambitious atmosphere of his laboratory. His encouragement and ongoing support have been very valuable for completing this work.

My special thanks go to Professor Dr. Karin Hoppe-Seyler for support and guidance. Her knowledge and skills in molecular and cell biology have allowed me to carry out this work under excellent supervision.

Also I would like to thank my thesis referees, Professor Dr. Stephan Urban (Department of Molecular Virology, University of Heidelberg) and Professor Dr. Hanswalter Zentgraf (Electron Microscopy, German Cancer Research Center), for their insight and critical evaluation. PD Dr. Karsten Rippe (Genome Organization and Function, German Cancer Research Center) kindly agreed to join the committee for thesis disputation.

All of my colleagues, past and present, are warmly thanked for unreserved assistance and for creating an enjoyable, pleasant atmosphere to work. I express my gratitude to Claudia Lohrey, Angela Heilig, and especially to Julia Bulkescher for organizing materials and reagents as well as for excellent support in the lab. Special thanks go to my colleagues Dr. Markus Vogt, Dr. Irena Crnkovic-Mertens, Dr. Nina Wagener, Dr. Stefanie Schmidt, Dr. Susanne Dymalla, Bettina Schuller, and especially to Dr. Christina Mensger, Dr. Daniela Holland and Dr. Claire Cullmann. I would also like to thank Thomas Holz for constant support not only as a computer expert but also as a very good friend.

This research did benefit tremendously from vital collaborative support. I would like to thank Professor Dr. Jennifer Reed (Structural Biochemistry, German Cancer Resarch Center) for performing circular dichroism spectroscopy, Dr. Martina Schnölzer (Functional Proteome Analysis, German Cancer Research Center) for mass spectrometry, Dr. Hans Heid (Helmholtz Group for Cell Biology, German Cancer Research Center) for Edman sequencing, Andreas Hunzicker (Oligonucleotide Synthesis and Sequencing Core Facility, German Cancer Research Center) for DNA sequencing, Dr. Rüdiger Pipkorn (Peptide Synthesis Core Facility, German Cancer Research Center) for peptide syntheses, and Professor Dr. Patrick S. Stayton (University of Washington, WA, USA) for the core streptavidin expression vector.

I thank all my friends in Heidelberg and Bavaria, especially Thomas Reithmeier, Rainer and Sandra Salzberger, Oliver Kühbeck, Dietmar Reithmeier, Silvia and Sonja Fiedler, Katrin Marold, Alexandra Ring, Tanja Müller, Karin Scheuermann, Roman Jowanowitsch, Dr. Katja Reuter, Dr. Nina Mossadegh, Dr. Florian Sonntag, Dr. Lars Krüger, Dr. Carlo Stresemann, Birte Seiffert, Christina Raupp, Mario Fix, Carolin Böhm, Verena Müller, Sophie Knobloch, Anne Faßl, Melanie Kretz, Nadine Michel, Karl Varadi, and Tobias Bauer. They play an important role in my life enabling me to find an invaluable balance between work and recreation.

I feel deeply privileged to have grown up in a warm and loving family giving me all the support I needed. I mainly owe a debt of gratitude to my wonderful parents, my sister and brother, my grandparents, and all the other relatives and friends of the family around me. I am deeply grateful to my parents, Gertraud and Hermann, for their enormous love and support. You have always believed in me and my skills. You have always done everything perfectly right.

Finally, I give my warmest thanks to my girlfriend Andrea for lasting love and endless support. You have shown me to recognize and esteem the small lovely things in life and so much more.

Danksagung

Die vorliegende Dissertation wurde in der Arbeitsgruppe „Molekulare Therapie Virus-assoziierter Tumore“ am Deutschen Krebsforschungszentrum in Heidelberg unter der wissenschaftlichen Anleitung von Herrn Professor Dr. Felix Hoppe-Seyler verfasst. Diese Arbeit stellt das Ende einer dreijährigen Reise dar, auf der ich von vielen Menschen begleitet wurde, denen ich nun an dieser Stelle für ihre wissenschaftliche sowie persönliche Unterstützung danken möchte.

Ich möchte mich sehr herzlich bei Herrn Professor Dr. Felix Hoppe-Seyler dafür bedanken, dass er mir die Möglichkeit gegeben hat, meine Idee von universellen zellpermeablen Transportsystemen in einem innovativen und ehrgeizigen Arbeitsumfeld umzusetzen. Seine Unterstützung hat maßgeblich zum Abschluss dieser Arbeit beigetragen.

Besonders möchte ich mich auch bei Frau Professor Dr. Karin Hoppe-Seyler für ihre Unterstützung bedanken. Ihr Fachwissen in der Molekular- und Zellbiologie ermöglichte es mir, diese Arbeit unter ausgezeichneter Betreuung zu erstellen.

Ebenso möchte ich meinen Gutachtern, Herrn Professor Dr. Stephan Urban (Abteilung Molekulare Virologie an der Universität Heidelberg) und Herrn Professor Dr. Hanswalter Zentgraf (Abteilung Elektronenmikroskopie am Deutschen Krebsforschungszentrum) für die Einsicht, die sie mir in ihr Fachgebiet gewährten sowie für ihre konstruktiven Bewertungen danken. Herr PD Dr. Karsten Rippe (Abteilung Genomorganisation und Funktion am Deutschen Krebsforschungszentrum) hat sich freundlicherweise dazu bereit erklärt, dem Komitee zur Disputation beizuwohnen.

Des Weiteren geht ein herzlicher Dank an all meine früheren und jetzigen Kolleginnen und Kollegen für ihre uneingeschränkte Mitwirkung und für die angenehme Arbeitsatmosphäre. Ich bedanke mich herzlich bei Claudia Lohrey, Angela Heilig und insbesondere bei Julia Bulkescher für die Organisation der Materialien und Reagenzien sowie für die ausgezeichnete Unterstützung im Labor. Bedanken möchte ich mich auch bei meinen Kolleginnen und Kollegen Dr. Markus Vogt, Dr. Irena Crnkovic-Mertens, Dr. Nina Wagener, Dr. Stefanie Schmidt, Dr. Susanne Dymalla, Bettina Schuller und besonders bei Dr. Christina Mensger, Dr. Daniela Holland und Dr. Claire Cullmann. An dieser Stelle möchte ich Herrn Thomas Holz nicht nur für seine beständige Unterstützung als Computerfachmann danken, sondern auch für seine Freundschaft.

Die vorliegende Arbeit wäre ohne die unerlässliche Unterstützung der folgenden Kolleginnen und Kollegen nicht möglich gewesen. Daher möchte ich mich bei Frau Professor Dr. Jennifer Reed (Abteilung Strukturbiologie am Deutschen Krebsforschungszentrum) für die Durchführung der Zirkulardichroismus-Spektroskopie, bei Frau Dr. Martina Schnölzer (Abteilung Funktionale Proteomanalyse am Deutschen Krebsforschungszentrum) für die Massenspektrometrie, bei Herrn Dr. Hans Heid (Helmholtzgruppe für Zellbiologie am Deutschen Krebsforschungszentrum) für die Edman-

Sequenzierung, bei Herrn Andreas Hunzicker (Oligonukleotidsynthese- und DNS-Sequenzierungseinheit am Deutschen Krebsforschungszentrum) für die DNS-Sequenzierung, bei Herrn Dr. Rüdiger Pipkorn (Peptidsyntheseeinheit am Deutschen Krebsforschungszentrum) für die Peptidsynthese und bei Herrn Professor Dr. Patrick S. Stayton (Universität Washington, WA, USA) für die Bereitstellung des Kern-Streptavidin-Expressionsvektors bedanken.

Ich danke all meinen Freunden in Heidelberg und zu Hause in Bayern, besonders Thomas Reithmeier, Rainer und Sandra Salzberger, Oliver Kühbeck, Dietmar Reithmeier, Silvia und Sonja Fiedler, Katrin Marold, Alexandra Ring, Tanja Müller, Karin Scheuermann, Roman Jowanowitsch, Dr. Katja Reuter, Dr. Nina Mossadegh, Dr. Florian Sonntag, Dr. Lars Krüger, Dr. Carlo Stresemann, Birte Seiffert, Christina Raupp, Mario Fix, Carolin Böhm, Verena Müller, Sophie Knobloch, Anne Faßl, Melanie Kretz, Nadine Michel, Karl Varadi und Tobias Bauer. Sie spielen eine wichtige Rolle in meinem Leben, was meine Balance zwischen Arbeit und Freizeit angeht.

Ich hatte das große Glück, inmitten einer herzlichen und liebevollen Familie aufzuwachsen, die mir sämtliche Unterstützung angedeihen ließ, die ich brauchte. Den meisten Dank schulde ich dabei meinen wundervollen Eltern, meiner Schwester und meinem Bruder, meinen Großeltern, allen Verwandten und Freunden der Familie. Ich bin meinen Eltern, Gertraud und Hermann, zutiefst dankbar für Ihre unendliche Liebe und Unterstützung. Ihr habt stets an mich und an meine Fähigkeiten geglaubt. Ihr habt immer alles richtig gemacht.

Letztendlich möchte ich meiner Freundin Andrea für Ihre grenzenlose Liebe und Unterstützung danken. Du hast mir gezeigt, die kleinen und schönen Dinge im Leben zu erkennen und schätzen zu lernen und noch so viel mehr.

Publications and patents

The findings of the present studies resulted in the following publications and patents:

PUBLICATIONS

MOOSMEIER MA, BULKESCHER J, REED J, SCHNÖLZER M, HEID H, HOPPE-SEYLER K, HOPPE-SEYLER F (2009). "Transtactin: A universal transmembrane delivery system for *Strep*-tag II-fused cargos." J Cellular Mol Med, in revision (impact factor 2007: 6.8)

POSTER PRESENTATIONS

MOOSMEIER MA, HOPPE-SEYLER K, HOPPE-SEYLER F (2007). "Transvidin: A universal transduction system for the *in vivo* delivery of siRNA- and peptide-based therapeutics." 12th DKFZ PhD Retreat, July 19-24, Weil der Stadt, Germany. Certificate: best poster award

MOOSMEIER MA, HOPPE-SEYLER K, HOPPE-SEYLER F (2007). "Transvidin: Delivering biotinylated therapeutic agents across cellular membranes." DKFZ PhD Poster Presentation, December 14, Heidelberg, Germany

MOOSMEIER MA, HOPPE-SEYLER K, HOPPE-SEYLER F (2008). "Transtactin: Delivering impermeable cargos across cellular membranes." 2nd Joint Scientific Conference in Life Sciences, September 22-23, Heidelberg, Germany

MOOSMEIER MA, BULKESCHER J, HOPPE-SEYLER K, HOPPE-SEYLER F (2009). „Transvidin: Delivering biotinylated proteins across cellular membranes." 9th Charles Rodolphe Brupbacher Symposium, February 11-13, Zurich, Switzerland

BOOK CHAPTERS

HOPPE-SEYLER F, DYMALLA S, MOOSMEIER MA, HOPPE-SEYLER K (2009). "Induction of apoptosis in human papillomavirus-positive cancer cells by peptide aptamers targeting the viral E6 oncoprotein." In: "Peptide-based drug discovery." (ed. B. Groner). Wiley-VCH, Weinheim, Germany, ISBN-10: 3527322051

PATENT APPLICATIONS

MOOSMEIER MA, HOPPE-SEYLER K, HOPPE-SEYLER F (2008). "Construct and method for the internalization of cargo molecules into a cell." European Patent EP 08161192.3

Chapter 1
Introduction

Chapter 1: Introduction

1.1 TARGETED THERAPY

One of the major objectives of molecular medicine is to understand the molecular basis of diseases and to translate this knowledge into novel therapeutic strategies. In principle, this can be achieved by a two-step scenario: (i) the determination of genetic or biochemical alterations which are responsible for a given disease and (ii) the development of molecular tools that specifically correct these alterations ("targeted therapy").

TARGETS OF THERAPEUTIC AGENTS

Different strategies for specifically interfering with the activity of genes and their products are feasible (figure 1-1). For instance, nucleic acids can be targeted on the DNA level by oligonucleotide-directed mutagenesis (IGOUCHEVA *et al.*, 2004) and on the RNA level by antisense molecules (CROOKE, 2004), ribozymes (BAGHERI and KASHANI-SABET, 2004), or RNA interference (RNAi) (FUCHS *et al.*, 2004). Intracellular and extracellular proteins (e.g. transcription factors and cell-surface receptors) can be targeted by organics, peptides, and protein binders, like antibodies (GRONER *et al.*, 2004) and their fragments (HOLLIGER and HUDSON, 2005), or non-antibody-derived protein binders (BINZ *et al.*, 2005). Examples of non-antibody-derived protein binders are peptide aptamers, based on thioredoxin (LAVALLIE *et al.*, 1993; HOPPE-SEYLER *et al.*, 2004), or anticalins, based on the lipocalin-fold (SCHLEHUBER and SKERRA, 2005; SKERRA, 2007; SKERRA, 2008).

In the case of cancer, the underlying pathogenesis can often be traced back to mutations in the genome. Transcription and translation finally lead to proteins with impaired functions or to altered protein levels (POIRIER, 2004). Inactivating mutations of tumor suppressor genes, like *p53* (WHIBLEY *et al.*, 2009), and activating mutations of proto-oncogenes, like *Ras* (DOWNWARD, 2003), play a major role for tumor development. In many cases, unaltered tumor suppressor proteins have an inhibitory effect on cell growth or promote apoptosis, whereas unaltered proto-oncoproteins stimulate cell growth and inhibit apoptosis. Consequently, the inactivation of tumor-suppressor genes and/or aberrant activation of proto-oncogenes can finally result in uncontrolled cell growth, as a hallmark of tumor cells (HANAHAN and WEINBERG, 2000). Conceivably, the correction of these defects may be of therapeutic value and diverse strategies have been developed to counteract the intracellular dysfunctions of these gene products, as delineated for the following examples.

The *p53* tumor suppressor gene is the most frequently mutated gene in human cancers and loss of normal p53 protein function is associated with cell cycle deregulation and resistance to apoptosis. Most of the *p53* mutations are missense point mutations that accumulate in the DNA-binding core domain, thereby resulting in the disruption of DNA binding and loss of transcriptional transactivation of p53 target genes. Notably, mutant p53 core domain misfolding is reversible. For instance, a synthetic peptide

derived from the p53 C-terminal domain restored the specific DNA binding function of mutant p53 proteins, resulting in growth inhibition and apoptotic tumor cell death (SELIVANOVA and WIMAN, 2007). Moreover, the transcriptional transactivation function of mutant p53 was also restored by intracellularly expressed single chain (sc) Fv fragments derived from anti-p53 monoclonal antibodies (CARON DE FROMENTEL *et al.*, 1999).

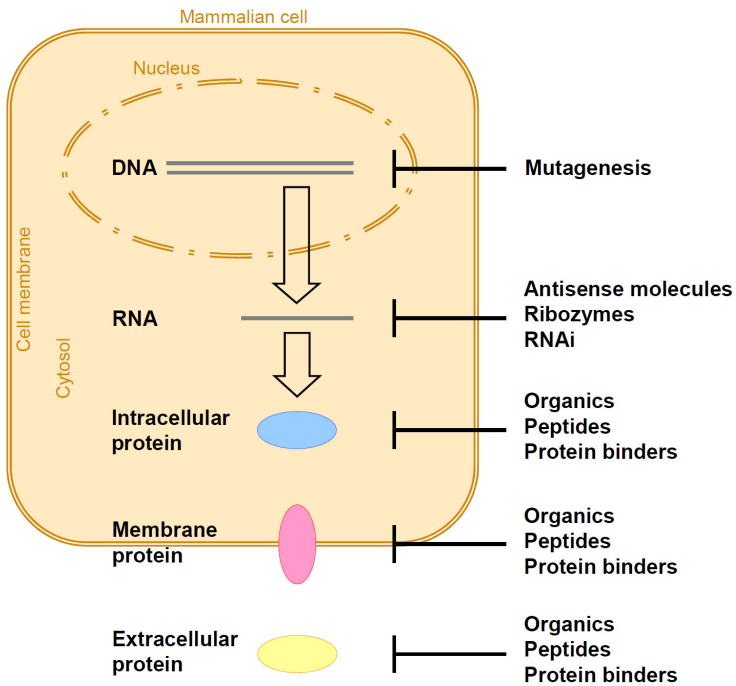

Figure 1-1. Different strategies for interfering with the activity of genes and proteins: Nucleic acids can be specifically targeted on the DNA level by site-directed mutagenesis and on the RNA level by antisense molecules, ribozymes, or RNA interference. Intracellular and extracellular proteins can be targeted by organics, peptides, and protein binders.

Activating mutations of the growth-promoting cellular *RAS* genes are found in approximately 20 % of all human cancers and can reach high frequencies for particular tumor types, being detectable, for example, in approximately 90 % of pancreatic and 50 % of colorectal cancers (DOWNWARD, 2003). Therapeutic agents that can interfere with aberrant RAS signalling are therefore considered to bear great potential for the development of novel cancer treatments (DOWNWARD, 2003). Several agents which target RAS at the protein level have been developed, including peptide aptamers that can specifically inhibit oncogenic RAS proteins as opposed to wildtype RAS (XU and LUO, 2002).

Oncogenes involved in human carcinogenesis can also be of viral origin. For example, specific types of human papillomaviruses (HPVs), including the high-risk types HPV-16 and HPV-18, cause cervical

cancer. The anti-apoptotic HPV E6 oncoprotein plays a crucial role for maintenance of the malignant phenotype of HPV-positive cancer cells (ZUR HAUSEN, 2002). Since E6, as a viral oncoprotein, is not expressed in healthy cells, E6 inhibitors should allow a selective attack on HPV-positive cells. As proof of concept, intracellularly expressed peptides (DYMALLA *et al.*, 2008) and protein binders (BUTZ *et al.*, 2000; GRIFFIN *et al.*, 2006; LAGRANGE *et al.*, 2007), which specifically bind to E6, induced apoptosis in HPV-positive cancer cells.

Thus, the reactivation of tumor suppressors and/or inactivation of cellular or viral oncoproteins by intracellularly expressed therapeutic peptides and protein binders should bear remarkable potential for targeted cancer therapy. This could be achieved by the intracellular expression of such inhibitors from therapeutic genes. Yet, the internalization of genetic material into eukaryotic cells either using viral vectors or by non-viral mechanisms, such as membrane permeabilization, microinjection, or electroporation, remains problematic: Firstly, viral vectors often suffer from significant problems such as immunogenicity, lack of specificity of transgene delivery, and/or insertional mutagenesis (THOMAS *et al.*, 2003). Secondly, membrane permeabilization can only be efficiently used in *ex vivo* cellular assays (NITIN *et al.*, 2004). Thirdly, microinjection and electroporation are invasive and may cause severe damage to cells (NITIN *et al.*, 2004). Therefore, many efforts are currently undertaken to develop methods which enable the transmembrane delivery of therapeutic peptides and proteins.

1.2 TRANSMEMBRANE DELIVERY OF THERAPEUTIC AGENTS

Most of the therapeutic agents prescribed today belong to the group of cell-permeable small molecules which are derived from organics and peptides. In general, small molecules enter the cell by free diffusion (figure 1-2) and interact with intracellular targets in defined ways, for instance by blocking the target's active site with sufficient affinity or by irreversible covalent binding. However, many small molecules suffer from lack of specificity, leading to unwanted side effects and toxicity. Macromolecular therapeutic agents based on nucleic acids, peptides, or proteins have several hypothetical advantages over organics (LEADER *et al.*, 2008). Firstly, they possess a highly specific and complex set of functions that cannot be mimicked by small molecules. Secondly, since nucleic acids, peptides, and proteins target molecules in a highly specific way, they often have less potential to induce unspecific side effects than small molecules which can bind to similarly shaped pockets of proteins other than the target. Thirdly, protein therapeutics can provide effective replacement treatment for diseases in which proteins are mutated, truncated, or not expressed.

On the other hand, most of the macromolecular therapeutic agents cannot penetrate cellular membranes of intact cells due to their biophysical properties, like size, charge, and polarity. This is especially true for nucleic-acid-based therapeutics or for peptides and protein binders (e.g. peptide aptamers). Nevertheless, due to their potential advantages in comparison to small molecules, there has been growing interest in the use of therapeutic macromolecular agents against intracellular targets. The

transmembrane delivery of such molecules into cells is still a major technical obstacle. In the following, two possible strategies to make therapeutic agents cell-permeable are described in-depth.

RECEPTOR-MEDIATED ENDOCYTOSIS

One way to achieve target cell-specific internalization is the fusion of therapeutic agents to ligands of cell-surface receptors. Following receptor-ligand interaction, the ligand-fused therapeutic agent is taken up into endosomal compartments by receptor-mediated endocytosis (figure 1-2) (WILEMAN *et al.*, 1985; ALLEN, 2002; QIAN *et al.*, 2002). After endosomal escape, the therapeutic agent can, for instance, inhibit a given oncoprotein by occupying its active site. However, this method requires the covalent coupling of a ligand to the cargo which often leads to altered properties with respect to ligand affinity as well as to the activity of the cargo. Moreover, this approach is highly restricted to specific cell types that express a certain cell-surface receptor and to the internalization properties of the targeted receptor. An alternative way to induce cell-membrane permeability of cargos is their linkage to peptide and protein transduction domains (PTDs).

PROTEIN TRANSDUCTION DOMAINS

PTDs, also known as cell penetrating peptides (CPPs) or membrane permeable peptides (MPPs), are short, in general 5 to 20 amino acids long peptides, comprising amino acid sequences which enable their own internalization into a variety of mammalian and human cell types (table 1-1, figure 1-2) (DIETZ and BAHR, 2004). PTDs can be classified into cationic and non-cationic peptides. Examples of well-studied cationic PTDs are the Tat13 peptide of the HIV-1 *trans*-activator protein (FRANKEL and PABO, 1988; GREEN and LOEWENSTEIN, 1988; FAWELL *et al.*, 1994; VIVES *et al.*, 1997; HONDA *et al.*, 2005), penetratin, also known as Ant16 (DEROSSI *et al.*, 1994; HONDA *et al.*, 2005), and Ant7 (FISCHER *et al.*, 2001; HONDA *et al.*, 2005), the two latter derived from the homeodomain of the *Drosophila melanogaster* Antennapedia protein, or polyarginines like R_9 (MITCHELL *et al.*, 2000; FUTAKI *et al.*, 2001; HONDA *et al.*, 2005). TLM12, derived from the pre-S domain of HBV, is an example of a non-cationic PTD forming an α-helix with an amphipathic structure (OESS and HILDT, 2000; STOECKL *et al.*, 2006).

PTD	Sequence
Tat13	YGRKKRRQRRRPP
Ant16	RQIKIWFQNRRMKWKK
Ant7	RRMKWKK
R_{13}	RRRRRRRRRRRRR
R_9	RRRRRRRRR
TLM12	PLSSIFSRIGDP

Table 1-1. Protein transduction domains: Amino acid sequences of cationic and non-cationic PTDs.

The precise uptake mechanism of PTDs is currently a topic of lively discussion. However, in the case of cationic PTDs, it is most likely that the positively charged side chains of the PTDs interact with the anionic structure at the cell surface leading to an increased local concentration of PTDs, subsequently

allowing cellular entry by a fluid-phase endocytotic mechanism (figure 1-2) (RICHARD *et al.*, 2003; BROOKS *et al.*, 2005; GUMP and DOWDY, 2007). It is remarkable that molecules that are bound to PTDs can be internalized concomitantly (GROS *et al.*, 2006). The uptake of non-cationic PTDs is also receptor-independent but, apart from that, their internalization mechanisms are still largely unclear.

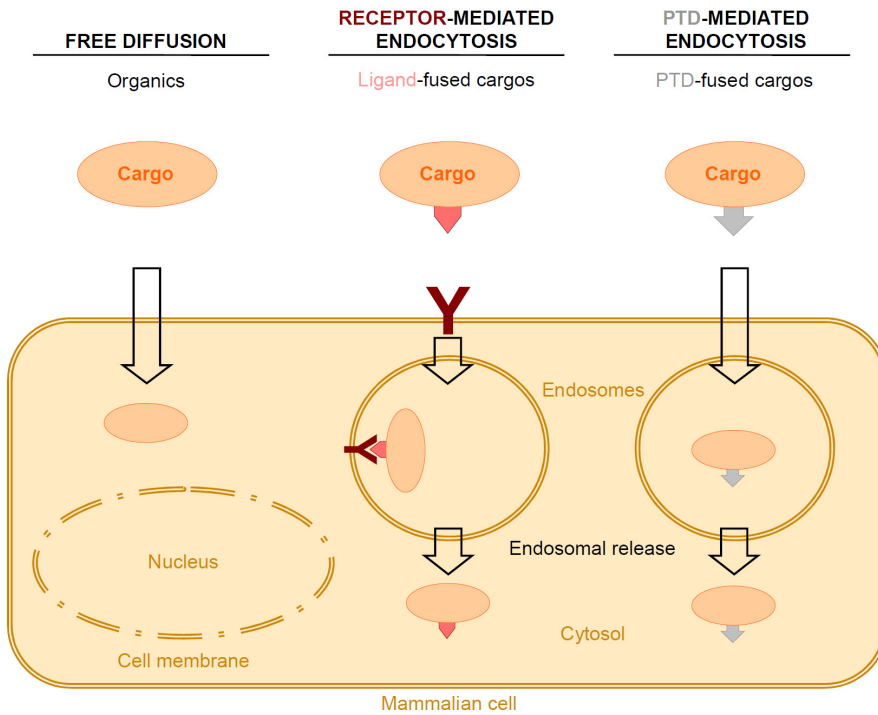

Figure 1-2. Ways through the cell membrane: Cell-permeable organics can enter the cell by free diffusion. Ligand-fused macromolecular therapeutic agents can be internalized by receptor-mediated endocytosis. PTDs can induce their own internalization via receptor-independent endocytosis, thereby mediating the internalization of bound non-cell-permeable cargos.

Since their discovery in 1988 (FRANKEL and PABO, 1988; GREEN and LOEWENSTEIN, 1988), a broad variety of bioactive molecules, ranging from nucleic acids, peptides, proteins, and even liposomes and particles, has been delivered by PTDs into cells both *in vitro* and *in vivo* (DIETZ and BAHR, 2004). This technology is thus considered to bear enormous potential to introduce macromolecular therapeutics into living cells (TREHIN and MERKLE, 2004; GUMP and DOWDY, 2007). Notably, there are reports indicating that PTDs can also penetrate intact epidermis and dermis which may enable the transdermal delivery of cargos upon topical application (ROTHBARD *et al.*, 2000; JIN *et al.*, 2001; PARK *et al.*, 2002).

One drawback of this technology is the genetic fusion of PTDs to cargos that can result in reduced protein expression and purification levels (HONDA *et al.*, 2005). Furthermore, the genetic or chemical linkage of PTDs can have an impaired effect on the biophysical properties of the cargo (HONDA *et al.*, 2005).

1.3 UNIVERSAL TRANSMEMBRANE DELIVERY SYSTEMS

In view of these obstacles, attempts have been made to generate transmembrane delivery systems that allow the concomitant internalization of non-covalently bound cargos. As further outlined below, these delivery systems often use the unrivalled high affinity of streptavidin (SA) to its natural ligand biotin as a basis for linking the therapeutic effect of a drug to the internalization property of a PTD.

THE SA/BIOTIN SYSTEM

SA is an extracellular homotetrameric protein secreted by the bacterium *Streptomyces avidinii* (TAUSIG and WOLF, 1964). Its name is derived from its bacterial source and from its structurally (LIVNAH *et al.*, 1993) and functionally (CHAIET and WOLF, 1964) analogous protein avidin (GREEN, 1975). SA was discovered in the early 1960s when the fermentation filtrates of *Streptomycetes* were searched for antibiotic activity (CHAIET *et al.*, 1963). This antibiotic activity is related to its ability to strongly bind the small growth factor biotin with an affinity constant (K_A) of $2.5 \cdot 10^{13}$ M^{-1} which is among the strongest non-covalent bonds known in nature. Cloning and sequencing of the SA gene of *Streptomyces avidinii* (ARGARANA *et al.*, 1986) showed that the gene coded for a 183 amino acid long protein. The first 24 amino acids comprise a signal sequence for secretion. After secretion, the matured SA monomer subunit is composed of 159 amino acids with a MW of 16.5 kDa, which is subsequently cleaved both at the N- and C-terminus by extracellular proteases (BAYER *et al.*, 1989). The resulting core SA monomer consists of 125 to 127 amino acids (MW = 13.2 kDa) and can be expressed as cytosolic inclusion bodies in *Escherichia coli* (*E. coli*) (SANO and CANTOR, 1990; THOMPSON and WEBER, 1993). Core SA is stable against further proteolytic degradation and retains its full biotin-binding activity. The crystal structure of core SA was resolved in the late 1980s (PAHLER *et al.*, 1987). Each subunit consists of eight antiparallel β-strands, which fold to an up-and-down β-barrel (figure 1-3). Subunit pairs of SA are hydrogen-bonded to each other forming a symmetric dimer with a pair of dimers interfacing each other and thus constituting the naturally occurring tetrameric structure. Each subunit possesses one exposed biotin-binding pocket. Therefore, the SA tetramer can bind up to four biotin molecules. Apart from its exceptional ligand-binding properties, SA bears unusual high stability against heat (GONZALEZ *et al.*, 1999), denaturants, extreme pH, and against the activity of proteolytic enzymes (LAITINEN *et al.*, 2006). Due to these unexampled characteristics, SA is widely utilized for different disciplines of biosciences and biomedicine.

BIOTIN

Biotin, also known as vitamin B_7, vitamin H, or coenzyme R (MW = 244 Da), was first discovered as a growth factor in 1901. It consists of two fused rings and an aliphatic valeric acid side chain with a carboxyl group in the end (figure 1-3). The natural function of biotin is to carry carboxyl groups and

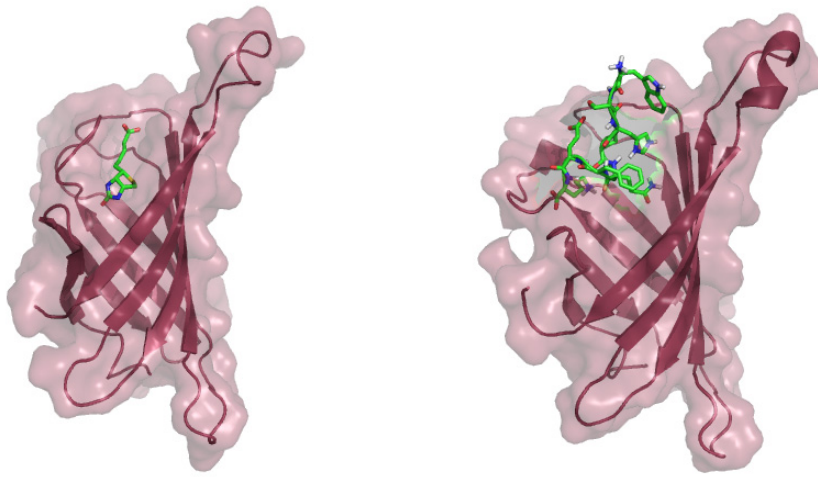

SA and biotin (green), PDB entry 1STP (WEBER *et al.*, 1989)

SA and *Strep*-tag II (green), PDB entry 1RSU (SCHMIDT *et al.*, 1996)

Figure 1-3. Crystal structures of monomeric SA with biotin and *Strep*-tag II.

to function as a cofactor for carboxylation reactions catalyzed by biotin-dependent carboxylases. Most prokaryotes and plants are able to synthesize biotin by themselves, whereas animals and humans need biotin in their diet. Various biotin derivatives were designed for biotechnological applications. They include 2-iminobiotin (HOFMANN *et al.*, 1980) and desthiobiotin (GREEN, 1975; VOSS and SKERRA, 1997), which show reversible binding and therefore are used for purification processes.

SA-BINDING PEPTIDES

In addition to biotin and its derivatives, various peptide motifs were designed which can occupy the biotin-binding pocket reversibly (table 1-2). The *Strep*-tag represents a nine amino acid peptide that

SA-binding peptides	Sequence
Strep-tag	AWRHPQFGG
Strep-tag II	WSHPQFEK
Nano-tag$_9$	DVEAWLGAR
Nano-tag$_{15}$	DVEAWLGARVPLVET
SBP	MDEKTTGWRGGHVVEGLAGELEQLRARLEHHPQGQREP

Table 1-2. SA-binding peptides: Amino acid sequences of SA-binding peptide motifs.

requires the peptide carboxylate group of C-terminal glycine to form a salt bridge with the guanidinium group of R^{84} of wildtype SA and therefore can only be fused to the C-terminus of recombinant proteins (SCHMIDT and SKERRA, 1993; SCHMIDT *et al.*, 1996). To overcome this limitation, a terminus-independent *Strep*-tag II peptide was generated (VOSS and SKERRA, 1997; SKERRA and SCHMIDT, 1999; KORNDORFER and SKERRA, 2002; SCHMIDT and SKERRA, 2007). The coding sequence of the *Strep*-tag II peptide can be easily fused to recombinant proteins during DNA subcloning. Moreover, *Strep*-tag II is biologically inert, proteolytically stable, and does usually not interfere with membrane translocation or protein function (SCHMIDT and SKERRA, 2007). Further examples of SA-binding peptides are Nano-tag_9 (LAMLA and ERDMANN, 2004), Nano-tag_{15} (LAMLA and ERDMANN, 2004), and the SBP-tag (KEEFE *et al.*, 2001), which all bind to SA with a nanomolar affinity. *Strep*-tag II bears a lower affinity to SA (K_D = 72 µM) than the previous *Strep*-tag (K_D = 37 µM). Therefore, *Strep*-Tactin (ST), as an SA-derivative with amino acid substitutions $E^{44}I$, $S^{45}G$, and $V^{47}R$ (numbering according to wildtype SA) was developed (VOSS and SKERRA, 1997). Recombinant proteins carrying an N- or C-terminal *Strep*-tag II (K_D = 1 µM) can be directly purified from the host cell extract by affinity chromatography on immobilized ST.

STREPTAVIDIN-BASED UNIVERSAL TRANSMEMBRANE DELIVERY SYSTEMS USING RECEPTOR-TARGETING

Various agents have been delivered into cells by receptor-mediated endocytosis using SA-based transporter systems. For instance, biotinylated cargos have been internalized into mammalian cells by using SA and biotinylated RNA aptamers which bind to specific surface receptors (CHU *et al.*, 2006) or by chimeric SA transporters with an N-terminally fused peptide targeting a receptor expressed on cancer cells (MASUDA *et al.*, 2006).

STREPTAVIDIN-BASED UNIVERSAL TRANSMEMBRANE DELIVERY SYSTEMS USING PROTEIN TRANSDUCTION DOMAINS

As an alternative to receptor-targeting, attempts have been made to generate universal cell permeable transporters based on SA that allow the concomitant internalization of cargos by non-covalent binding of biotin-fused cargos. For instance, Nitin *et al.* used SA to bridge the internalization properties of a biotinylated PTD to a biotinylated molecular beacon as an example for a nucleic-acid-based diagnostic agent (NITIN *et al.*, 2004). In a similar setting, biotinylated siRNA molecules were internalized by using SA and biotinylated PTDs (WANG *et al.*, 2007). Furthermore, model cargos (e.g. β-galactosidase) fused to SA as scaffolds were delivered into cells by PTD-biotin (MAI *et al.*, 2002). *Vice versa*, SA fused to the Tat11 PTD (YGRKKRRQRRR) was generated as a cell-permeable transporter (Tat11-SA) for biotinylated proteins (figure 1-4) (ALBARRAN *et al.*, 2005; RINNE *et al.*, 2007).

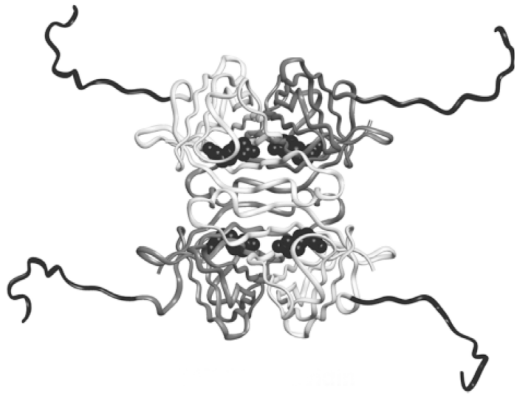

Figure 1-4. Model of Tat11-SA: Tat11 peptides are shown in black, SA monomers in light and dark gray. Biotin is shown in black spheres. Adopted from (ALBARRAN *et al.*, 2005).

However, biotinylation requires chemical linkage and may be inefficient for some cargos leading to the biotinylation of only a small portion of the cargo. Furthermore, it cannot be excluded that biotinylation of a cargo or its fusion to a scaffold, like SA, may impair its activity. To overcome possible difficulties due to chemical modifications of the cargo, Futaki *et al*. synthesized a cell-permeable nickel-nitrilotriacetic acid (R_8-Ni-NTA) for polyhistidine tagged recombinant proteins (FUTAKI *et al.*, 2004). Moreover, Mie *et al.* developed a system where the cargo is captured by an antibody and internalized due to the interaction with PTD-fused protein A that interacts with the Fc portion (MIE *et al.*, 2003; MIE *et al.*, 2006). However, this system consists of several components and requires an antibody that recognizes the target with high affinity and at the same time does not change the target's activity.

1.4 RESEARCH OBJECTIVES

INTERNALIZATION OF NON-MODIFIED PROTEIN SCAFFOLDS BY PTD-FUSED LIGANDS

The first goal of this thesis was the development of a novel and biologically safe two-component delivery system for the internalization of a non-modified protein binder. The system consists of (i) a non-cell permeable protein binder containing a binding pocket for an intracellular target molecule and (ii) a ligand which interacts with the same pocket more weakly and is fused to a PTD. Binding of the PTD-ligand to the protein binder should allow subsequent internalization of the complex. At the intracellular level, the ligand should then be displaced by the intracellular target which exhibits a higher binding affinity to the pocket. In principle, such a system could allow the intracellular sequestration and, consequently, functional inactivation of the target molecule. The system should be developed and tested by introducing SA via PTD-*Strep*-tag II. Subsequently, PTD-*Strep*-tag II should be replaced by biotin which binds to the same SA pocket with higher affinity.

DEVELOPMENT OF CELL-PERMEABLE TRANSMEMBRANE TRANSPORTERS FOR BIOTIN- AND *STREP*-TAG II-FUSED CARGOS

The design and generation of PTD-fused cargos (e.g. PTD-fused therapeutic agents) can result in reduced expression and purification levels and in altered biophysical properties of the cargos (HONDA *et al.*, 2005). Therefore, as a second goal, a universal transmembrane delivery system should be developed which circumvents covalent PTD fusion to the cargo. Mechanistically, the system takes advantage of the interaction of SA and ST proteins with biotin and SA-binding peptides, like *Strep*-tag II. Specifically, PTD-fused SA and ST molecules should be tested for their potential to internalize biotin- or *Strep*-tag II-fused molecules into human cells. The intracellular distribution of the transporter and the cargo should be analyzed and the functionality of an introduced model enzyme tested. In principle, this system could allow the cellular internalization of any biotin- or *Strep*-tag II-linked compound.

Chapter 2
Results

Chapter 2: Results

For the implementation of the projects, a series of model cargos and transporters were produced, namely SA and ST, which served as cargos to be internalized by PTD-fused biotin and *Strep*-tag II. In addition, (i) SA, fused to various PTDs, termed Transvidins (from transduction and streptavidin), and (ii) ST, fused to various PTDs, termed Transtactins (from transduction and *Strep*-Tactin) had to be constructed, produced, and characterized. The ultimate aim for these latter molecules was to evolve them into universal transporters for biotinylated and/or *Strep*-tag II-fused cargos.

2.1 CONSTRUCTION, EXPRESSION, AND PURIFICATION OF STREPTAVIDIN AND ITS DERIVATIVES

CONSTRUCTION OF EXPRESSION VECTORS

For large-scale production of core SA, the pSA1 expression vector (figure 2-1) was utilized (kindly provided by P. S. Stayton) which expresses the core *SA* gene from the pET21a vector backbone (CHILKOTI *et al.*, 1995).

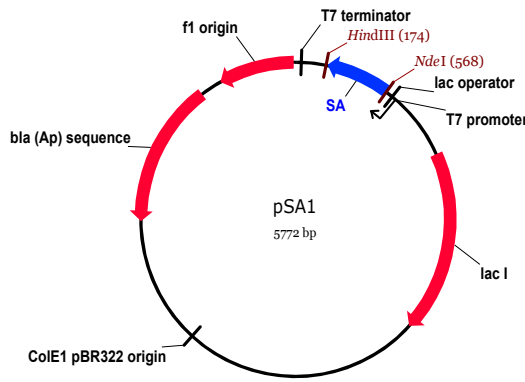

Figure 2-1. Scheme of the vector pSA1 for large-scale expression of core SA: The expression vector contains a *lac* I gene which codes for the lac repressor protein, a T7 promoter which is specific to T7 RNA polymerase, a lac operator which blocks transcription, f1 and ColE1 origins of replication, and the *bla* ampicillin resistance gene.

Vector pST1 for the large-scale expression of ST was generated from pSA1 by replacement of the triplets coding for E^{33}, S^{34}, and V^{36} (numbering according to core SA) using *in vitro* Quik-change side-directed mutagenesis. The desired mutations were verified by DNA sequencing using T7 promoter and T7 terminator oligonucleotide primers. Sequences of *SA* and *ST* genes were aligned in figure 2-2, the mutated nucleotides converting *SA* to *ST* were highlighted in red.

```
      1       10        20        30        40        50        60
      |       |         |         |         |         |         |
pST1  ATGGCTGAAGCTGGTATCACCGGCACCTGGTACAACCAGCTGGGATCCACCTTCATCGTT
pSA1  ATGGCTGAAGCTGGTATCACCGGCACCTGGTACAACCAGCTGGGATCCACCTTCATCGTT
      ************************************************************
     61       70        80        90       100       110       120
      |       |         |         |         |         |         |
pST1  ACCGCTGGTGCTGACGGTGCTCTGACCGGTACCTACATCGGTGCGAGGGGTAACGCTGAA
pSA1  ACCGCTGGTGCTGACGGTGCTCTGACCGGTACCTACGAATCCGCTGTTGGTAACGCTGAA
      ************************************      **    ************
    121      130       140       150       160       170       180
      |       |         |         |         |         |         |
pST1  TCTAGATACGTTCTGACCGGTCGTTACGACTCCGCTCCGGCTACCGACGGTTCCGGAACC
pSA1  TCTAGATACGTTCTGACCGGTCGTTACGACTCCGCTCCGGCTACCGACGGTTCCGGAACC
      ************************************************************
    181      190       200       210       220       230       240
      |       |         |         |         |         |         |
pST1  GCTCTGGGTTGGACCGTTGCTTGGAAAAACAACTACCGTAACGCTCACTCCGCTACCACC
pSA1  GCTCTGGGTTGGACCGTTGCTTGGAAAAACAACTACCGTAACGCTCACTCCGCTACCACC
      ************************************************************
    241      250       260       270       280       290       300
      |       |         |         |         |         |         |
pST1  TGGTCTGGCCAGTACGTTGGTGGTGCTGAAGCTCGTATCAACACCCAGTGGTTGTTGACC
pSA1  TGGTCTGGCCAGTACGTTGGTGGTGCTGAAGCTCGTATCAACACCCAGTGGTTGTTGACC
      ************************************************************
    301      310       320       330       340       350       360
      |       |         |         |         |         |         |
pST1  TCCGGCACCACCGAAGCTAACGCGTGGAAATCCACCCTGGTTGGTCACGACACCTTCACC
pSA1  TCCGGCACCACCGAAGCTAACGCGTGGAAATCCACCCTGGTTGGTCACGACACCTTCACC
      ************************************************************
    361      370       380       390
      |       |         |         |
pST1  AAAGTTAAACCGTCCGCTGCTTCCTAATAA
pSA1  AAAGTTAAACCGTCCGCTGCTTCCTAATAA
      ****************************
```

Figure 2-2. Sequence alignment of the 387 bp long *SA* and *ST* genes: Start and stop codons are highlighted in blue. The mutated nucleotides for the amino acid substitutions $E^{33}I$, $S^{34}G$, and $V^{36}R$ are shown in red.

Both *SA* and *ST* genes were translated *in silico* into their amino acid sequences and aligned to confirm the amino acid substitutions $E^{33}I$, $S^{34}G$, and $V^{36}R$ (figure 2-3).

```
      1       10        20        30        40        50        60   65
      |       |         |         |         |         |         |    |
ST    MAEAGITGTWYNQLGSTFIVTAGADGALTGTYIGARGNAESRYVLTGRYDSAPATDGSGTALGWT
SA    MAEAGITGTWYNQLGSTFIVTAGADGALTGTYESAVGNAESRYVLTGRYDSAPATDGSGTALGWT
      ********************************  * ******************************
     66  70        80        90       100       110       120     128
      |   |         |         |         |         |         |       |
ST    VAWKNNYRNAHSATTWSGQYVGGAEARINTQWLLTSGTTEANAWKSTLVGHDTFTKVKPSAAS
SA    VAWKNNYRNAHSATTWSGQYVGGAEARINTQWLLTSGTTEANAWKSTLVGHDTFTKVKPSAAS
      ************************************************************
```

Figure 2-3. Alignment of the SA and ST amino acid sequences: The amino acid substitutions $E^{33}I$, $S^{34}G$, and $V^{36}R$ to convert SA into ST are highlighted in red.

For generating different Transvidin and Transtactin variants, the coding sequences for the cationic PTDs Ant16, Ant7, Tat13, R_9, R_{13}, and for the non-cationic PTD TLM12 were fused in frame to the 5' end of the *SA* or *ST* genes and subcloned into pET-21a. A triplet encoding glycine was introduced between the coding sequences for the PTDs and the *SA* or *ST* genes to increase the flexibility of the

```
              1 3                                                   4 6
              | |                                                   | |
       SA/ST  ATG-----------------------------------------------------GCT
ANT16-SA/ST   ATGCGCCAGATTAAGATTTGGTTCCAGAACCGCCGCATGAAGTGGAAGAAGGGTGCT
 ANT7-SA/ST   ATGCGTC-------------------------GTATGAAGTGGAAGAAGGGTGCT
  R13-SA/ST   ATGAGACGCAGAAGAC---------GCAGAAGACGCAGAAGAAGAAGAAGGGTGCT
   R9-SA/ST   ATGAGACGCAGAAGAA---------GAAGAAGACGCAGA------------GGTGCT
TAT13-SA/ST   ATGTACGGAAGAAAGA---------AGCGCAGACAAAGAAGACGTCCACCAGGTGCT
TLM12-SA/ST   ATGCCCTTATCGTCAAT------------CTTCTCGAGGATTGGGGACCCTGGTGCT
              ***                                                   ***
```

Figure 2-4. DNA sequence alignment of the different PTDs: PTDs, highlighted in blue, were fused in frame to the 5' end of the *SA* and *ST* genes, shown in green. The triplet for glycine between the coding sequences of the PTDs and the *SA*/*ST* genes is shown in black. Numbering according to the *SA* gene.

```
                1                 2      10        20
                |                 |       |         |
       SA/ST    M                 AEAGITGTWYNQLGSTFIV
ANT16-SA/ST     MRQIKIWFQNRRMKWKKGAEAGITGTWYNQLGSTFIV
 ANT7-SA/ST     M---------RRMKWKKGAEAGITGTWYNQLGSTFIV
  R13-SA/ST     M---RRRRRRRRRRRRGAEAGITGTWYNQLGSTFIV
   R9-SA/ST     M--------RRRRRRRRGAEAGITGTWYNQLGSTFIV
TAT13-SA/ST     M---YGRKKRRQRRRPPGAEAGITGTWYNQLGSTFIV
TLM12-SA/ST     M    PLSSIFSRIGDPGAEAGITGTWYNQLGSTFIV
                *                 ******************
```

Figure 2-5. Alignment of the amino acid sequences of the Transvidin and Transtactin proteins after *in silico* translation: The various PTDs are highlighted in blue, SA and ST in green. The glycine residue which was introduced to increase the flexibility of the PTDs is shown in black. Numbering according to SA.

PTDs. All obtained expression vectors were verified by analytical restriction analysis (data not shown) and by DNA sequencing (figure 2-4). Figure 2-5 shows an alignment of the amino acid sequences of the PTD-fused SA and ST proteins after *in silico* translation.

EXPRESSION

E. coli-K12-strain BL21(DE3) was transformed for large-scale expression of SA, ST, Transvidin, and Transtactin proteins. Recombinant proteins were expressed overnight by IPTG-induction as cytosolic inclusion bodies. Coomassie-stained SDS-polyacrylamide gels of separated bacterial whole cell protein extracts sampled after 20 hours indicated that - apart from R_{13}-SA/ST - all individual recombinant proteins were expressed in full length, exhibiting a migration behavior similar as expected for their calculated MWs (table 2-1, figure 2-6). The lack of R_{13}-SA/ST expression may be related to the highly biased *E. coli* codon usage. In particular, the arginine AGA codon which was predominantly used for

primer design is extremely rare and the tRNA of this codon is poorly produced in *E. coli* (IKEMURA, 1981; KOMINE *et al.*, 1990). This may also explain the lower expression levels observed for recombinant R_9-SA/ST proteins.

Protein	MW [Da]	ε [$M^{-1}cm^{-1}$]
SA	13402.6	41940
Ant16-SA	15688.4	52940
Ant7-SA	14473.9	47440
R_{13}-SA	15490.1	41940
R_9-SA	14865.3	41940
Tat13-SA	15195.7	43430
TLM12-SA	14730.1	41940
ST	13413.7	41940
Ant16-ST	15699.4	52940
Ant7-ST	14485.0	47440
R_{13}-ST	15501.1	41940
R_9-ST	14876.4	41940
Tat13-ST	15206.8	43430
TLM12-ST	14741.2	41940

Table 2-1. Calculated MWs and extinction coefficients (εs) of SA and its derivatives: MWs and εs of all recombinant proteins were calculated according to their amino acid sequences.

In the case of Ant16- and R_{13}-fusion protein productions, the samples taken after an IPTG-induction of 20 hours indicated the overexpression of an additional protein with an MW of approximately 22 kDa (figure 2-6). No further attempts were started to identify this protein.

PURIFICATION

Inclusion bodies containing individual Transvidins and Transtactins were harvested and denatured proteins were refolded and purified by fractionated ammonium sulfate precipitation, as previously published for SA (SCHMIDT and SKERRA, 1994). Ant16-SA and Ant16-ST could not be refolded (figure 2-7), most likely due to the N-terminal part of the Ant16 PTD, since Ant7-SA and Ant7-ST inclusion bodies could be refolded without any problem. The yields of purified PTD-SA/ST proteins depended on the expression level as well as on the refolding process and ranged from 10 mg to 80 mg per 1 L expression volume. Purified SA showed a protein yield of approximately 30 mg/L.

2.2 BIOPHYSICAL CHARACTERIZATION OF STREPTAVIDIN AND ITS DERIVATIVES

After purification, all recombinant proteins were characterized by sodium dodecyl sulfate-polyacrylamide gel electrophoresis (SDS-PAGE), matrix-assisted-laser desorption/ionization time-of-flight mass

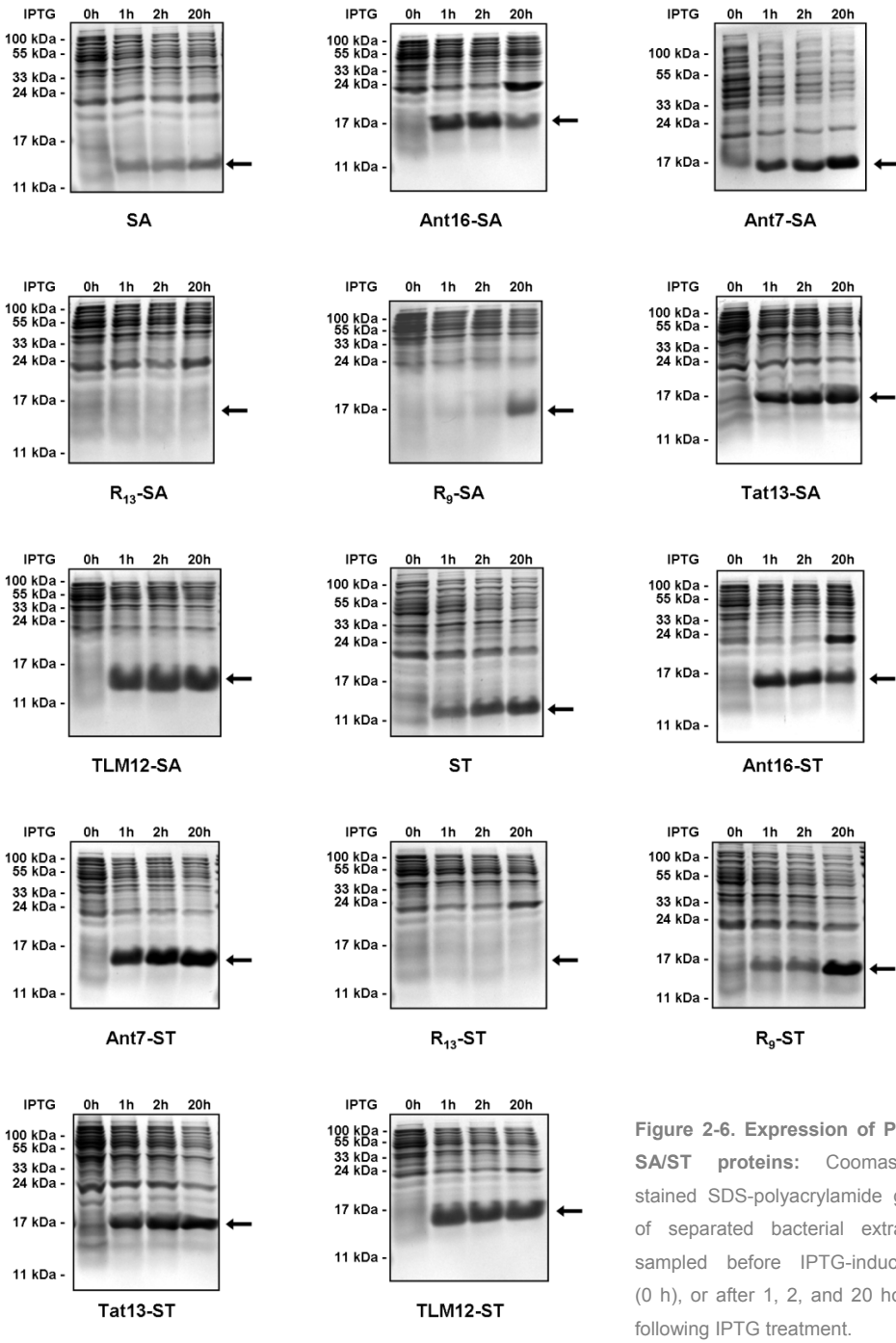

Figure 2-6. Expression of PTD-SA/ST proteins: Coomassie-stained SDS-polyacrylamide gels of separated bacterial extracts sampled before IPTG-induction (0 h), or after 1, 2, and 20 hours following IPTG treatment.

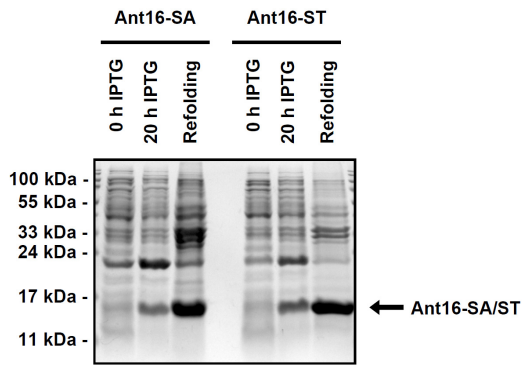

Figure 2-7. Coomassie-stained SDS-polyacrylamide gel analyzing Ant16-SA/ST refolding: The pelleted fractions after refolding attempts indicated that Ant16-SA and Ant16-ST proteins remained denatured.

spectrometry (MALDI-TOF MS), Edman sequencing, far-UV circular dichroism (CD) spectroscopy, and thermal (tetramer) stability analysis.

SDS-PAGE Analyses

SDS-PAGE analyses were performed to estimate MWs and purities of SA, ST, and their PTD-linked derivatives (figure 2-8).

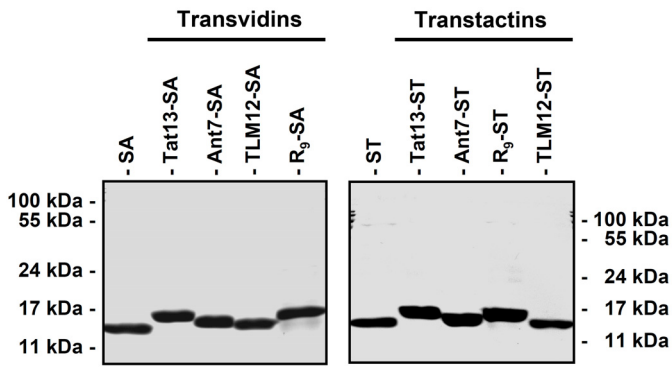

Figure 2-8. Coomassie-stained SDS-polyacrylamide gels of purified proteins.

Purified proteins exhibited a migration behavior similar to their expected theoretical masses (table 2-1) and showed more than 95 % in purity as estimated by Coomassie-staining (figure 2-8).

Mass Spectrometry

MALDI-TOF MS analyses of desalted protein samples were performed to determine their mass-to-charge (m/z, MH^+) values. Figure 2-9 exemplarily shows the result for Ant7-ST.

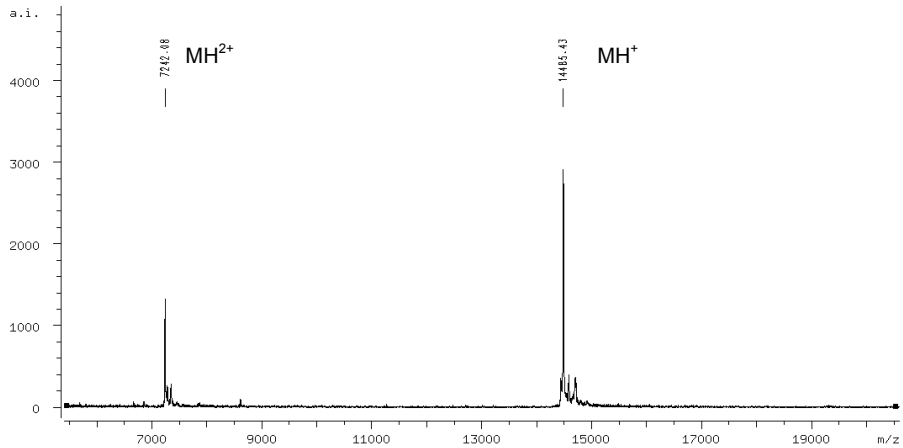

Figure 2-9. MALDI-TOF MS analyses: Purified Ant7-ST protein showed an observed MH^+ value (right peak) similar to its calculated average MH^+(av) value.

The observed MH^+ values of Tat13-SA/ST, Ant7-SA/ST, and R_9-SA/ST were similar to their average theoretical (MH^+(av)) values with discrepancies of less than 5 Da (table 2-2). Differences between the observed and theoretical values of SA/ST and TLM12-SA/ST could be explained by removal of the N-terminal methionines due to the activity of the *E. coli* methionine aminopeptidase which removes the start-methionine, depending on the side chain length of the second amino acid (MOGK *et al.*, 2007).

EDMAN SEQUENCING

N-terminal methionine removal from SA/ST and TLM12-SA/ST was confirmed by Edman sequencing. All cationic PTDs retained the start methionine (table 2-2).

Protein	MALDI-TOF MS			Start-methionine
	Theoretical MH^+(av)	Observed MH^+	Difference MH^+(av) – MH^+	
SA	13403.7	13273.8	129.9	-
TAT13-SA	15196.9	15196.5	0.4	+
ANT7-SA	14475.1	14474.5	0.6	+
R_9-SA	14866.5	ND	ND	+
TLM12-SA	14731.2	14598.4	132.8	-
ST	13414.8	13287.5	127.3	-
TAT13-ST	15207.9	15205.1	2.8	+
ANT7-ST	14486.2	14485.4	0.8	+
R_9-ST	14877.5	14882.4	-4.9	+
TLM12-ST	14742.3	14613.0	129.3	-

Table 2-2. MALDI-TOF MS and Edman sequencing: MALDI-TOF MS and Edman sequencing of selected proteins confirmed that unfused SA/ST and TLM12-SA/ST proteins lacked the N-terminal start-methionine. Start-methionine present (+), absent (-). ND: not determined.

THERMAL TETRAMER STABILITY

SA and ST tetramerization (VOSS and SKERRA, 1997) is essential for forming the binding pocket for biotin and *Strep*-tag II which lies at the interface between SA and ST subunits, respectively (SANO and CANTOR, 1995). SA and ST tetramers are extremely stable even in the presence of SDS and therefore can be detected on SDS-polyacrylamide gels (BAYER *et al.*, 1996; WANER *et al.*, 2004; HUMBERT *et al.*, 2005). Temperature dependence of tetramer breakup was studied by heating and subsequent SDS-PAGE analyses, as exemplified for Tat13-SA either analyzed alone, or in complex with biotin, *Strep*-tag, or *Strep*-tag II (figure 2-10). Temperature-dependent tetramer stabilities of all recombinant proteins were compiled in figure 2-11. Up to a temperature of 65 °C, SA proteins were detectable exclusively in a tetrameric state. Notably, all PTD fusions increased the tetramer stability of SA up to 70 °C. SA and all those Transvidins complexed with biotin showed increased tetramer stabilities up to 90 °C. *Strep*-tag and *Strep*-tag II peptides induced no changes in the temperature-dependent tetramer breakup of SA compared to the ligand-free protein preparations. The amino acid substitutions which were required to convert SA into ST decreased the tetramer stability by 5 °C. The Tat13-ST and R_9-ST Transtactins showed similar stabilities compared to the Transvidin proteins. Ant7-ST and TLM12-ST tetramers were stable up to 65 °C. All pre-incubations of unfused ST or individual Transtactins with biotin, *Strep*-tag, and *Strep*-tag II, respectively, had no effect on temperature-dependent ST tetramer breakup. Summed up, these data indicated that all investigated transporters were stable over a wide range of temperatures with regard to their tetramer forming capacity.

CIRCULAR DICHROISM SPECTROSCOPY

Since PTD fusions can influence the biophysical properties of cargos (HONDA *et al.*, 2005), CD spectroscopy was performed to assess possible alterations in the secondary structures of SA and ST proteins caused by their N-terminal PTD-fusions. Protein preparations, dialyzed against H_2O, were analyzed by far-UV CD spectroscopy from 190 nm to 240 nm. The spectra of all SA derivatives showed almost identical curve progressions, similar to the CD spectrum of core SA (figure 2-12). CD spectra were interpreted using PEPFIT (REED and REED, 1997). The fractions of secondary structure were compared with the crystal structures of SA (HYRE *et al.*, 2006) and ST (KORNDORFER and SKERRA, 2002) (figure 2-13). Both, the line shapes of the CD spectra and the PEPFIT results suggested that all proteins shared similar β-sheet rates of approximately 44.5 % to 58 % and α-helix rates up to 7 % (figure 2-13). These minor differences could be explained by small effects of the N-terminal PTD-fusions or slight skewing of the analyses of CD spectra due to the need to compensate for the unusually pronounced positive peaks at 230 nm (GREEN and MELAMED, 1966). These peaks most likely reflect one lobe on an exciton interaction between aromatic side chains (MANDAL *et al.*, 1985; GRISHINA and WOODY, 1994).

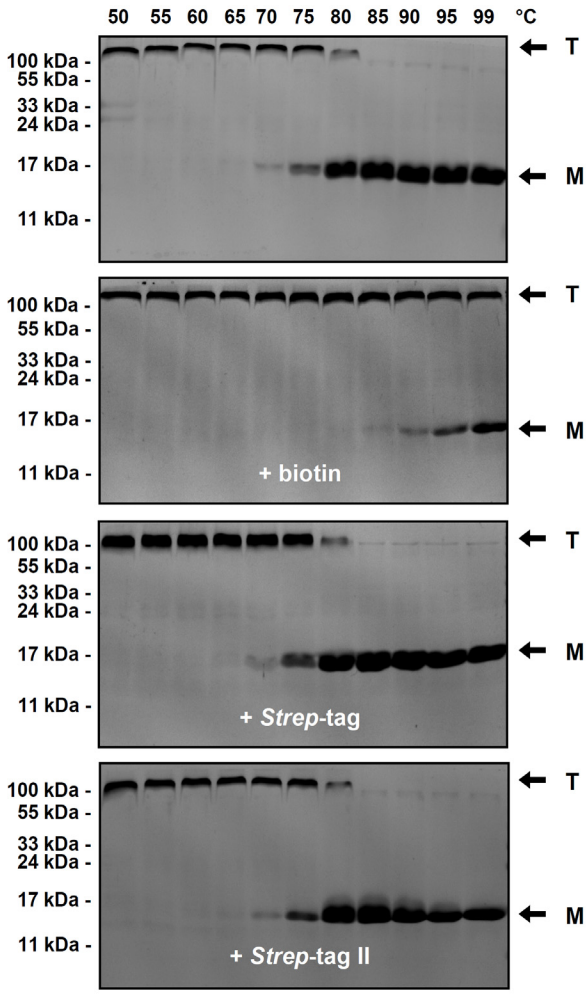

Figure 2-10. Thermal tetramer stability of Tat13-SA protein preparations: SDS-PAGE analyses of Coomassie-stained Tat13-SA proteins without ligand or pre-incubated with biotin, *Strep*-tag, or *Strep*-tag II at various temperatures. Tetrameric (T) and monomeric (M) states of Tat13-SA were indicated. Tetrameric Tat13-SA proteins appeared at MWs that differed from their theoretical values since the electrophoretic mobility strongly depends *inter alia* on the protein folding.

Legend for figure 2-11 which is printed on the following page. Compilation of thermal tetramer stabilities of SA and ST, as well as of Transvidins and Transtactins, either in the absence or presence of the ligands biotin, *Strep*-tag, or *Strep*-tag II: Tetrameric and monomeric protein amounts less than 10 %, with respect to the deployed amount of protein, remained unconsidered.

PTD	SA/ST	Ligand	Temperature [°C] 50	55	60	65	70	75	80	85	90	95	99
-	SA	-											
		biotin											
		Strep-tag											
		Strep-tag II											
Tat13	SA	-											
		biotin											
		Strep-tag											
		Strep-tag II											
Ant7	SA	-											
		biotin											
		Strep-tag											
		Strep-tag II											
R_9	SA	-											
		biotin											
		Strep-tag											
		Strep-tag II											
TLM12	SA	-											
		biotin											
		Strep-tag											
		Strep-tag II											
-	ST	-											
		biotin											
		Strep-tag											
		Strep-tag II											
Tat13	ST	-											
		biotin											
		Strep-tag											
		Strep-tag II											
Ant7	ST	-											
		biotin											
		Strep-tag											
		Strep-tag II											
R_9	ST	-											
		biotin											
		Strep-tag											
		Strep-tag II											
TLM12	ST	-											
		biotin											
		Strep-tag											
		Strep-tag II											

Tetramer

Tetramer / monomer

Monomer

See previous page for figure legend 2-11

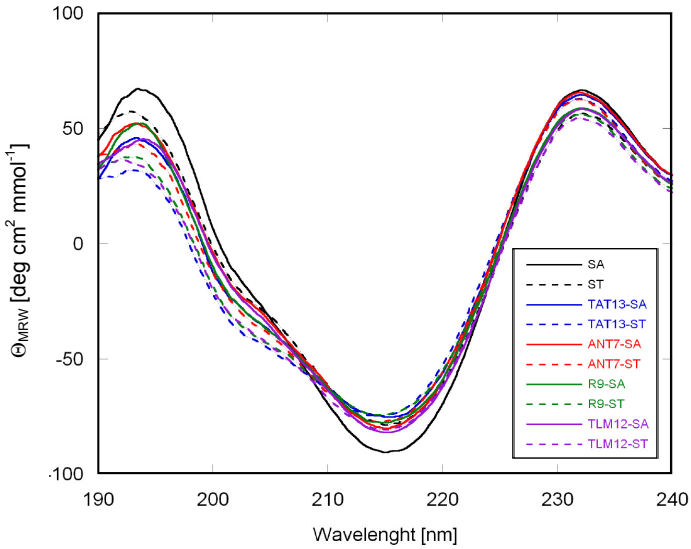

Figure 2-12. Far-UV CD spectroscopy: Spectra of SA, ST, Transvidin, and Transactin proteins showed almost identical curve progressions. Note the unusually pronounced peaks at 230 nm which most likely reflect one lobe on an exciton interaction.

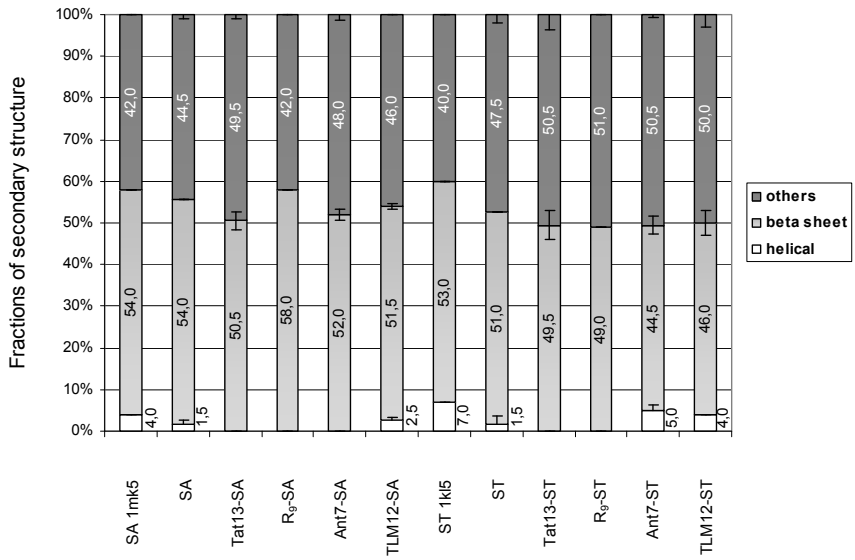

Figure 2-13. Interpretation of CD spectra by PEPFIT analyses: Fractions of the secondary structures were compared with the crystal structures of SA (PDB entry 1mk5) (HYRE *et al.*, 2006) and ST (PDB entry 1kl5) (KORNDORFER and SKERRA, 2002).

THERMAL DENATURATION

In-line with the data obtained by the temperature-dependent tetramer breakup experiments, thermal unfolding analyses using CD spectroscopy revealed that conformational stabilities of SA and ST, as well as of individual Transvidins and Transtactins, were consistent with high melting temperatures (T_ms). These ranged from 74.63 °C for R_9-ST to 83.67 °C for SA. Figure 2-14 (A) exemplarily shows the thermal denaturation curve for Tat13-SA, figure 2-14 (B) its normalized (see Materials and Methods) thermal denaturation curve. All normalized melting curves were summarized in figures 2-14 (C) and (D). Table 2-3 shows a compilation of all T_ms.

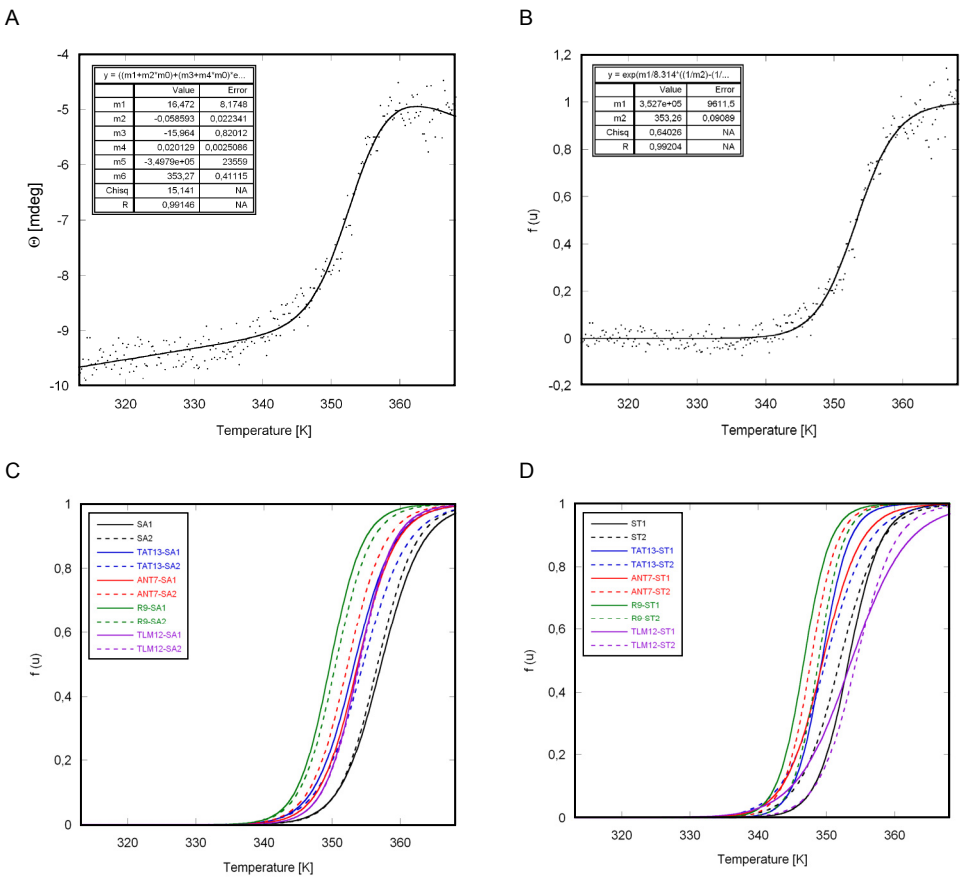

Figure 2-14. Thermal denaturation: (A) Thermal denaturation of a Tat13-SA preparation with a T_m of 80.11 °C. (B) Normalized thermal denaturation curve of Tat13-SA. Compilations of two independently determined melting curves of (C) Transvidin and (D) Transtactin proteins.

Protein	T_m [°C]
SA	83.67 ± 0.34
Tat13-SA	80.68 ± 0.91
Ant7-SA	79.83 ± 1.04
R_9-SA	76.95 ± 0.56
TLM12-SA	80.77 ± 0.09
ST	79.21 ± 0.76
Tat13-ST	76.46 ± 0.37
Ant7-ST	75.45 ± 1.22
R_9-ST	74.63 ± 1.51
TLM12-ST	80.74 ± 0.63

Table 2-3. Thermal denaturation: Compilation of all T_ms.

2.3 INTERNALIZATION OF STREPTAVIDIN AND *STREP*-TACTIN BY PTD-FUSED LIGANDS

Next, the above generated tools were tested functionally. The first transmembrane delivery system analyzed consisted of two components: (i) SA, as a non-cell permeable model for a protein binder, and (ii) PTD-fused *Strep*-tag II which more weakly interacts with the binding pocket of SA than the intracellular target molecule biotin. Hypothetically, upon PTD mediated internalization, *Strep*-tag II should be replaced on SA by biotin (figure 2-15, upper part of the panel). This principle should also be applicable for other protein binders (e.g. anticalins (SCHLEHUBER and SKERRA, 2005; SKERRA, 2007)), acting on defined intracellular targets (figure 2-15, lower part of the panel).

In an initial set of experiments, Tat13-PEO_3-biotin was used to internalize SA and to characterize its intracellular distribution upon internalization. Analogous experiments were then performed utilizing Tat13-*Strep*-tag II as transporter and SA/ST as cargos. These experiments also addressed the question whether the binding affinity of the ligands might influence the efficiency of transmembrane delivery. Finally, the intracellular displacement of Tat13-*Strep*-tag II by biotin was investigated. This latter analysis took advantage of the observation that biotin binding leads to an increased thermal tetramer stability of SA when compared to Tat13-*Strep*-tag II complexes (figure 2-11).

INTERNALIZATION OF SA BY TAT13-PEO_3-BIOTIN

INTRACELLULAR DISTRIBUTION

In general, PTD-mediated internalized cargos appear in two major distribution patterns, either cytosolically solubilized or in a punctuated pattern which is likely to reflect endosomal compartments (RINNE *et al.*, 2007). Whether the same is true for SA internalized by Tat13-PEO_3-biotin was investigated by fluorescence microscopy. Titration experiments revealed that externally applied concentrations of as low as 100 nM SA complexed with 100 nM Tat13-PEO_3-biotin could be visualized by immunofluorescence upon internalization (data not shown). For the following experiments, HeLa

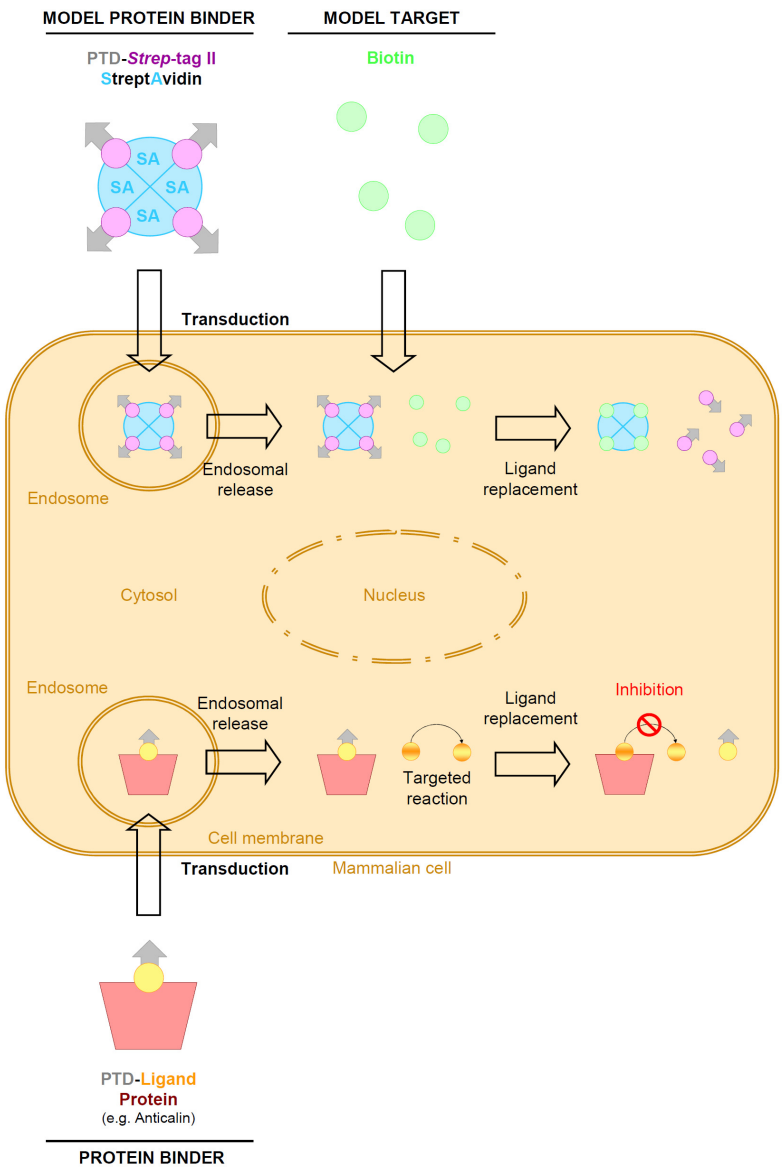

Figure 2-15. Model for the internalization of protein binders by PTD-fused ligands: SA is internalized into mammalian cells by PTD-*Strep*-tag II, most likely via the endosomal route (upper part of the panel). In the cytoplasm, PTD-*Strep*-tag II is replaced by the higher affinity ligand biotin which is internalized by means of the multivitamin transporter. If this system is principally functional, one could envision the application of therapeutically useful protein binders, e.g. anticalins, using low affinity PTD-ligands for internalization (lower part of the panel). Subsequently, this ligand will be replaced by a higher affinity intracellular target molecule, leading to the functional inactivation of the latter by sequestration.

cells were incubated with 10 µM SA pre-complexed with 10 µM Tat13-PEO_3-biotin. Non-complexed SA served as negative control. After 2 hours of incubation, cells were trypsinized to remove extracellularly attached proteins, plated on glass coverslips for paraformaldehyde (PFA) fixation, and subsequently analyzed by immunofluorescence. It was found that Tat13-PEO_3-biotin internalized its cargo SA into almost 100 % of the HeLa cells (figure 2-16). Control-treated cells showed no internalization. Higher resolution microscopy analyses showed that Tat13-internalized SA proteins were typically detected in two major intracellular distribution patterns (figure 2-17), either punctuated around the cell nucleus or cytosolically solubilized.

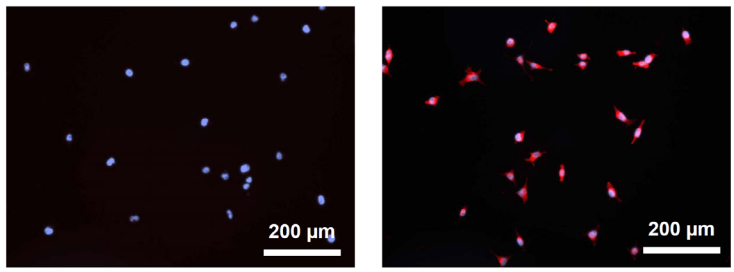

Figure 2-16. Internalization of SA by Tat13-PEO_3-biotin: Internalized SA was detected by immunofluorescence analysis. DNA-staining with DAPI in blue, SA is shown in red.

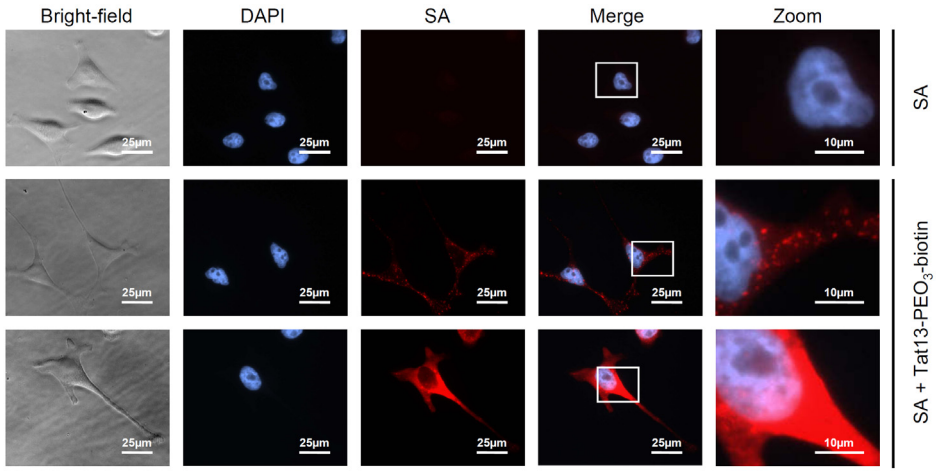

Figure 2-17. Intracellular distribution of SA internalized by Tat13-PEO_3-biotin: HeLa cells were treated with SA alone (upper panel, negative control) or with SA complexed with Tat13-PEO_3-biotin (lower two panels).

Internalization of SA-Fusion Proteins by Tat13-PEO_3-Biotin

To quantify the efficiency of transmembrane delivery, horseradish peroxidase (HRP) fused to SA was applied as cargo. HeLa cells were incubated with 1 µM of SA-HRP complexed with 2 µM Tat13-PEO_3-

biotin. High enzymatic HRP-activities were measured only in lysates of HeLa cells treated with SA-HRP complexed with Tat13-PEO_3-biotin (figure 2-18, upper panel). Untreated cells or cells incubated with SA-HRP alone showed only low background enzymatic HRP activities. An SA-HRP calibration curve

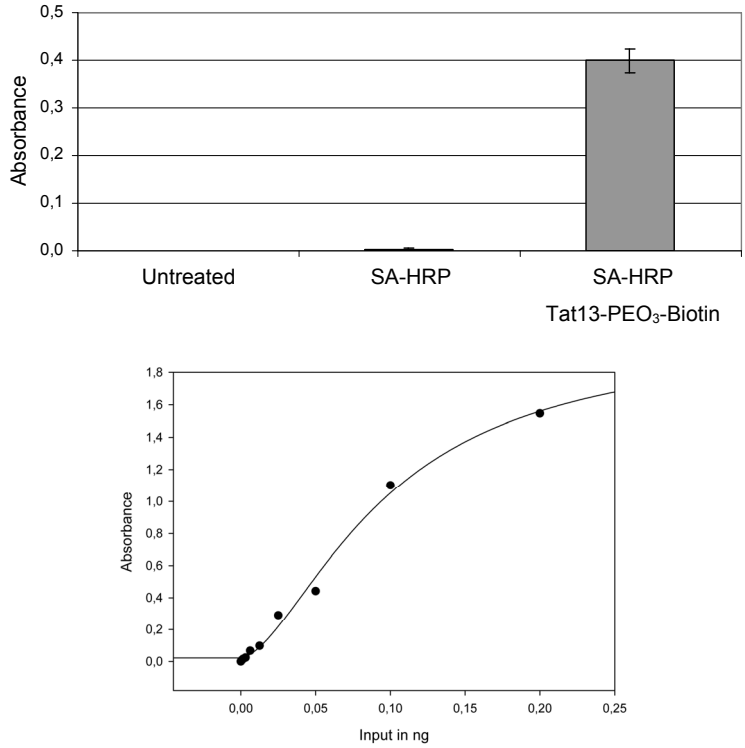

Figure 2-18. Internalization of SA-HRP by Tat13-PEO_3-biotin: Analyses of enzymatic HRP activities in HeLa cell lysates (upper panel). Calibration curve of the SA-HRP enzyme activity to determine internalization rates (lower panel).

(figure 2-18, lower panel) was calculated to estimate the amount of Tat13-PEO_3-biotin internalized SA-HRP. Regarding the theoretical maximum amount of internalized SA-HRP, which equaled the molarity of the Tat13-PEO_3-biotin transporter, 0.74 % of functional SA-HRP were introduced by Tat13-PEO_3-biotin, which equaled 26 pmol per mg total amount of protein (table 2-4).

Transporter and cargo
Tat13-PEO_3-biotin SA-HRP
Quantification
(0.27 - 1.03) % (26 - 72) pmol/mg

Table 2-4. Quantification of the internalization of SA-HRP by Tat13-PEO_3-biotin: Internalized amounts of HRP were calculated with respect to the theoretical maximum amount of internalized SA-HRP in percent or in pmol of internalized SA-HRP normalized to the total amount of protein (for details, see Materials and Methods).

INTERNALIZATION OF ST BY TAT13-*STREP*-TAG II

INTRACELLULAR DISTRIBUTION

The internalization efficiency and intracellular distribution of ST internalized by Tat13-*Strep*-tag II were investigated as described for SA and Tat13-PEO_3-biotin. Again, HeLa cells treated with complexes of ST and Tat13-*Strep*-tag II were almost 100 % ST-positive, as shown by fluorescence microscopy (figure 2-19). Alike SA, the internalized ST, also appeared cytosolically solubilized or in a punctuated pattern around the nucleus (figure 2-20).

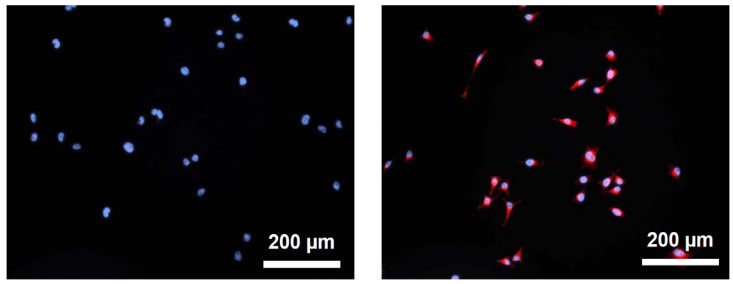

Figure 2-19. Internalization of ST by Tat13-*Strep*-tag II: Internalized ST was detected using an anti-SA primary antibody. DNA-staining with DAPI in blue, ST is shown in red.

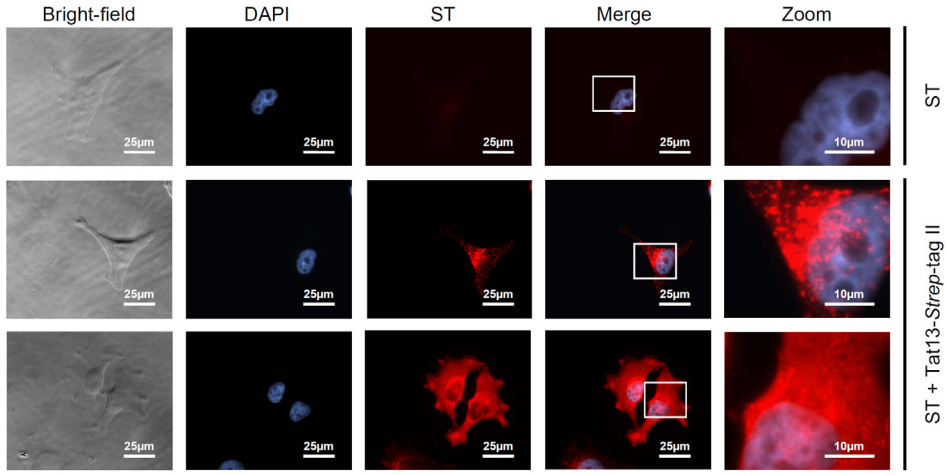

Figure 2-20. Intracellular distribution of ST internalized by Tat13-*Strep*-tag II: HeLa cells were treated with ST alone (upper panel, negative control) or in a complex with Tat13-*Strep*-tag II (lower two panels).

INTERNALIZATION OF ST-FUSION PROTEINS BY TAT13-*STREP*-TAG II

Tat13-*Strep*-tag II was also able to internalize functional ST-HRP conjugates. High enzymatic activities were detected in lysates of HeLa cells incubated with ST-HRP complexed with Tat13-*Strep*-tag II (figure 2-21, upper panel). In contrast, untreated cells showed no enzymatic activity. Cells treated with ST-HRP

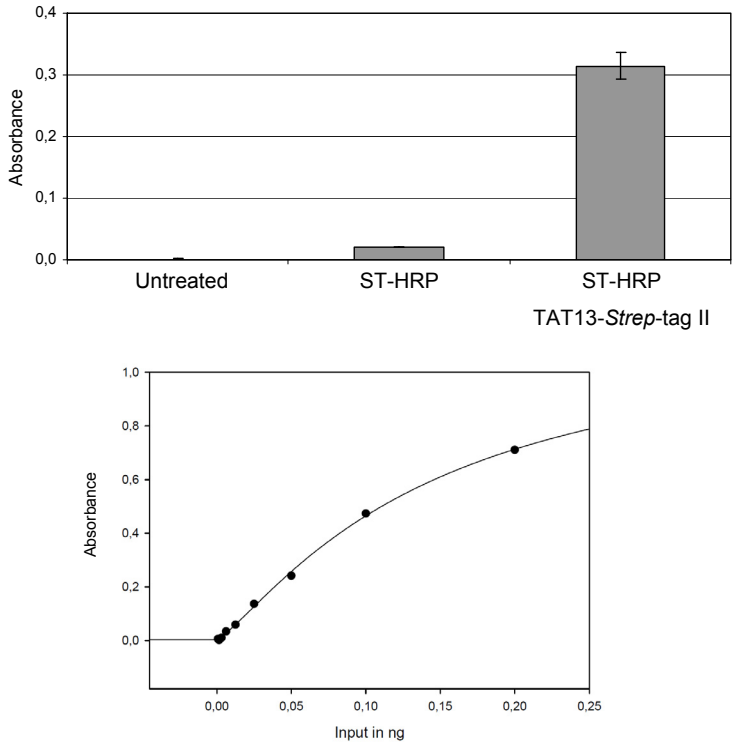

Figure 2-21. Internalization of ST-HRP by Tat13-*Strep*-tag II: Analyses of enzymatic HRP activities in HeLa cell lysates (upper panel). Calibration curve of ST-HRP (lower panel).

alone showed only low background enzymatic HRP signals. Regarding the theoretic maximum amount of internalized ST-HRP, 0.68 ‰ of ST-HRP were successfully internalized, which equaled 4.2 pmol per mg total protein (table 2-5).

Transporter and cargo
Tat13-*Strep*-tag II ST-HRP
Quantification
(0.68 - 0.76) ‰ (4.2 - 14) pmol/mg

Table 2-5. Quantification of the internalization of ST-HRP by Tat13-*Strep*-tag II.

The observed range of internalization of ST-HRP by Tat13-*Strep*-tag II (K_D = 1 µM) was lower compared to the internalization of SA-HRP by Tat13-PEO_3-biotin (K_D ~ 10^{-14} M). This can partly be explained by means of the law of mass action (see Materials and Methods). According to that, only 58 % of ST-HRP were theoretically complexed with Tat13-*Strep*-tag II and therefore suitable for cellular internalization.

INTERNALIZATION OF SA BY TAT13-*STREP*-TAG II AND ST BY TAT13-PEO_3-BIOTIN

Finally, the internalization of SA by Tat13-*Strep*-tag II and ST by Tat13-PEO_3-biotin was tested. Again, HeLa cells were almost 100 % SA/ST-positive after treatment with the corresponding complexes, as depicted in figure 2-22. Control-treated cells showed no cargo internalization (data not shown). Internalized SA and ST proteins appeared in similar distribution patterns (data not shown) as found for Tat13-PEO_3-biotin and SA (figure 2-17).

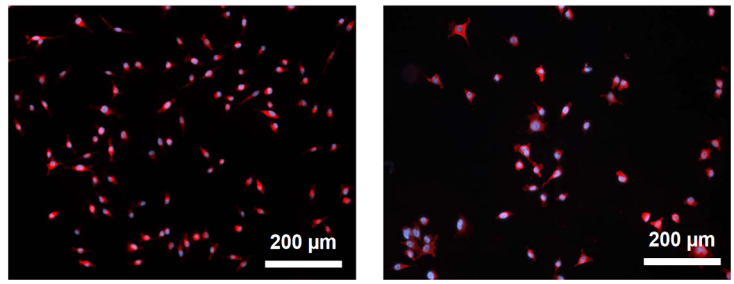

SA + Tat13-*Strep*-tag II ST + Tat13-PEO_3-Biotin

Figure 2-22. Internalization of SA by Tat13-*Strep*-tag II and ST by Tat13-PEO_3-biotin: Internalized SA and ST proteins were detected by immunofluorescence analyses using anti-SA primary antibodies. DNA-staining with DAPI in blue, SA and ST are shown in red.

Next, the internalization efficiencies of Tat13-*Strep*-tag II for SA-HRP (figure 2-23, upper panel) and Tat13-PEO_3-biotin for ST-HRP (figure 2-24, upper panel) were determined as described above. High enzymatic HRP-activities were measured only in lysates of HeLa cells incubated with SA/Tat13-*Strep*-tag II and ST/Tat13-PEO_3-biotin, respectively. Untreated cells or cells incubated with SA/ST-HRP alone showed no or low background enzymatic HRP activities. Regarding the theoretical maximum amount of internalized HRP, 0.24 ‰ of SA-HRP and 0.62 % of ST-HRP were functionally internalized by Tat13-fused *Strep*-tag II and biotin (table 2-6). This equaled 1.5 pmol/mg SA-HRP and 22 pmol/mg ST-HRP, respectively.

The observed internalization efficiency for SA-HRP by Tat13-*Strep*-tag II (K_D = 72 µM) was lower than for ST-HRP and Tat13-*Strep*-tag II (K_D = 1 µM). This can be partly explained by applying the law of mass action. According to that, only 2.7 % of SA-HRP and Tat13-*Strep*-tag II were theoretically

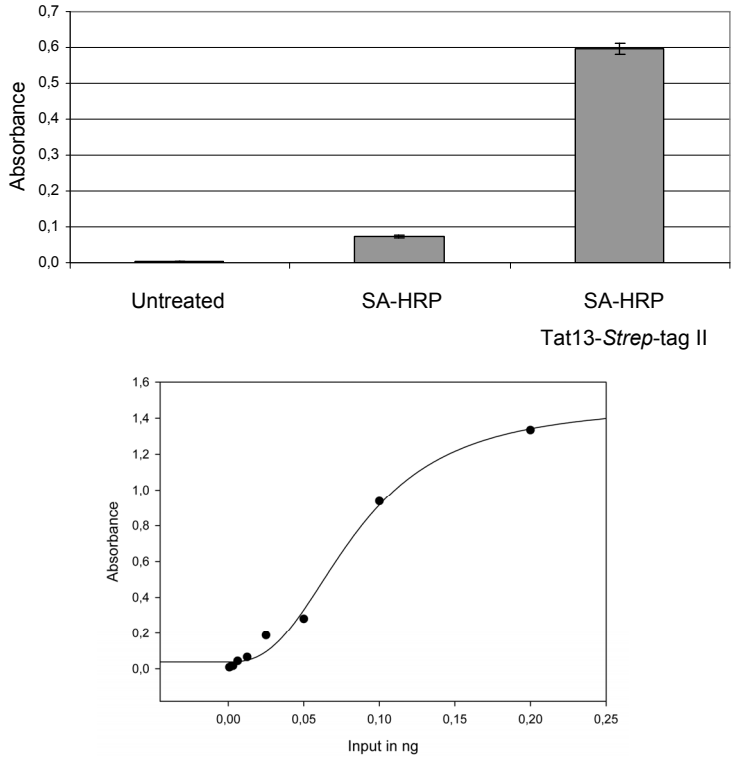

Figure 2-23. Internalization of SA-HRP by Tat13-*Strep*-tag II: Analyses of enzymatic HRP activities in HeLa cell lysates (upper panel). Calibration curve of SA-HRP (lower panel).

complexed. The internalization efficiencies for ST-HRP (K_D < 1 µM, ND) and SA-HRP (K_D ~ 10^{-14} M) by Tat13-PEO_3-biotin were in a similar range.

LIGAND-REPLACEMENT BY AN INTRACELLULAR TARGET

According to the model depicted in figure 2-15, Tat13-*Strep*-tag II will be replaced on internalized SA by its natural higher-affinity binding ligand biotin. This should result in increased thermal tetramer stability since biotin binding stabilizes SA tetramers (figure 2-11).

To investigate this issue, HeLa cells were first treated with complexes of 10 µM SA and 20 µM Tat13-*Strep*-tag II. After 2 hours, the cells were extensively washed and, subsequently, a 2-fold molar excess of biotin was added to the cells. Biotin-uptake was supported by means of the mammalian multivitamin transporter (PRASAD and GANAPATHY, 2000). After 2 additional hours, cell lysates were prepared and analyzed by immunoblotting (figure 2-25, lower panel).

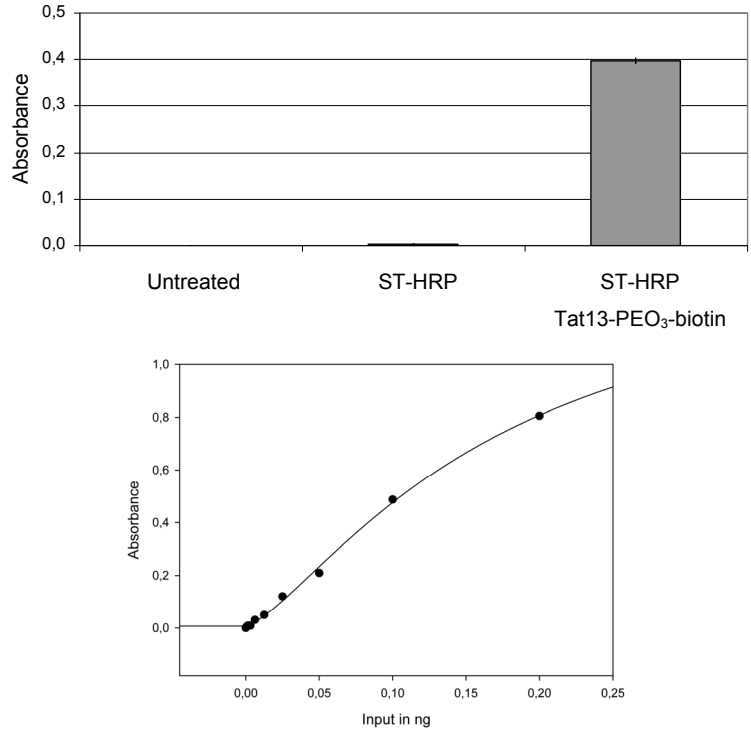

Figure 2-24. Internalization of ST-HRP by Tat13-PEO_3-biotin: Analyses of enzymatic HRP activities in HeLa cell lysates (upper panel). Calibration curve of ST-HRP (lower panel).

Transporter and cargo	Quantification
SA-HRP Tat13-*Strep*-tag II	(0.17 - 0.24) ‰ (0.56 - 1.5) pmol/mg
ST-HRP Tat13-PEO_3-biotin	(0.62 - 0.87) % (22 - 29) pmol/mg

Table 2-6. Quantification of the internalization of SA/ST-HRP by Tat13-fused ligands.

As shown in figure 2-11, stabilization of SA tetramers is reflected by decreased amounts of SA monomers. In-line with this, intracellular Tat13-SA tetramers (positive control) were thermally stabilized by the addition of biotin to the cells, as indicated by the decreased amount of SA monomers at 85 °C (figure 2-25, fourth panel). For Tat13-PEO_3-biotin internalized SA, external addition of biotin is not expected to result in a further stabilization of SA tetramers, since Tat13-PEO_3-biotin is a biotin-derivative which already strongly binds to the SA pocket. Indeed, upon SA internalization by Tat13-PEO_3-biotin, the addition of biotin to the cells did not affect the amount of SA monomers at high temperatures (figure 2-25, third panel). This finding strongly differed from the data for Tat13-*Strep*-tag II-internalized SA, where SA was no longer monomeric at 85 °C upon addition of biotin to the cells (figure 2-25, second panel). These results strongly suggest that biotin induced the thermal stabilization of SA tetramers by

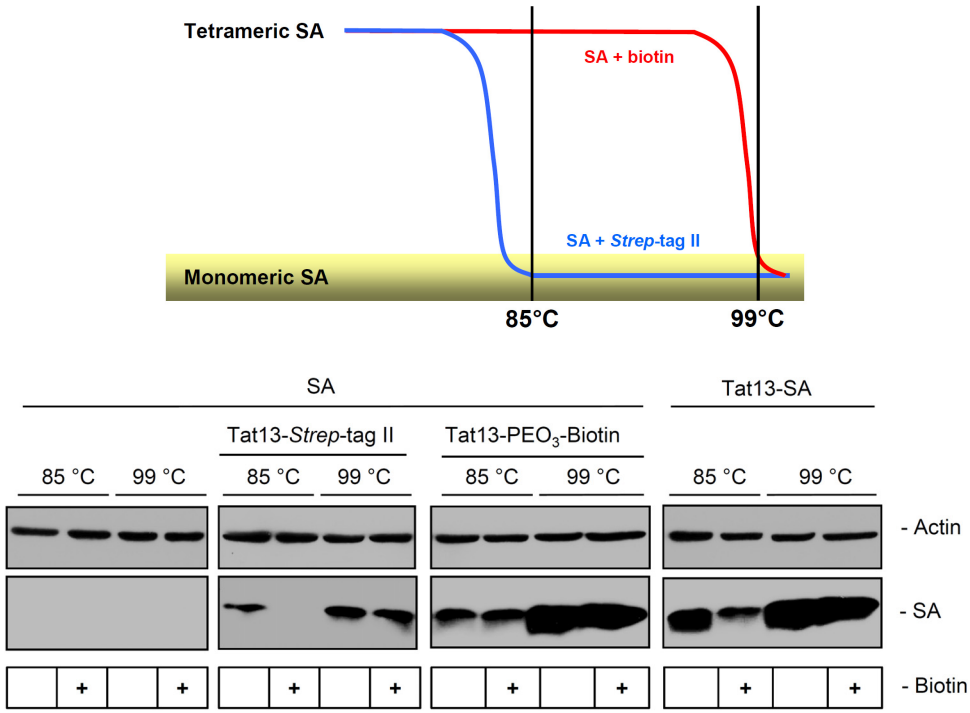

Figure 2-25. Intracellular replacement of Tat13-*Strep*-tag II on SA by biotin: (A) Scheme for the temperature-dependent tetramer breakup of SA complexed with biotin (red) or *Strep*-tag II peptide (blue). Tetrameric and monomeric SA proteins are indicated. Monomeric SA was investigated to show intracellular ligand replacement (yellow). (B) Immunoblot analysis of monomeric SA. Actin: loading control.

replacing Tat13-*Strep*-tag II on SA. Thus, the internalization of a protein binder by a low affinity ligand fused to a PTD is feasible and can be utilized for subsequent ligand replacement in the cytoplasm.

2.4 INTERNALIZATION OF TRANSVIDINS AND TRANSTACTINS

PTDs were fused to SA (Transvidins) and ST (Transtactins) in an attempt to convert both proteins into universal cell-permeable transporters for biotinylated and *Strep*-tag II-fused cargos, respectively (figure 2-26). To investigate the ability of the transporters to internalize into mammalian cells, HeLa and SiHa cervical carcinoma as well as U-2 OS osteosarcoma cells were incubated with 1 µM of individual Transvidins and Transtactins for 2 hours. Cells were trypsinized to remove extracellularly attached proteins. Subsequently, cell lysates were prepared and analyzed by immunoblotting. Under these experimental conditions, Tat13- and R_9-fused SA and ST proteins, but not TLM12-SA/ST, internalized at

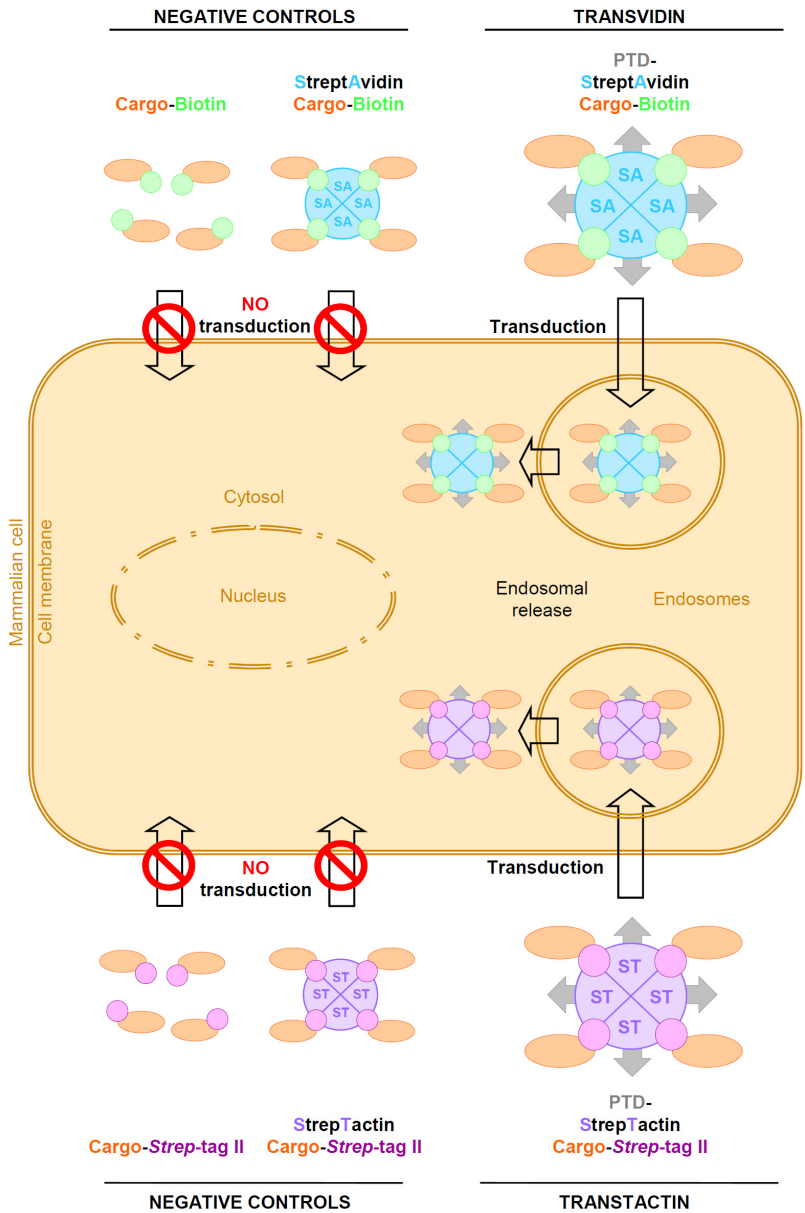

Figure 2-26. Model for the internalization of Transvidins and Transtactins: Cargos bind via biotin- and *Strep*-tag II-fused ligands to Transvidin and Transtactin transporters. The PTD portion of the Transvidins/Transtactins mediates the transmembrane delivery of the complexes via the endosomal route into mammalian cells. Ligand-fused cargos *per se*, or ligand-fused cargos bound to unfused SA or ST proteins, are not internalized (negative controls).

readily detectable levels (figure 2-27). The results for Ant7-fused transporters differed in the fact that the Ant7-SA uptake was not detectable by Western blot analysis, in contrast to Ant7-ST. Notably, Tat13-SA/ST and R_9-SA/ST displayed a more efficient internalization than Ant7-ST (figure 2-27).

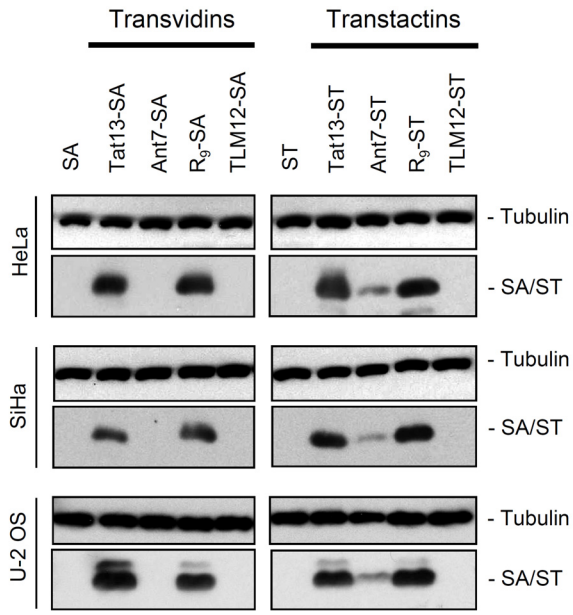

Figure 2-27. Internalization of Transvidins and Transtactins into HeLa, SiHa, and U-2 OS cells: Immunoblot analyses of intracellular monomeric SA/ST proteins upon treatment with the indicated transporters. Tubulin: loading control.

For immunofluorescence analyses, HeLa cells were treated with 10 µM of Transvidins (figure 2-28, panels to the left) or 10 µM of Transtactins (figure 2-28, panels to the right). All cells were almost 100 % SA/ST-positive, except for TLM12-SA/ST treated cells where the percentage of cells showing internalization was below 1 %. SA and ST, lacking PTDs, served as negative controls.

Next, the intracellular distribution of internalized Tat13-SA/ST, Ant7-SA/ST, and R_9-SA/ST was analyzed. Transvidins (figure 2-29) and Transtactins (figure 2-30) were detected in two major distribution patterns, either in a punctuated pattern around the cell nucleus or cytosolically solubilized. In the case of unfused SA and ST, serving as negative controls, no internalized proteins were detected. Treatment of SiHa or U-2 OS cells yielded identical results (data not shown).

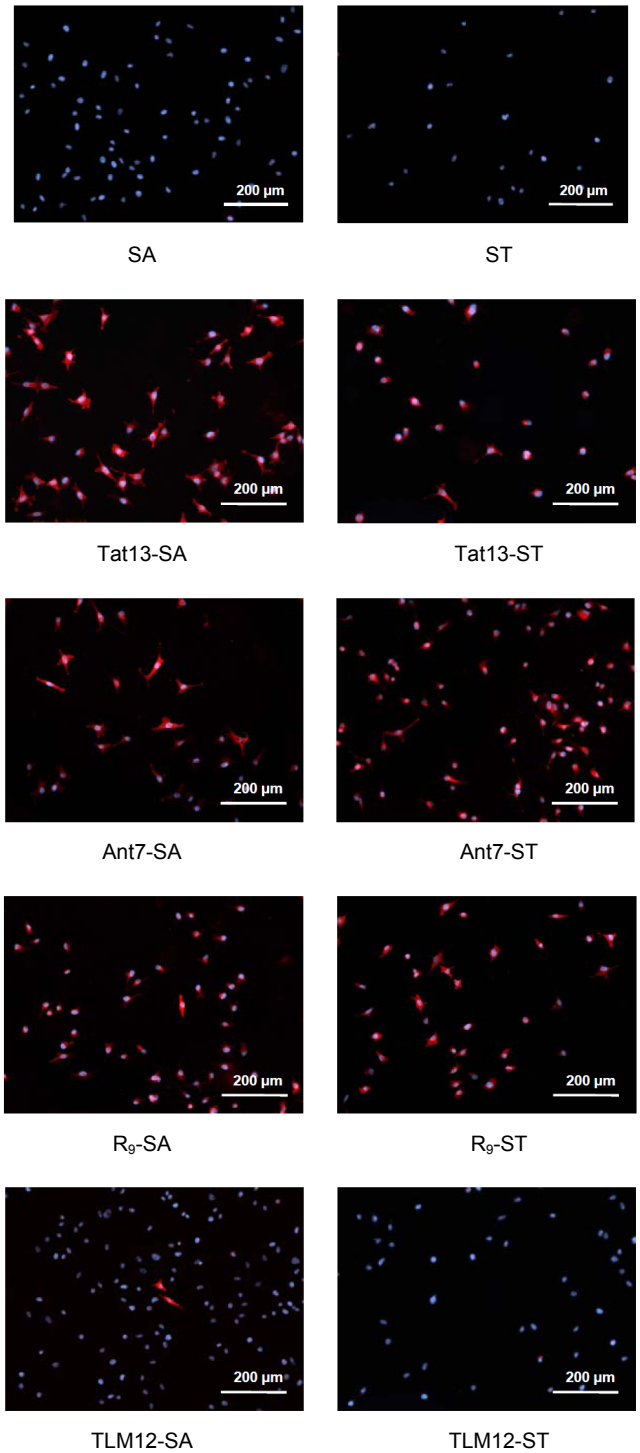

Figure 2-28. Internalization efficiencies of Transvidins and Transactins in HeLa cells: Immunofluorescence analyses using an anti-SA primary antibody which recognizes both SA and ST. DNA-staining with DAPI in blue, SA and ST are shown in red.

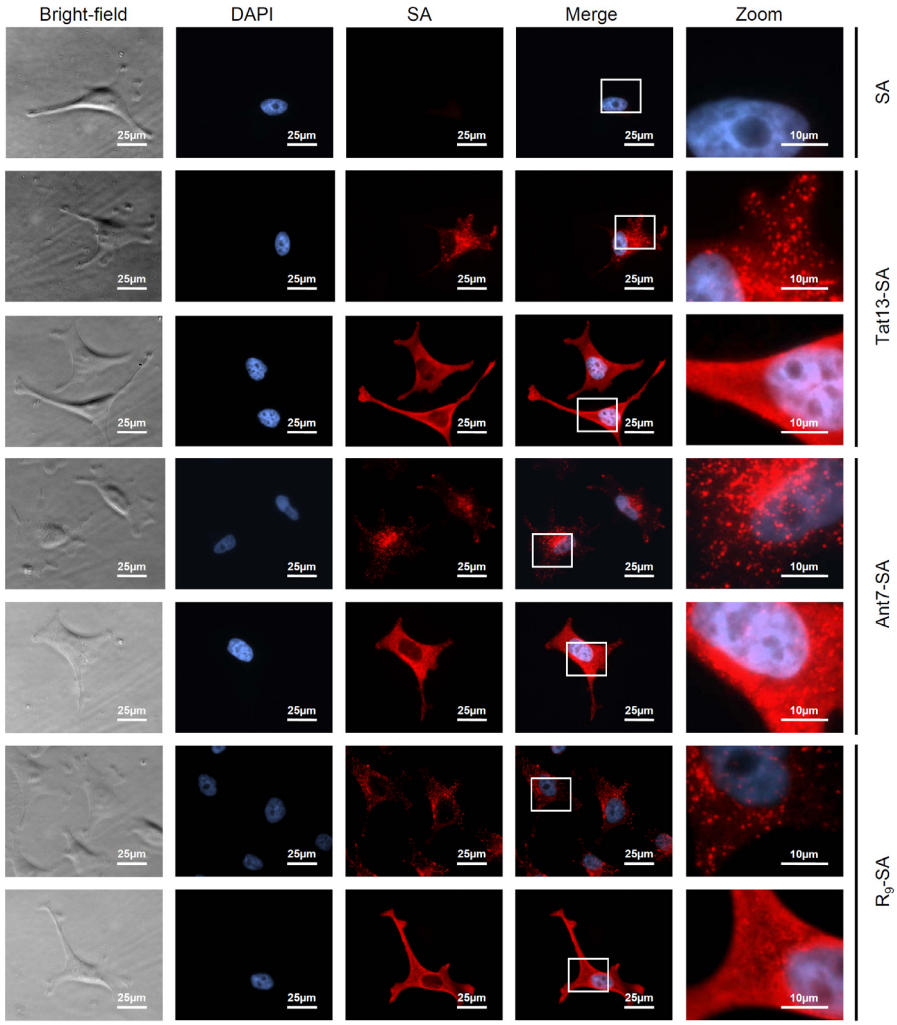

Figure 2-29. Intracellular distribution of Transvidins: Larger magnifications of immunofluorescence analyses of HeLa cells treated with SA alone (upper panel, negative control) or with Tat13-SA, Ant7-SA, and R_9-SA proteins (lower panels). Internalized Transvidins were detected using an anti-SA antibody.

In summary, Tat13-SA/ST and R_9-SA/ST proteins fulfilled the required internalization properties, both at high and at low applied external doses. Ant7-SA/ST internalization could only be detected at high doses (figures 2-29 and 2-30). TLM12 failed as a PTD, since it could not internalize covalently bound SA/ST (figures 2-27 and 2-28). Therefore, the following experiments aiming at the concomitant internalization of biotinylated or *Strep*-tag II-fused cargos focused on Tat13-SA/ST, Ant7-SA/ST, and R_9-SA/ST transporters.

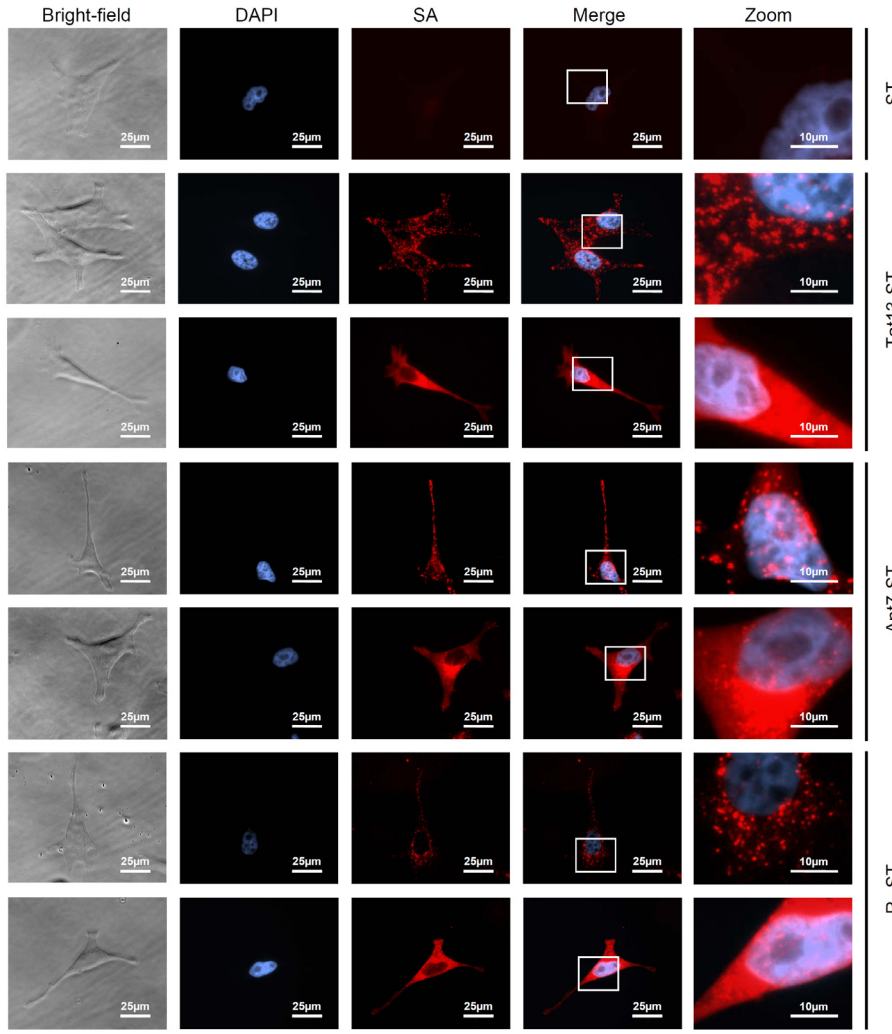

Figure 2-30. Intracellular distribution of Transtactins: Larger magnifications of immunofluorescence analyses of HeLa cells treated with ST alone (upper panel, negative control) or with Tat13-ST, Ant7-ST, and R_9-ST (lower panels). Internalized Transtactins were detected using an anti-SA antibody.

2.5 TRANSVIDINS AS UNIVERSAL DELIVERY SYSTEMS FOR BIOTINYLATED CARGOS

Next, the abilities of Transvidins to deliver cargos into intact cells were tested by using biotinylated organics, peptides, proteins, and proteinaceous multicomponent complexes.

INTERNALIZATION OF FITC-BIOTIN AS A MODEL CARGO FOR ORGANICS

In order to investigate whether Transvidins were able to co-internalize a biotinylated cell-membrane impermeable organic, HeLa cells were treated with 10 µM Tat13-SA, Ant7-SA, or R_9-SA complexed with 10 µM FITC-biotin. Figure 2-31 shows that FITC-biotin was clearly internalized by Transvidin transporters. In contrast, cells control-treated with FITC-biotin alone or in a complex with SA (devoid of a PTD) showed no FITC fluorescent signals. The staining pattern for FITC-biotin was punctual,

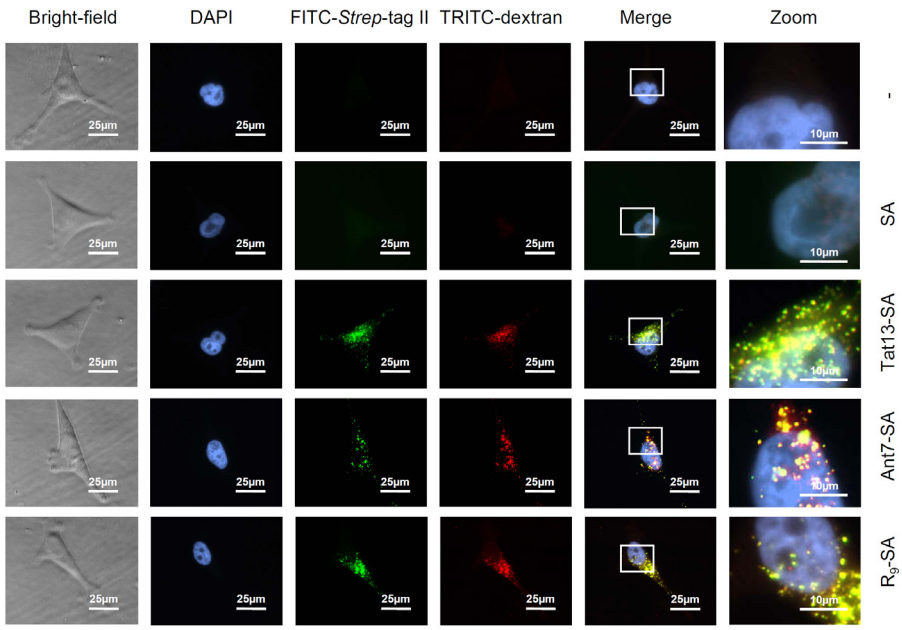

Figure 2-31. Intracellular distribution of FITC-biotin internalized by Transvidins: Fluorescence microscopy of HeLa cells treated with FITC-biotin alone, with FITC-biotin bound to SA (upper two panels, negative controls), Tat13-SA, Ant7-SA, or R_9-SA (lower panels). TRITC-dextran: fluid-phase endosomal marker, which was present in the medium.

indicating enrichment in distinct cellular compartments. These signals co-stained with TRITC-dextran, a fluid-phase endosomal marker, indicating that FITC-biotin was enriched in endosomal compartments.

INTERNALIZATION OF HRP-BIOTIN AS A MODEL CARGO FOR PROTEINS

Transvidins were also tested for the transmembrane delivery of biotinylated proteins into cultured HeLa cells. 200 nM Transvidins were incubated with 400 nM HRP-biotin. High enzymatic HRP activities were measured in lysates of cells treated with Tat13-SA and R_9-SA (figure 2-32, upper panel). Cells

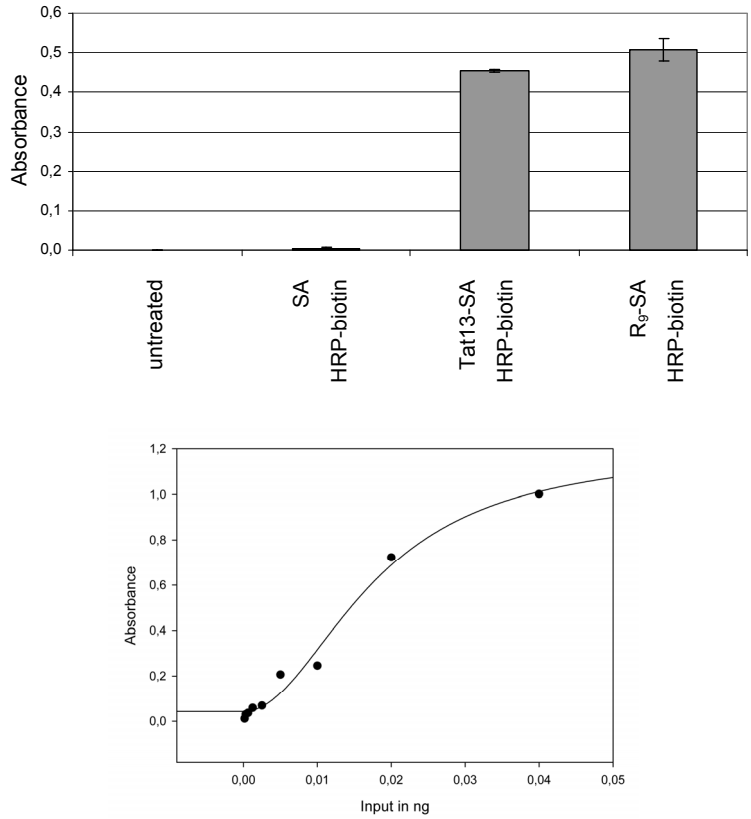

Figure 2-32. Internalization of functional HRP-biotin by Transvidins: Analyses of enzymatic HRP-biotin activities in HeLa cell lysates (upper panel). Calibration curve of HRP-biotin bound to SA (lower panel).

Transporter and cargo	Quantification
Tat13-SA HRP-biotin	(0.10 - 0.21) % (1.6 - 16) pmol/mg
R_9-SA HRP-biotin	(0.10 - 0.23) % (1.8 - 9.3) pmol/mg

Table 2-7. Quantification of the internalization of HRP-biotin by Transvidins.

incubated with Ant7-SA or TLM12-SA showed only low enzymatic activities (data not shown). Untreated cells and cells treated with complexes of HRP-biotin and SA (devoid of a PTD) showed no or only low background enzyme activities (figure 2-32, upper panel, negative controls). R_9-SA possessed the highest internalization rate of 0.23 % regarding the theoretical maximum amount of internalized HRP-biotin, which equaled 3.3 pmol per mg total protein (table 2-7).

INTERNALIZATION OF PROTEINACEOUS MULTICOMPONENT COMPLEXES

Additional experiments were performed to find out whether Transvidins were also able to deliver multicomponent complexes into cells. To this end, HeLa cells were incubated with 200 nM Transvidins

complexed with 300 nM His_6-PEO_3-biotin and 400 nM Ni-NTA-HRP. In this scenario, the Ni-NTA-HRP portion should be non-covalently linked to Transvidin via His_6-PEO_3-biotin and internalized. Indeed, high enzymatic HRP activities were measured only in cellular lysates of HeLa cells incubated with Tat13-SA or R_9-SA complexed with His_6-PEO_3-biotin and Ni-NTA-HRP (figure 2-33, upper panel). Untreated cells or cells incubated with a complex of SA (devoid of a PTD), His_6-PEO_3-biotin, and Ni-NTA-HRP showed no or only low background HRP activities. Low enzymatic HRP activities were also measured in lysates of HeLa cells incubated with Ant7-SA (data not shown). R_9-SA complexed with His_6-PEO_3-biotin

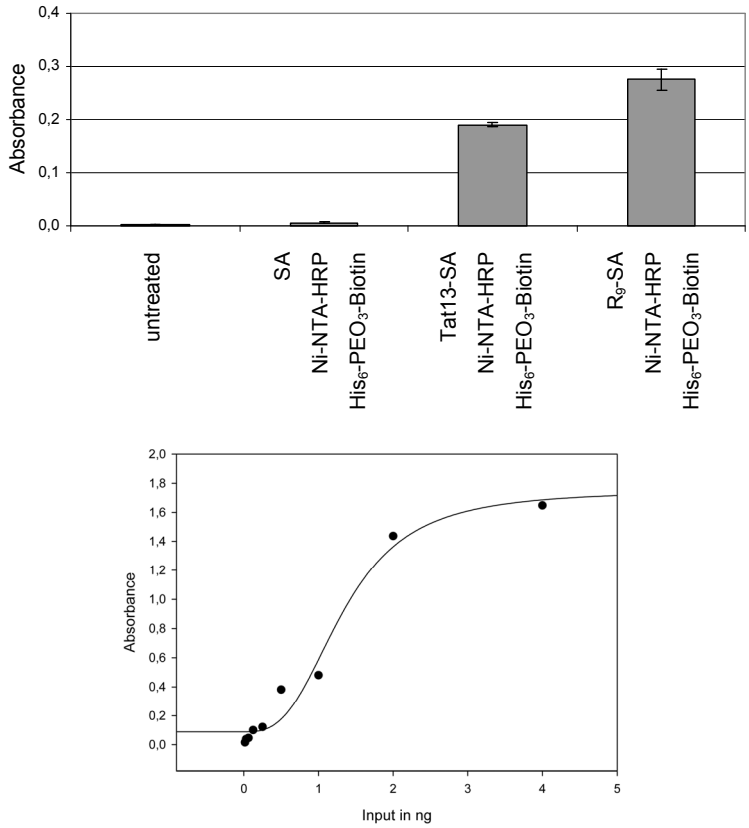

Figure 2-33. Internalization of Ni-NTA-HRP by Transvidins via His_6-PEO_3-biotin: Analyses of enzymatic HRP-activities in HeLa cell lysates (upper panel). Calibration curve of Ni-NTA-HRP bound to SA via His_6-PEO_3-biotin (lower panel).

Transporter and cargo	Quantification
Tat13-SA His_6-PEO_3-biotin Ni-NTA-HRP	(0.11 - 0.40) % (2.0 - 16) pmol/mg
R_9-SA His_6-PEO_3-biotin Ni-NTA-HRP	(0.18 - 0.51) % (4.9 - 14) pmol/mg

Table 2-8. Quantification of the internalization of Ni-NTA-HRP by Transvidins.

possessed the highest internalization rate of 0.51 % regarding the theoretical maximum amount of internalized Ni-NTA-HRP which equaled 14 pmol per mg total protein (table 2-8).

2.6 TRANSTACTINS AS UNIVERSAL DELIVERY SYSTEMS FOR *STREP*-TAG II-FUSED CARGOS

Corresponding experiments, as described for Transvidin, were performed to test the potential of Transtactin transporters to concomitantly internalize various model cargos into living cells.

INTERNALIZATION OF FITC-*STREP*-TAG II AS A MODEL FOR ORGANICS

Strep-tag II-fused FITC served as a model organic to be introduced by Transtactins. Upon treatment of HeLa cells with 10 µM Transtactins complexed with 10 µM FITC-*Strep*-tag II, Tat13-ST, Ant7-ST, and R_9-ST clearly internalized FITC-*Strep*-tag II (figure 2-34, lower panels). In contrast, cells control-treated with FITC-*Strep*-tag II alone or with FITC-*Strep*-tag II complexed with ST (devoid of a PTD) showed no FITC fluorescent signals (figure 2-34, upper two panels). Intracellular staining at higher magnification was punctual for FITC-*Strep*-tag II and co-stained with TRITC-dextran, indicating that FITC-*Strep*-tag II was enriched in endosomal compartments (figure 2-34).

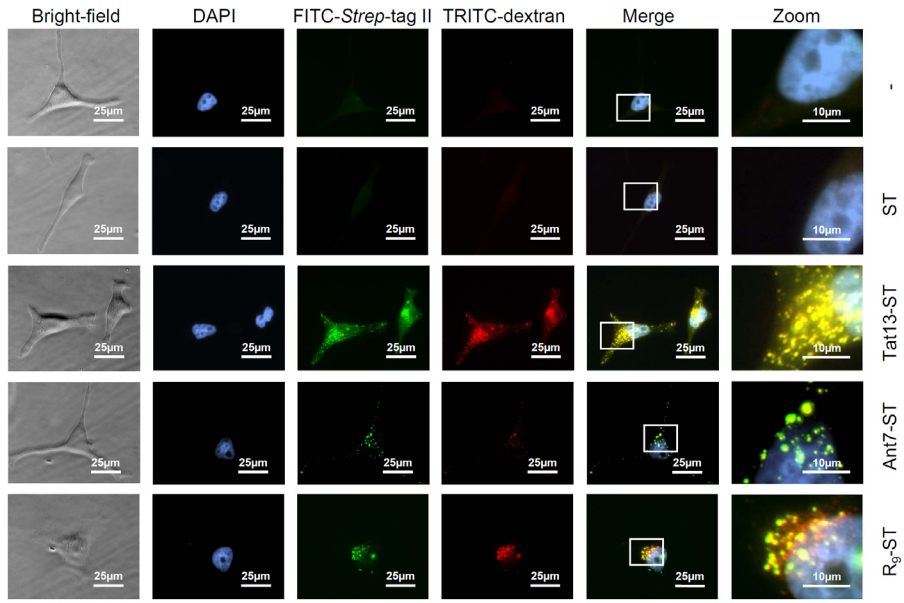

Figure 2-34. Intracellular distribution of FITC-*Strep*-tag II internalized by Transtactins: Fluorescence microscopy of HeLa cells treated with FITC-*Strep*-tag II alone or in a complex with ST (upper two panels, negative controls), Tat13-ST, Ant7-ST, or R_9-ST (lower panels). TRITC-dextran: fluid-phase endosomal marker.

INTERNALIZATION OF HRP-BIOTIN AS A MODEL CARGO FOR PROTEINS

The capacity of Transtactins to internalize proteins in an intracellularly functional form was analyzed by using HRP-biotin as a cargo (figure 2-35). High enzymatic HRP activities were measured in HeLa cells treated with complexes of 1 µM Tat13-ST or 1 µM R_9-ST with 2 µM HRP-biotin. In contrast, cells

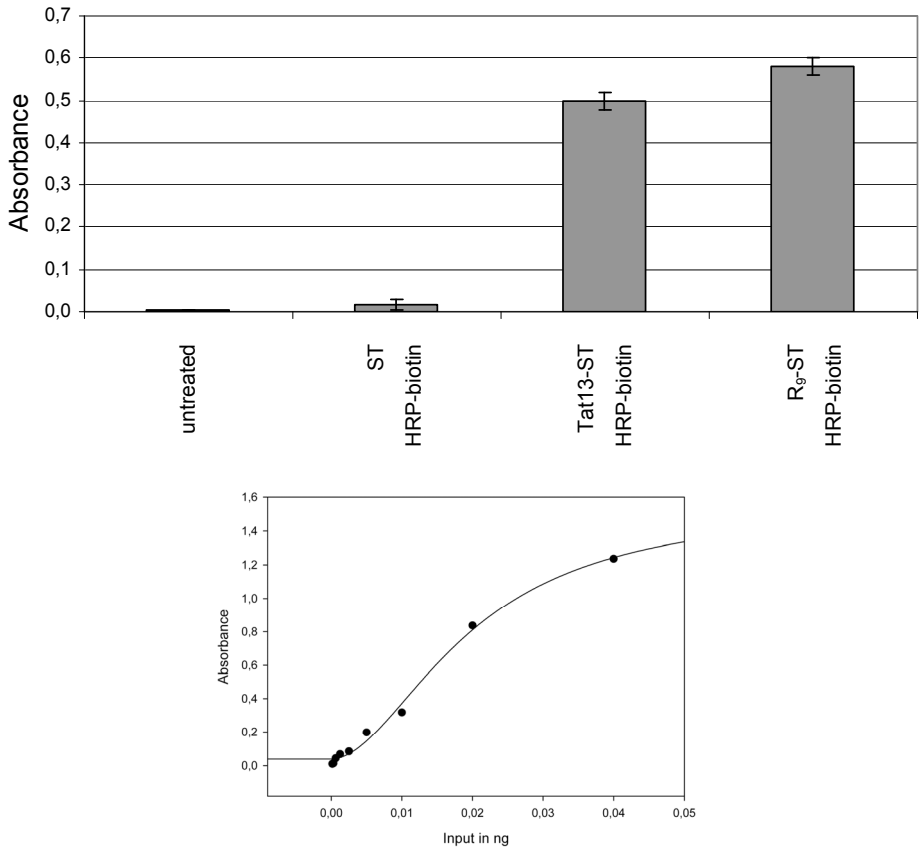

Figure 2-35. Internalization of HRP-biotin by Transtactins: Analyses of enzymatic HRP activities in HeLa cell lysates (upper panel). Calibration curve of HRP-biotin bound to ST (lower panel).

incubated with HRP-biotin alone or in a complex with ST (devoid of a PTD) showed no or only low background HRP activities. Regarding the theoretical maximum amount of internalized HRP, 0.22 % of HRP-biotin were successfully internalized by R_9-ST, which equaled 19 pmol/mg (table 2-9).

Transporter and cargo	Quantification
Tat13-ST HRP-biotin	(0.04 - 0.19) % (7.0 - 15) pmol/mg
R_9-ST HRP-biotin	(0.04 - 0.22) % (9.0 - 19) pmol/mg

Table 2-9. Quantification of the internalization of HRP-biotin by Transtactins.

INTERNALIZATION OF PROTEINACEOUS MULTICOMPONENT COMPLEXES AS MODELS FOR THERAPEUTIC PEPTIDES AND PROTEINS

Finally, it was tested whether Transtactins were able to deliver multicomponent complexes into intact cells. To this end, HeLa cells were incubated with 1 µM Transtactin proteins complexed with 1.5 µM His_6-*Strep*-tag II and 2 µM Ni-NTA-HRP. In this scenario, the Ni-NTA-HRP portion should be non-covalently linked to Transtactin via His_6-*Strep*-tag II and internalized concomitantly. Indeed, high enzymatic HRP activities were measured in lysates of cells treated with Tat13-ST and R_9-ST complexed with His_6-*Strep*-tag II and Ni-NTA-HRP (figure 2-36, upper panel). Untreated cells and cells incubated with a complex of ST (devoid of a PTD) with His_6-*Strep*-tag II and Ni-NTA-HRP showed no or only background HRP activities. Regarding the theoretical maximum amount of internalized Ni-NTA-HRP, 0.24 % of functional Ni-NTA-HRP were successfully internalized by R_9-ST which equaled 26 pmol/mg (table 2-10).

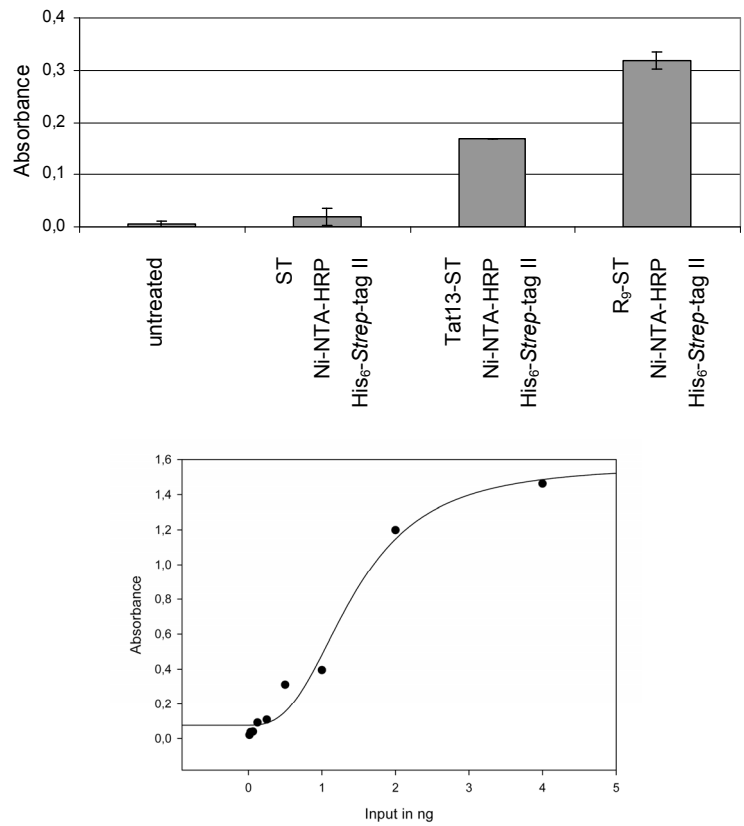

Figure 2-36. Internalization of Ni-NTA-HRP linked to Transtactins via a His_6-*Strep*-tag II peptide: Analyses of enzymatic HRP activities in HeLa cell lysates (upper panel). Calibration curve of Ni-NTA-HRP bound to ST via His_6-*Strep*-tag II (lower panel).

Transporter and cargo	Quantification
Tat13-ST His_6-*Strep*-tag II Ni-NTA-HRP	(0.06 - 0.15) % (14 - 23) pmol/mg
R_9-ST His_6-*Strep*-tag II Ni-NTA-HRP	(0.06 - 0.24) % (15 - 26) pmol/mg

Table 2-10. Quantification of the internalization of Ni-NTA-HRP by Transtactins.

Chapter 3
Discussion

Chapter 3: Discussion

3.1 TRANSMEMBRANE DELIVERY OF CARGOS

The efficient internalization of therapeutic agents through the plasma membrane remains a major hurdle for drug delivery. One way to achieve cell membrane permeability of cargos, such as therapeutic agents, is their genetic or biochemical fusion to PTDs (DIETZ and BAHR, 2004). PTDs can internalize covalently and non-covalently bound cargos (GROS *et al.*, 2006) in a non-cell-specific manner by a fluid-phase endocytotic mechanism (GUMP and DOWDY, 2007). Since their discovery in the late 1980s, a broad range of bioactive molecules has been successfully delivered into intact cells using PTDs (DIETZ and BAHR, 2004).

In this work, two novel transporter systems for the transmembrane delivery of non-covalently bound cargos were developed. The first model system was based on non-covalently bound PTD-fused ligands which were generated in order to deliver non-modified protein binders acting on intracellular targets. Specifically, SA was internalized by its weakly bound ligand *Strep*-tag II which itself was coupled to a Tat13 PTD. After internalization, the intracellular target biotin was sequestered by displacing Tat13-*Strep*-tag II in the SA binding pocket. For the second model system, cell permeable SA and ST derivatives, termed Transvidins and Transtactins, were developed as universal transporters for biotin- or *Strep*-tag II-linked compounds. Successfully internalized cargos included FITC-biotin and FITC-*Strep*-tag II as model compounds for cell-impermeable organics, HRP-biotin as a model protein cargo, and Ni-NTA-HRP bound to His_6-PEO_3-biotin or His_6-*Strep*-tag II as models for multicomponent proteinaceous complexes. The introduction of *Strep*-tag II-fused cargos revealed that a K_D of 1 µM was sufficient for Transtactin-mediated internalization. The introduced HRPs were enzymatically active, showing that both Transvidins and Transtactins allowed the internalization of functionally active proteins. Both transporter systems developed in this work may thus allow the circumvention of technical obstacles which are currently still associated with transmembrane delivery.

3.2 INTERNALIZATION OF NON-MODIFIED CARGOS

Unlike cell-permeable organics, many macromolecular agents with therapeutic potential cannot penetrate cellular membranes, due to their biophysical properties. This is especially true for peptides and proteins. Yet, compared to organics, therapeutic proteins possess several theoretical advantages, including increased target specificity (LEADER *et al.*, 2008). So far, therapeutic proteins have been almost exclusively used to target extracellular molecules, like tumor-specific cell-surface receptors. The development of transporter systems which may allow employing proteins as intracellularly active therapeutics is thus a topic of intense research efforts (TREHIN and MERKLE, 2004; GUMP and DOWDY, 2007). Notably, however, the genetic linkage of PTDs can result in both reduced expression and purification levels, as well as in altered biophysical properties of cargos (HONDA *et al.*, 2005).

Therefore, the first part of this work concentrated on the design of a transporter system for a non-modified cargo which is able to bind and sequester an intracellular target. SA was chosen as a model molecule to be internalized by the reversible interaction with *Strep*-tag II-fused PTDs.

INTERNALIZATION OF UNMODIFIED PROTEIN BINDERS BY PTD-FUSED LIGANDS AND SUBSEQUENT LIGAND-REPLACEMENT BY AN INTRACELLULAR TARGET

The components of this system consisted of (i) SA, a model protein binder containing a binding pocket for its intracellular target biotin, (ii) the PTD-fused ligand *Strep*-tag II, a cell-permeable transporter which more weakly interacts with the same pocket, and (iii) biotin, which should replace the PTD-*Strep*-tag II ligand at the intracellular level due to its higher binding affinity to SA. Both immunoblot and immunofluorescence analyses demonstrated that Tat13-*Strep*-tag II mediated the successful transmembrane delivery of non-covalently bound SA. Moreover, supplemented biotin, internalized by means of the mammalian multivitamin transporter (PRASAD and GANAPATHY, 2000), displaced the weakly bound Tat13-*Strep*-tag II as confirmed by an increased thermal tetramer stability of internalized SA. Thus, this system allows the internalization of a protein binder which then can be used to sequester a given intracellular target with higher binding affinity to the protein binder.

INTRACELLULAR DISTRIBUTION

The PTD-mediated uptake mechanism is currently a topic of lively discussion. In the case of cationic PTDs, like Tat13, it is most likely that the positively charged side chains interact with the anionic structure at the cell surface, thereby leading to an increased local concentration of PTDs. This subsequently allows entry by a fluid-phase endocytotic mechanism via endosomal compartments (BROOKS *et al.*, 2005). Consistent with this proposed mechanism, internalized SA was found in the present study either diffusively distributed in the cytoplasm or in a more punctuated pattern (ALBARRAN *et al.*, 2005; RINNE *et al.*, 2007). Similar distribution patterns were observed for SA or ST internalized by Tat13-PEO_3-biotin and for ST internalized by Tat13-*Strep*-tag II. The internalization of SA and ST by Tat13-fused ligands was found to be highly efficient since almost 100 % of the treated cells were positive for SA or ST. Similar efficiencies have been reported for the use of other PTDs (LEA *et al.*, 2003).

QUANTIFICATION OF THE INTERNALIZATION

The efficiency of internalization mediated by Tat13-fused *Strep*-tag II was quantified using functionally active HRP fused to SA. It was lower (~ 1 pmol per mg of total cellular protein) than the reported efficiency of the internalization of FITC-SA by Tat11-biotin (23 pmol/mg) (EL-ANDALOUSSI *et al.*, 2007). This lowered amount of internalization could be explained by the twofold increased MW of SA-HRP (~ 134 kDa) if compared to FITC-SA (~ 60 kDa) and by the law of mass action which describes the proportion of theoretically formed complexes. The increased uptake of SA-HRP by Tat13-PEO_3-biotin (~ 52 pmol/mg) compared to FITC-SA and Tat11-biotin (EL-ANDALOUSSI *et al.*, 2007) could be

explained by the increased incubation times and doses applied in the present study, and by the PEO_3 spacer between PTD and biotin which could increase the accessibility of the Tat13 PTD.

ADVANTAGES AND DISADVANTAGES

The delivery of cargos by the non-covalent binding of PTD-fused ligands has several theoretical advantages over the internalization of cargos which are covalently bound to PTDs. Notably, covalent linkage of a PTD can lead to reduced expression and purification yields and/or to impaired biophysical properties (HONDA *et al.*, 2005). The system developed in the present work avoids these potential obstacles since it allows the delivery of a non-modified cargo. Moreover, in contrast to previously designed transmembrane delivery systems, such as Tat11-SA (ALBARRAN *et al.*, 2005; RINNE *et al.*, 2007) or Tat11-fused protein A (MIE *et al.*, 2003; MIE *et al.*, 2006), the transporter employed here is less bulky since it only consists of low-MW components: a PTD and a small ligand. Finally, since the active site of the internalized cargo is reversibly occupied by the PTD-fused ligand, only molecules possessing a higher affinity to the cargo should be able to displace the ligand. Therefore, unwanted side-reactions could be reduced. A drawback of the system is the fact that PTD-fused ligands have to be newly designed for every cargo, which can be challenging, time-consuming, labor-intensive, and expensive.

FUTURE PERSPECTIVES

The findings in this study for non-modified SA indicate that - in principle - various engineered protein binders, such as anticalins (SCHLEHUBER and SKERRA, 2005; SKERRA, 2007) or peptide aptamers (HOPPE-SEYLER *et al.*, 2004; BORGHOUTS *et al.*, 2008), could be utilized for the intracellular sequestration of a given target molecule. These protein binders could be internalized by a PTD-fused molecule which was derived, for instance, from the intracellular target by chemical modification leading to reduced binding affinity. After PTD-mediated internalization, this weakly bound PTD-ligand should be displaced by the higher affinity intracellular target, as shown here for the replacement of PTD-*Strep*-tag II by biotin. In many cases, the sequestration of the target should ultimately lead to its functional inhibition, thereby providing a new strategy to specifically block the intracellular activities of pathologically relevant factors.

3.3 TRANSVIDIN AND TRANSTACTIN TRANSPORTERS

The second delivery system developed in this work was based on cell-permeable SA and ST derivatives that internalized biotin- and/or *Strep*-tag II-tagged cargos.

PRODUCTION OF CELL-PERMEABLE TRANSPORTERS

It is known that PTDs interact with cellular membranes and thereby can diminish the success of both the expression and purification of soluble PTD-fused proteins (HONDA *et al.*, 2005). The purification of Transvidins and Transtactins from harvested inclusion bodies seemed to prevent these common problems since high amounts - ranging from 10 mg to 80 mg per 1 L expression volume - were purified for all recombinant proteins in the present studies. Differences in the obtained amounts for individual purified proteins could be explained by varying expression levels and by different efficiencies of the refolding process. Notably, among the Transvidins and Transtactins, only Ant16-fused SA and ST could not be refolded and purified, in contrast to Ant7-fused SA/ST. Although not further explored here, it is likely that this differential biochemical behavior is due to activities of the additional N-terminal 9 amino acid sequence present in Ant16.

STABILITIES OF TRANSVIDINS AND TRANSTACTINS

Since covalent PTD linkage can change the biophysical properties of proteins (HONDA *et al.*, 2005), it was necessary to analyse possible alterations in the secondary structures of SA and ST upon fusion to the various PTDs. It was found that the fusion of Tat13, Ant7, R_9, and TLM12 only slightly altered the secondary structures of SA/ST, as determined by far-UV CD spectroscopy and subsequent PEPFIT analyses. This indicated that both cargos were extremely rigid protein scaffolds and can well tolerate different PTD fusions. Thermal unfolding using CD spectroscopy also revealed high thermal stabilities of Transvidins and Transtactins, similar to those of unfused SA and ST. This conformational stability is an essential requirement for the functionality of the transporters since the biotin- and *Strep*-tag II-binding properties must be retained. In-line with these spectroscopic results, it was found that all engineered Transvidin and Transtactin variants exhibited high thermal tetramer stabilities (up to at least 70 °C) which is similar to the published thermal tetramer stability of SA (BAYER *et al.*, 1996; WANER *et al.*, 2004; HUMBERT *et al.*, 2005). This tetramerization of SA and ST proteins (VOSS and SKERRA, 1997) is essential to correctly form the biotin- and *Strep*-tag II-binding pocket which lies in the interface between SA and ST subunits, respectively (SANO and CANTOR, 1995). Summed up, these results indicate that both Transvidins and Transtactins are conformationally stable within a wide temperature range, thereby retaining the binding capacities for their ligands. Under a more practical aspect, these findings also imply that no cooling at the bench or during storage and shipping is necessarily required to preserve the functionality of these transporters.

INTERNALIZATION AND INTRACELLULAR DISTRIBUTION OF TRANSVIDINS AND TRANSTACTINS

All Transvidin and Transtactin proteins - apart from TLM12-SA/ST - efficiently induced their own internalization into human cell lines which stemmed from epithelial (HeLa, SiHa) or connective tissues (U2- OS). This is in-line with previous reports showing that PTD-linked molecules can penetrate into a wide range of cell types derived from different histological backgrounds (DIETZ and BAHR, 2004). The internalization of Transvidins and Transtactins was highly efficient since almost 100 % of the treated

cells were SA/ST-positive. Titration experiments revealed that internalization of Tat13-SA/ST and R_9-SA/ST could be detected upon external applications of doses as low as 100 nM. Immunofluorescence analyses revealed that the internalized Transvidin and Transtactin transporters were found either diffusively distributed in the cytoplasm or in a more punctuated pattern, the latter most likely reflecting endosomal compartments, as previously described for other PTD-linked molecules (BROOKS *et al.*, 2005; RINNE *et al.*, 2007).

INTERNALIZATION OF CARGOS

Likewise, FITC-labeled biotin and *Strep*-tag II internalized by Tat13-SA/ST, Ant7-SA/ST, and R_9-SA/ST transporters co-stained with the fluid-phase endosomal marker TRITC-dextran, supporting the idea that the transporters enter cells via the endosomal route. In addition to FITC, serving as an example of a small organic compound, Transvidins and Transtactins were even able to internalize proteins (HRP-biotin) or proteinaceous complexes (His_6-PEO_3-biotin or His_6-*Strep*-tag II peptides complexed with Ni-NTA-HRP). This indicates that both transporter systems should be useful for a multitude of applications. Since internalization strongly depends on the properties of the cargo (TUNNEMANN *et al.*, 2006), one would expect that lower MW cargos will be favorably internalized by Transvidin and Transtactin transporters as opposed to larger compounds or multicomponent complexes. Notably, however, even bulky HRP cargos, with a total MW of up to 160 kDa, were internalized by Transvidin and Transtactin transporters. The internalization efficiencies depended on the transporter used, the cargo employed, and the doses employed for the treatment of the cells. Internalization for HRP ranged between 1.6 pmol and 26 pmol per mg protein which was within the same range as reported for Tat11-biotin-internalized FITC-SA (EL-ANDALOUSSI *et al.*, 2007). As previously reported for other PTD-fused cargos (MITCHELL *et al.*, 2000; FUTAKI *et al.*, 2001), the internalization efficiencies of individual Transvidins and Transtactins also increased with a rising number of positively charged residues within their PTD portions (Ant7 < Tat13 < R_9).

ADVANTAGES AND DISADVANTAGES

In general, the application of Transvidins and Transtactins is straightforward. Only a short incubation step of the transporter with the cargo in buffer conditions is necessary for complex formation. Then, the complex is injected into a serum- and biotin-free medium of cultured cells. Free biotin in the cell culture medium can be removed with avidin, a biotin-binding protein that does not interfere with *Strep*-tag II (SCHMIDT and SKERRA, 2007). No further treatment or expensive laboratory equipment is required for internalization.

Under functional aspects, the transmembrane delivery of cargos by Transvidins and Transtactins bears several advantages above the introduction of cargos which are directly linked to PTDs. For example, PTD-fused agents have been shown to penetrate intact skin (ROTHBARD *et al.*, 2000; JIN *et al.*, 2001; PARK *et al.*, 2002) which indicates that they could pose a health risk for experimentators working with potentially hazardous compounds. The fact that - for the use of Transvidins and Transtactins - the

transporter and the cargo can be produced separately should increase the bio-safety during preparation, since (i) SA and ST have no reported biological functions apart from their biotin-binding properties and (ii) the cargo cannot penetrate into cells without the transporter.

Furthermore, both Transvidins and Transtactins should possess advantages over existing cargo delivery systems: Firstly, up to four different cargos can be theoretically internalized simultaneously by using the homotetrameric Transvidins and Transtactins, in contrast to the previously described R_8-Ni-NTA transporter (FUTAKI *et al.*, 2004) which carries only one binding site for His_6-fused cargos. This distinction should allow Transvidins and Transtactins to co-transport pH-sensitive endosomal releasing polymers like PPAA (ALBARRAN *et al.*, 2005) or peptides like HA2 (WADIA *et al.*, 2004) to enhance cytoplasmic delivery (figure 3-1). To avoid cross-linking of the transporters in the case of dimeric or

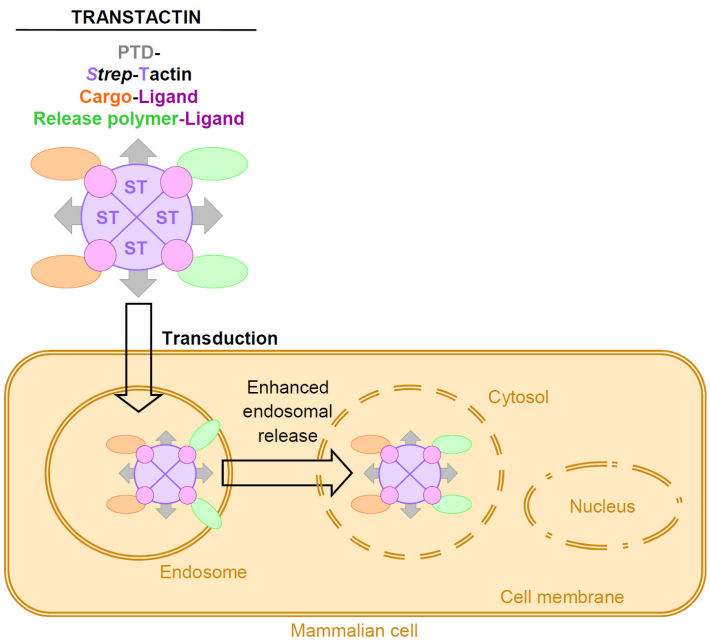

Figure 3-1. Enhanced endosomal release by pH-sensitive polymers: Loading of tetravalent Transtactin with both the cargo-ligand and a release polymer-ligand which should disrupt endosomal membranes and thereby further increases cytoplasmic delivery.

multimeric cargos, SA could be replaced by a monovalent SA derivative bearing only one biotin-binding site (HOWARTH *et al.*, 2006). Secondly, Transtactins possess advantages over Tat11-SA (ALBARRAN *et al.*, 2005; RINNE *et al.*, 2007) or Transvidin transporters. Specifically, the ST/*Strep*-tag II system has become very common for the purification of various cargos, since the *Strep*-tag II sequence can be easily fused to the N- or C-terminus of any kind of recombinant protein during subcloning and *Strep*-tag II-expression vectors are available for a broad variety of host organisms (SCHMIDT and SKERRA, 2007). Thus, no elaborate chemical linkage, as in the case of biotin, is necessary. Notably, biotinylation

may disturb cargo functions due to the chemical linkage, unlike *Strep*-tag II (SCHMIDT and SKERRA, 2007). In addition, biotinylation often requires spacer arms between biotin and the cargo to reduce steric hindrance. However, typical spacers used for biotinylation, such as a 6 carbon spacer (HNATOWICH *et al.*, 1987), can reduce the solubility of the cargo in aqueous media which is problematic for *in vivo* applications where organic solvents cannot be used. In contrast, *Strep*-tag II requires, if at all, only a short two-amino-acid spacer to ensure accessibility (SCHMIDT and SKERRA, 2007). Thirdly, in contrast to the PTD-fused protein A transporter developed before (MIE *et al.*, 2003; MIE *et al.*, 2006), no cargo-specific antibody as linker between the transporter and the cargo is required for the use of Transvidins and Transtactins.

TRANSVIDINS AND TRANSTACTINS: FUTURE PERSPECTIVES

Apart from biotinylated cargos or cargos bearing an SA-binding peptide (e.g. *Strep*-tag II), it is also conceivable to employ Transvidins and Transtactins in order to internalize alternatively tagged proteins. This could be achieved by employing suitable linkers, e.g. using Ni-NTA-biotin (O'SHANNESSY *et al.*, 1995; MCMAHAN and BURGESS, 1996; REICHEL *et al.*, 2007) or Ni-NTA-*Strep*-tag II for polyhistidine-tagged proteins (figure 3-2).

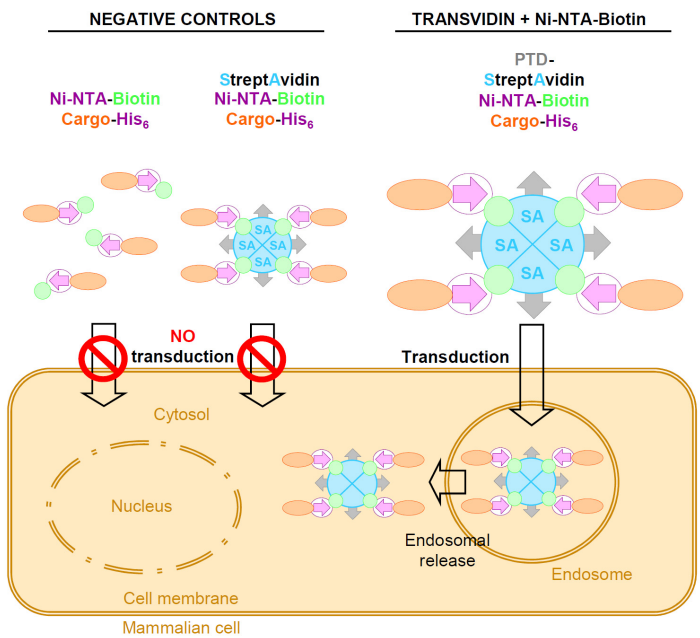

Figure 3-2. Model for the internalization of polyhistidine-fused cargos by Transvidin: His_6-fused cargos bind via Ni-NTA-biotin linkers to Transvidin transporters and are concomitantly internalized (right part of the panel). Similarly, the internalization of His_6-fused cargos by Transtactins via Ni-NTA-*Strep*-tag II or Ni-NTA-biotin linkers is also conceivable (not shown).

Apart from the described internalization of non-cell-permeable organics, peptides, proteins, and proteinaceous complexes, it also could be envisioned to use both transporters for the internalization of biotinylated nucleic-acid-based therapeutic agents, such as siRNAs (MEADE and DOWDY, 2007) or antisense molecules (WANG *et al.*, 2007).

The intracellular activity of a cargo internalized by Transvidin and Transtactin might be impaired by steric problems due to the transporter/ligand complex formation. However, as shown in the present work for Tat13-*Strep*-tag II and SA, it is possible to increase the release of a cargo by adding a higher affinity ligand, such as biotin. The same should be true for *Strep*-tag II-fused cargos internalized by Transtactins (figure 3-3). Furthermore, the usage of cleavable linkers possessing for instance a reducible disulfide bond (FEENER *et al.*, 1990) or an endosomal and/or cytosolic cleavage site (KELLER *et al.*, 2001) could as well increase the release of cargos in the cytoplasm after internalization by Transvidins and Transtactins.

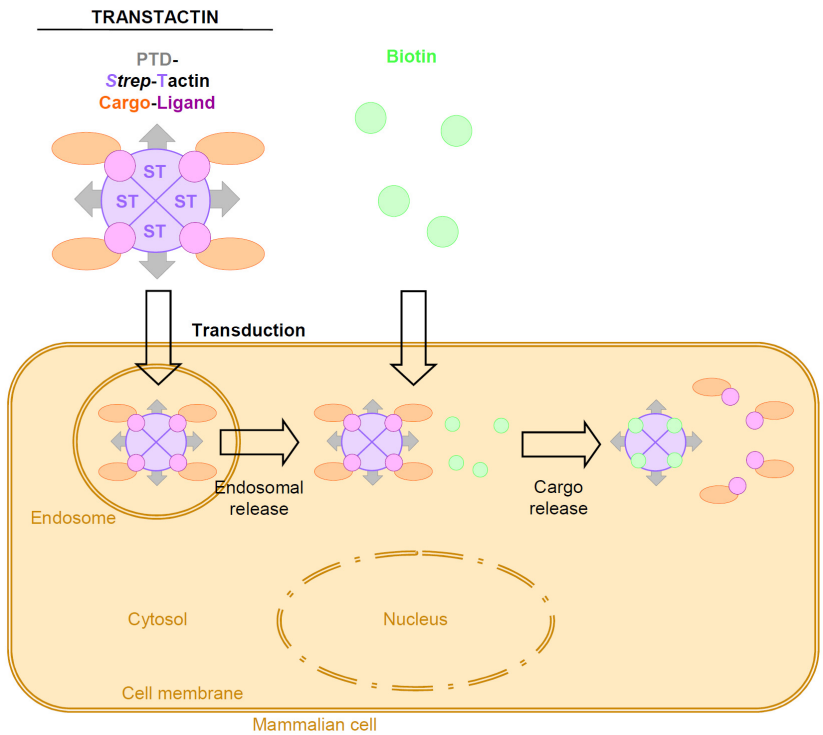

Figure 3-3. Internalization of *Strep*-tag II-fused cargos by Transtactin with subsequent cargo-release: *Strep*-tag II-fused cargos are displaced after the supplementation of biotin which is internalized by means of the mammalian multivitamin transporter.

In summary, Transvidins and Transtactins meet the requirements for universal delivery systems for biotinylated, *Strep*-tag II-, His_6-, or Ni-NTA-fused cargos. They thus fill the remaining gap between unspecific traditional transfection methods and cell-surface receptor-mediated endocytosis of ligand-fused cargos. Possible applications of Transvidins and Transtactins range from basic proteomics research to high-throughput testing of non-cell permeable intracellularly active diagnostics (SAWYER *et al.*, 2003; HONDA *et al.*, 2005) and therapeutic peptides (BORGHOUTS *et al.*, 2005; PRIVE and MELNICK, 2006) and proteins (COLAS, 2000; HOPPE-SEYLER *et al.*, 2004; BORGHOUTS *et al.*, 2008) like antibodies (ADAMS and WEINER, 2005), their fragments (HOLLIGER and HUDSON, 2005), and non-antibody-derived binders (BINZ *et al.*, 2005). Since PTDs penetrate the epidermis and dermis (ROTHBARD *et al.*, 2000; JIN *et al.*, 2001; PARK *et al.*, 2002), Transvidin and Transtactin transporters could also enable the transdermal delivery of concomitantly bound diagnostic and therapeutic agents upon *in vivo* topical applications.

3.4 THERAPEUTIC IMPLICATIONS

Both the transmembrane delivery of protein binders as well as the utilization of the Transvidin/Transtactin transporter systems should bear therapeutic potential. However, due to the proteinaceous nature of these molecules, this issue currently still faces many technical hurdles which are associated with protein therapeutics in general. These include proteolytic instability of PTDs (FUCHS and RAINES, 2005) and antigenicity of SA (BREITZ *et al.*, 2000). Possible solutions to reduce the potential antigenicity of Transvidins and Transtactins include site-directed mutagenesis of solvent-exposed side chains, as shown for SA (MEYER *et al.*, 2001), or replacement of SA/ST by non-immunogenic protein binders, like human-derived lipocalins (SKERRA, 2000; SCHLEHUBER and SKERRA, 2005), engineered to bind protein tags, such as *Strep*-tag II or His_6 (LAZAR, 2007).

For some therapeutic applications, the delivery of cargos into the cell nucleus will be required. Internalization into the cell nucleus could be realized by utilizing nuclear localization sequences (NLSs) (ESCRIOU *et al.*, 2003), such as the simian virus 40 (SV40) T large antigen NLS-sequence (CARTIER and RESZKA, 2002). The NLS could be inserted between the PTD and the SA/ST portion of Transvidin and Transtactin transporters with a prefixed cytosolic cleavage site (KELLER *et al.*, 2001) to release the PTD into the cytoplasm after successful transmembrane delivery.

Moreover, PTDs internalize cargos receptor-independently into a variety of mammalian and human cell types (DIETZ and BAHR, 2004). Due to this lack of cell specificity, PTDs are restricted to local or topical applications which could be a major drawback for clinical applications (VIVES *et al.*, 2008). Attempts have been made to target PTDs to certain cell types. For instance, Jiang *et al.* linked the R_9 PTD via a hairpin loop exhibiting a matrix metalloprotease cleavage site to its polyanionic counterpart through ionic interactions (JIANG *et al.*, 2004). Tumor cells that have overexpressed matrix metalloproteases at the cell surface can cleave the recognition site. This leads to the drift-away of the polyanionic counterpart.

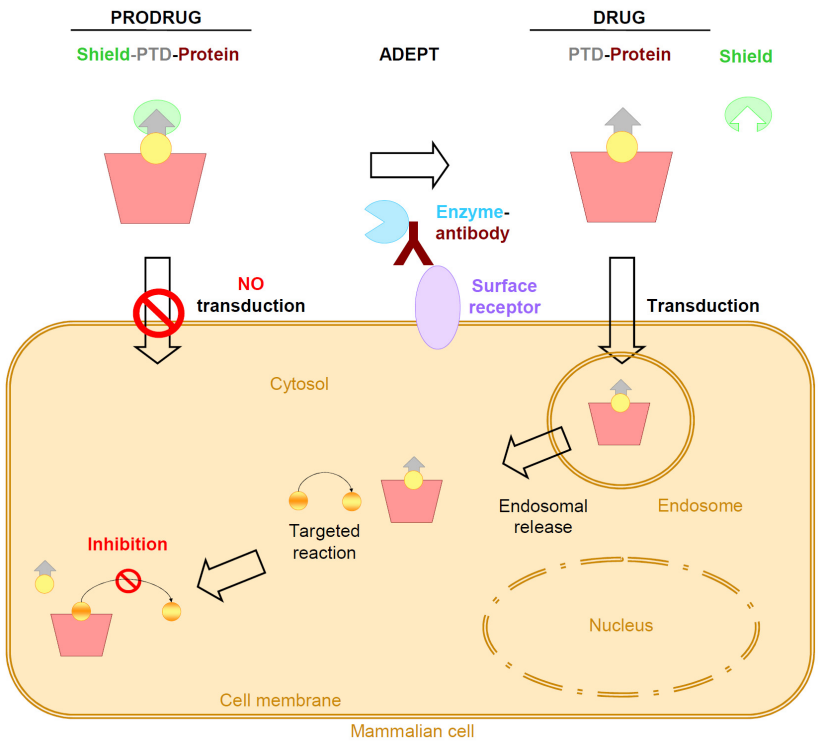

Figure 3-4. Targeted delivery of PTDs: The PTD is temporarily shielded (e.g. by an anionic counterpart) until cleavage by a protease. Specific proteases can be present on tumor cells or targeted to disease-related cell surface antigens via protein binders (e.g. antibodies): “ADEPT - antibody-directed enzyme prodrug therapy”.

The PTD is finally unshielded and mediates the local internalization of cargos. In a similar setting, cationic PTDs fused to ligands for the internalization of non-modified cargos (figure 3-4) or of the various Transvidin and Transtactin transporters could be shielded in a similar way for a cell-specific internalization of cargos.

Chapter 4
Materials and methods

Chapter 4: Materials and methods

4.1 MATERIALS

ESCHERICHIA COLI-K12-STRAINS

TG2	*E. coli supE hsd*Δ5 *thi* Δ(*lac-proAB*) Δ(*srl-recA*)306::Tn*10*(*tet*^{r}) (SAMBROOK and RUSSELL, 2001)
BL21(DE3)	*E. coli* B F$^-$ *dcm ompT hsdS*(r_B^- m_B^-) *gal* λ (DE3) (Stratagene, Heidelberg, Germany)

PLASMID

pET-21a	Novagen, Darmstadt, Germany

OLIGONUCLEOTIDES

MM-SA-ST-For	5′- G ACC GGT ACC TAC ATC GGT GCG AGG GGT AAC GCT GAA TC -3′
MM-SA-ST-Rev	5′- GA TTC AGC GTT ACC CCT CGC ACC GAT GTA GGT ACC GGT C -3′
MM-Ant16-For	5′- G GAA TTC CAT ATG CGC CAG ATT AAG ATT TGG TTC CAG AAC CGC CGC ATG AAG TGG AAG AAG GGT GCT GAA GCT GGT ATC ACC GGC ACC -3′
MM-Ant7-For	5′- G GAA TTC CAT ATG CGT CGT ATG AAG TGG AAG AAG GGT GCT GAA GCT GGT ATC ACC GGC ACC -3′
MM-Tat13-For	5′- G GAA TTC CAT ATG TAC GGA AGA AAG AAG CGC AGA CAA AGA AGA CGT CCA CCA GGT GCT GAA GCT GGT ATC ACC GGC ACC -3′
MM-R_{13}-For	5′- G GAA TTC CAT ATG AGA CGC AGA AGA CGC AGA AGA CGC AGA AGA AGA AGA AGA GGT GCT GAA GCT GGT ATC ACC GGC ACC -3′
MM-R_9-For	5′- G GAA TTC CAT ATG AGA CGC AGA AGA AGA AGA AGA CGC AGA GGT GCT GAA GCT GGT ATC ACC GGC ACC -3′
MM-TLM12-For	5′- G GAA TTC CAT ATG CCC TTA TCG TCA ATC TTC TCG AGG ATT GGG GAC CCT GGT GCT GAA GCT GGT ATC ACC GGC ACC -3′
MM-SA-Rev	5′- CGC AAG CTT TTA TTA GGA AGC AGC GG -3′

Underlined nucleotides denote mutations for amino acid substitutions or PTD sequence insertions. Oligonucleotides were supplied by the Oligonucleotide Synthesis Core Facility of the German Cancer

Research Center (Heidelberg, Germany) or by MWG Biotech (Ebersbach, Germany). All oligonucleotides were purified by reversed-phase (RP) high-performance liquid chromatography (HPLC) and solved in water.

PROTEINS AND ENZYMES

Benzonase	Merck, Darmstadt, Germany
Biotin-HRP	Pierce, Rockford, IL, USA
BSA	New England Biolabs, Schwalbach, Germany
CIAP	Fermentas, St. Leon-Roth, Germany
Cytochrom c	Bruker Daltonics, Bremen, Germany
Myoglobin	Bruker Daltonics
Ni-NTA-HRP	Qiagen, Hagen, Germany
PfuUltra polymerase, hotstart (2.5 U/µL)	Stratagene
Restrction endonucleases	New England Biolabs
	Fermentas
	Promega, Mannheim, Germany
SA-HRP	Pierce
ST-HRP	IBA, Göttingen, Germany
T4 DNA ligase (5 U/µL)	Fermentas
Taq DNA polymerase (5 U/µL)	Invitrogen, Karlsruhe, Germany
Ubiquitin	Bruker Daltonics

CHEMICALS

Molecular biology grade reagents and buffer components were used where possible. Otherwise the purest materials available were chosen.

Acetonitrile	Karl Roth, Karlsruhe, Germany
Acetic acid	Merck
Adenosine 5'-triphosphate	Gibco BRL, Eggenstein, Germany
Agar-agar	Karl Roth
Agarose	Sigma-Aldrich, Taufkirchen, Germany
Ammonium persulfate	Karl Roth
Ammonium sulfate	Karl Roth
Ampicillin	Sigma-Aldrich
β-Androsterone	Sigma-Aldrich
Biotin	Sigma-Aldrich
Bradford working solution	Amersham, Braunschweig, Germany
Bromphenol Blue	Sigma-Aldrich
1-Butanol	Applichem, Darmstadt, Germany
Cesium chloride	Applichem

Coomassie Blue R-250	Serva, Heidelberg, Germany
4',6-Diamidino-2-phenylindole dihydrochloride	Roche, Penzberg, Germany
Dulbecco's minimal essential medium	Gibco BRL
Dimethyl sulfoxide	Merck
Deoxynucleotide	Epicentre, Madison, USA
Dioxane	Sigma-Aldrich
Di-sodium hydrogen phosphate hexahydrate	Fluka, Buchs, Switzerland
Ethylenediaminetetraacetic acid	Acros Organics, Geel, Belgium
Ethanol	Riedel-de Haën, Hannover, Germany
Ethidium bromide	Sigma-Aldrich
Fetal bovine serum	Gibco BRL
FITC-biotin (Biotin-4-FITC)	Sigma-Aldrich
D(+)-Glucose	Applichem
L-Glutamine	Sigma-Aldrich
Glycerol	Gibco BRL
Glycine	GERBU, Gaiberg, Germany
Guanidine thiocyanate	Sigma-Aldrich
Hydrochloric acid	Fluka
Isopropyl β-D-1-thiogalactopyranoside	Applichem
2-Mercaptoethanol	Merck
Lithium chloride	Karl Roth
Magnesium chloride hexahydrate	Merck
Magnesium sulfate heptahydrate	Merck
Methanol	Fluka
Milk powder, non-fat dry	Saliter, Obergünzburg, Germany
Nonidet P-40	Fluka
Pefablock	Biomol, Hamburg, Germany
Penicillin-Streptomycin solution	Sigma-Aldrich
Polyacrylamide	Karl Roth
Poly(ethylene glycol) 8000	Sigma-Aldrich
Potassium acetate	Karl Roth
Potassium chloride	Acros Organics, Geel, Belgium
Potassium dihydrogen phosphate	Merck
2-Propanol	Sigma-Aldrich
Protease inhibitor cocktail P8340	Sigma-Aldrich
Reporter lysis buffer	Promega
Sodium acetate	Merck
Sodium chloride	Riedel-de Haën
Sodium dodecyl sulfate	Bio-Rad, Munich, Germany
Sodium deoxycholate	Sigma-Aldrich
Sodium hydroxide	Mallinchrodt Baker, Griesheim, Germany
Sucrose	Calbiochem
Sulfuric acid	Merck

Tetramethylen diamine	Sigma-Aldrich
3,3',5,5'-Tetramethylbenzidine	Pierce
Trifluoroacetic acid	Pierce
Tris(hydroxymethyl)-aminomethan	Sigma-Aldrich
Trypsin-EDTA	Gibco BRL
Tryptone	Difco, Augsburg, Germany
Tween-20	MP Biomedicals, Eschwege, Germany
Xylencyanol	Sigma-Aldrich
Yeast extract	Difco

KITS

Plasmid Mini, Midi Kit	Qiagen
QIAquick Gel Extraction Kit	Qiagen
QIAquick PCR Purification Kit	Qiagen
QuikChange II Site-Directed Mutagenesis Kit	Stratagene

MEDIA, ANTIBIOTICS AND GENERAL SOLUTIONS

MEDIA AND SOLUTIONS

All media and solutions for the work with bacteria, proteins, or DNA were autoclaved (20 min, 121 °C) or sterilized using 0.22 µm filters (Millipore, Billerica, MA, USA). All solutions were generated with double distilled water or with water for injection purposes (B. Braun, Melsungen, Germany) except for culture media which were assessed with desalted water. Buffers were pH adjusted utilizing a 761 Calimatic pH-Meter (Knick, Berlin, Germany). Culture plates were stored at 4 °C, all media and solutions, if not otherwise declared, at room temperature (RT).

ANTIBIOTICS

The following antibiotic stock solution was used:

1000x Ampicillin (Amp)
100 mg/mL in H_2O

The stock solution was sterilized by filtration through a 0.22 µm filter and stored in light-tight containers at - 20 °C.

MEDIA

Luria-Bertani (LB) media

10 g/L	Tryptone
5 g/L	Yeast extract
10 g/L	NaCl

LB-Agar

10 g/L	Tryptone
5 g/L	Yeast extract
10 g/L	NaCl
15 g/L	Agar-agar

The pH was adjusted to 7.0 with NaOH.

Transformation media

10 % (w/v)	PEG 8000
5 % (v/v)	DMSO
50 mM	$MgCl_2$
15 % (v/v)	Glycerol
	in LB media

LB-agar was autoclaved, gently swirled to distribute the melted agar and after cooling down to approximately 50 °C to 60 °C, Amp was added. Between 30 mL to 35 mL of media were poured directly from the flask into sterile 90 mm petri dishes (Greiner Bio-one, Frickenhausen, Germany).

PH BUFFERS

10x Phosphate-buffered saline (PBS)

1.37 M	NaCl
27 mM	KCl
43 mM	$Na_2HPO_4 * 7\ H_2O$
14 mM	KH_2PO_4

10x Tris EDTA (TE)

100 mM	Tris/HCl (pH 8.0)
10 mM	ETDA (pH 8.0)

The pH was adjusted to 7.4 with HCl.

INDUCTION SOLUTION

1000x IPTG

500 mM	IPTG in H_2O

4.2 MOLECULAR BIOLOGY METHODS

CULTIVATION AND CONSERVATION OF *E. COLI* STRAINS

E. coli-K12-strain TG2 was used as a general host for cloning, BL21(DE3) for large-scale protein expression of SA and its derivatives.

Single colonies were generated by plating transformed bacteria on LB-agar culture plates and incubation for approximately 14 hours at 37 °C. The selection of bacteria for plasmids was carried out by the addition of Amp to the medium. Colonies on the plates were checked for identical appearance, look, and smell like *E. coli*. Culture plates with bacterial colonies were stored at 4 °C and used for inoculation for up to four weeks. For large-scale protein expression, BL21(DE3) *E. coli* was freshly transformed every time.

Liquid cultures were set up in LB media containing Amp. For precultures, single colonies were picked using an inoculating loop and suspended in 5 mL or 50 mL LB media. Main cultures were inoculated with a stationary preculture at a ratio of 1:50. Incubation took place at 37 °C and 200 rpm in an SM-30 culture shaker (Edmund Buehler, Hechingen, Germany). Cell densities were determined by measuring the optical density (OD) at a wavelength of 550 nm (OD_{550}) in 1 cm plastic cuvettes (Greiner Bio-One) using a GeneQuant spectral photometer (GE Healthcare Biosciences, Munich, Germany).

For conservation of transformed *E. coli* strains, 0.5 mL of an over-night stationary culture were mixed with 0.5 mL of sterile glycerol and stored at - 80°C.

COMPETENT BACTERIA

Transformation-competent bacteria (HANAHAN, 1985; INOUE *et al.*, 1990) of *E. coli* strains TG2 and BL21(DE3) were prepared by utilizing magnesium-enriched transformation media. Bacterial cells were grown in 500 mL LB media until OD_{550} = 0.5. Cells were pelleted (4000 rpm, 4 °C, 10 min), re-suspended in 50 mL transformation media, and subsequently frozen in liquid nitrogen (N_2, Air Liquide, Düsseldorf, Germany). 200 µL aliquots were stored at - 80°C.

TRANSFORMATION OF BACTERIA WITH PLASMID DNA

Transformation of bacteria with plasmid DNA was performed according to the protocol of Hanahan (HANAHAN, 1983). 20 ng to 100 ng of DNA or 5 µL of freshly ligated plasmid DNA were incubated with 100 µL of competent bacteria. After incubation on ice for 30 min, bacteria were heat-shocked at 42 °C for 60 seconds, cooled on ice for 60 seconds, and supplemented with 900 µL LB media. Samples were incubated at 37 °C for 1 hour with vigorous shaking using a 1.5 mL thermomixer (Eppendorf, Wesseling-Berzdorf, Germany) and streaked on Amp-containing LB-agar plates.

GEL ELECTROPHORESIS OF DNA

Double-stranded DNA fragments were separated according to their size by horizontal agarose-gel electrophoresis. The DNA was visualized with the fluorescent dye EtBr which intercalates between the stacked bases of DNA (MANIATIS *et al.*, 1982). Gel electrophoresis was used for analytical restriction analysis, estimation of the quantity, and for the preparative isolation of fragments after restriction digest or amplification by PCR.

For analytical agarose gel-electrophoresis, 1 % (w/v) agraose gels were used. Agarose was dissolved in TAE buffer at the boiling heat. The molten gel was cooled to approximately 55 °C. After adding 0.5 µg/mL EtBr, the solution was poured into horizontal gel chambers (Peqlab, Erlangen, Germany). After cooling down, the gel was set into a TAE buffer-filled electrophoresis chamber (Peqlab). 1 µg to 2 µg DNA, supplemented with DNA loading buffer, were loaded per lane and electrophoresis was performed at a constant voltage of 90 V (Standard Power Pack P25, Biometra, Göttingen, Germany) for 1 hour. DNA fragments were visualized in the form of EtBr-intercalats at 312 nm using a UV transilluminator system (Konrad Benda, Wiesloch, Germany). Gels were documented using a Gel Jet Imager (INTAS, Göttingen, Germany).

For preparative gel electrophoresis, 1.2 % (w/v) agarose gels were poured as described above. Slots were loaded with up to 50 µL DNA solution. Electrophoresis took place at 70 V (Standard Power Pack P25) for approximately 90 min. Gel cubes were cut out and the DNA fragments were extracted from the agarose using the QIAquick Gel Extraction Kit according to the manufacturer's protocol.

TAE buffer		6x DNA loading buffer	
40 mM	Tris	0.25 % (w/v)	bromphenol blue
5 mM	sodium acetate	0.25 %(w/v)	xylencyanol
1 mM	EDTA (pH 8.0)	30 % (v/v)	glycerol

DEPHOSPHORYLATION OF DNA 5'-TERMINI

The 5'-terminal phosphates of linearized vectors were hydrolyzed with calf intestinal alkaline phosphatase (CIAP) in the supplied reaction buffer. Dephoshorylation was carried out in a final volume of 50 µL with 5 U of CIAP for 45 min at 37 °C.

CLEAVAGE OF DOUBLE-STRANDED DNA WITH RESTRICTION ENDONUCLEASES

Restriction endonucleases (REs) were utilized following the supplier's buffer guidelines. In brief, analytical restriction analysis was performed using approximately 1 µg of plasmid DNA in a final volume of 20 µL employing 2 µL of 10x appropriate reaction buffer, 2 µL of 10x BSA, and 0.5 µL of RE. The reaction was performed at an appropriate temperature for 60 min. REs were heat-inactivated or removed using the QIAquick PCR Purification Kit according to the manufacturer's protocol.

DNA LIGATION

Purified PCR-amplified fragments and digested fragments were subcloned into linearized, 5'-dephosphorylated plasmid vectors. Ligation of cohesive-end termini was performed by employing T4 DNA ligase. An amount of 50 ng to 100 ng of vector and a three-fold molar excess of insert were incubated with 2 U of T4 DNA ligase in ligation buffer in a final volume of 20 µL in a water bath (Julabo, Seelbach, Germany) at 20 °C for 2 hours or over-night at 16 °C.

ETHANOL-PRECIPITATION

Aqueous DNA solutions were supplemented with 1:10 volume 3 M sodium acetate (pH 5.2) and mixed with 2.5-fold volume of ice-cold 100 % ethanol. After incubation at - 20 °C for at least 60 min, the precipitated DNA was pelleted (13200 rpm, 4 °C, 15 min). The pellet was washed in 70 % ethanol and again pelleted (13200 rpm, 4 °C, 5 min). The pellet was air-dried and dissolved in the appropriate buffer. Alternatively, the DNA was purified using the QIAquick PCR Purification Kit according to the manufacturer's protocol.

SITE DIRECTED MUTAGENESIS

The ST expression vector, comprising the point mutations for the amino acid substitutions $E^{33}I$, $S^{34}G$, and $V^{36}R$ (numbering according to core *SA*), was PCR-amplified from the SA expression vector pSA1 by one-step PCR mutagenesis following the protocol and primer design guidelines of the QuikChange Site-directed Mutagenesis Kit manual. In brief, PCR reactions (table 4-1) were performed in 50 µL *PfuUltra*

Step	Cycles	Temperature [°C]	Time [s]
1	1	95	120
2	18	95	30
		55	60
		68	360
3	1	4	-

Table 4-1. Site-directed mutagenesis: Cycling parameters for the QuikChange site-directed mutagenesis method to generate ST expression vectors.

buffer with 50 ng of template, 30 pmol MM-SA-ST-For primer, 30 pmol MM-SA-ST-Rev primer, 1 mM dNTPs, and 0.5 µL of *PfuUltra* DNA polymerase (2.5 U/µL). Subsequently, 1 µL of *Dpn*I endonuclease was added, an enzyme specific for methylated DNA and suitable for selectively digesting the parental DNA template. After incubating for 1 hour at 37 °C and enzyme removal, 5 µL of the sample were used for transformation of *E. coli* TG2.

ONE-SIDED-OVERLAP-EXTENSION PCR

The *PTD-SA*/*ST* genes were generated by one-sided overlap extension PCR (table 4-2) using overhang

Step	Cycles	Temperature [°C]	Time [s]
1	1	94	120
2	20	94	30
		52	30
		68	60
3	1	68	300
4	1	4	-

Table 4-2. One-sided-overlap-extension PCR: Cycling parameters for the PCR to generate *PTD-SA/ST* genes.

primers containing PTD coding sequences in frame (MM-PTD-For) and the reverse primer MM-SA-Rev. PCR reactions were performed in 50 µL *Taq* buffer with 50 ng of pSA1 or pST1 expression vectors as templates, 30 pmol of each primer, 1 mM $MgSO_4$, 0.3 mM dNTPs, and 0.5 µL *Taq* DNA polymerase (5 U/µL). The resulting PCR products flanking *Nde*I and *Hin*dIII restriction sites were ligated into linearized pET-21a. 5 µL of the samples were used for transformation of *E. coli* TG2.

CLONING CONTROL AND SEQUENCING

Clones were controlled by analytical digestion and sequenced according to the chain termination method (SANGER *et al.*, 1977) using double-stranded circular plasmid DNA (CHEN and SEEBURG, 1985). DNA sequencing was performed by the German Cancer Research Center Sequencing Core Facility to confirm correct insertions or presence of mutations. Sequence alignments were generated using the online tools ALIGN or CLUSTALW (http://workbench.sdsc.edu). Nucleotide sequences were translated into their amino acid sequences using SIXFRAME (http://workbench.sdsc.edu).

EXPRESSION, DENATURATION, AND REFOLDING OF STREPTAVIDIN AND ITS DERIVATIVES

ST, PTD-SA, and PTD-ST proteins were expressed, denatured, and refolded as published for SA (SCHMIDT and SKERRA, 1994). In brief, a single colony of *E. coli* BL21(DE3) freshly transformed with expression vectors for SA or its derivatives was used for inoculating 50 mL LB media containing 100 µg/mL Amp. After incubation overnight at 37 °C, 20 mL of the pre-cultures were transferred to 1 L of the same medium. At an OD_{550} of 0.6, protein expression was induced by the addition of 0.5 mM IPTG and shaking was continued overnight. Cells were pelleted by centrifugation (GSA rotor, Thermo/Sorvall, 5000 rpm, 15 min, 4 °C) and resuspended in 25 mL ice-cold Tris-buffer A. After centrifugation (GSA rotor, 11500 rpm, 30 min, 4 °C), the cells were resuspended in 15 mL ice-cold Tris-buffer B and passed through an EmulsiFlex-C5 homogenizer (Avestin, Mannheim, Germany) according to the manufacturer's protocol until complete lysis. The homogenates were centrifuged (GSA rotor, 11500 rpm, 30 min, 4 °C) in order to sediment inclusion bodies. After washing with 10 mL ice-cold Tris-buffer B for 15 min, the inclusion bodies were dissolved in 8 mL 6 M guanidine/HCl (pH 1.5) in order to remove traces of biotin (SANO and CANTOR, 1990). Dissolved inclusion bodies were centrifuged at 15000 rpm at 4 °C for 15 min (SS34 rotor, Thermo/Sorvall). Refolding was then accomplished by rapid dilution into 250 mL PBS buffer at 4 °C. The mixtures were slowly stirred overnight at 4 °C and cleared by centrifugation (11500 rpm, 30 min, 4 °C).

Tris-buffer A		Tris-buffer B	
50 mM	Tris/HCl (pH 8.0)	50 mM	Tris/HCl (pH 8.0)
500 mM	sucrose	1 mM	EDTA

BACTERIAL WHOLE CELL EXTRACTS

1 mL of Benzonase buffer was supplemented with 12.5 U of Benzonase. 1 mL of culture was pelleted (13200 rpm, 1 min, 4 °C) and subsequently dissolved in 75 µL benzonase buffer. Cells were lysed by adding 25 µL 4x protein sample buffer. Nucleic acids were hydrolyzed with Benzonase during a 60 min incubation step at 4 °C. Whole bacterial cell extracts were stored at - 20 °C until SDS-PAGE. 20 µL of protein extract were loaded for a cell culture sample with an OD_{550} of 0.25. Accordingly, for a cell culture sample with an OD_{550} of *OD*, a protein extract volume of *V* was loaded on SDS-polyacrylamide gels according to equation (1).

$$V = \frac{20 \cdot 0.25}{OD} \text{ [µL]} \qquad (1)$$

4x Protein sample buffer		Benzonase buffer	
0.47 M	Tris/HCl (pH 6.7)	100 mM	Tris/HCl (pH 8.0)
2 % (w/v)	SDS	5 mM	$MgCl_2$
16 % (v/v)	glyerole		
6 % (v/v)	2-mercaptoethanol		
0.4 % (w/v)	Bromphenol Blue		

AMMONIUM SULFATE PRECIPITATION

Refolded proteins were purified by fractionated ammonium sulfate precipitation as described for SA (SCHMIDT and SKERRA, 1994). Solid ammonium sulfate was slowly added to protein solutions in the cold to a saturation of 40 % (62.7 g). After slow stirring overnight at 4 °C, the precipitated contaminating proteins and monomeric, incompletely refolded SA/ST and PTD-SA/ST proteins, respectively, were removed by centrifugation (GSA rotor, 11500 rpm, 30 min, 4 °C). Then, the ammonium sulfate saturation was raised to 70 % by adding 59 g. After incubation at 4 °C for 4 hours, tetrameric SA/ST and PTD-SA/ST proteins were recovered (GSA rotor, 11500 rpm, 60 min, 4 °C) and resuspended in 9 mL of PBS-buffered 2.2 M ammonium sulfate solution for removal of residual impurities which became soluble under these conditions. After centrifugation (SS34 rotor, 15000 rpm, 30 min, 4 °C), the recombinant proteins were dissolved in 8 mL PBS buffer. The solutions were finally cleared by centrifugation (15000 rpm, 30 min, 4 °C). The protein concentrations were adjusted to 1 mg/mL. After sterile filtration using a 0.22 µm filter (Millipore), 1 mL aliquots were stored at - 80 °C. Recombinant proteins were quality-controlled by SDS-PAGE, MALDI-TOF MS, Edman-sequencing, and far-UV CD spectroscopy.

PBS-buffered ammonium sulfate solution

2.2 M ammonium sulfate
in 1x PBS

DETERMINATION OF PROTEIN CONCENTRATIONS

The concentration of purified proteins was determined by measuring the absorption at 280 nm (A_{280}) according to the law of Lambert-Beer where *c* denoted the protein concentration and *d* the path length:

$$A_{280} = \varepsilon \cdot c \cdot d \qquad (2)$$

The extinction coefficients ε were determined by means of the program ProtParam (www.expasy.org) and are summarized in table 4-3. Protein concentrations were measured with a NanoDrop ND-1000 UV-Vis spectrophotometer (Thermo).

Protein	MW [Da]	ε [$M^{-1}cm^{-1}$]	Number of amino acids
SA	13271.4	41940	127
Ant16-SA	15688.4	52940	145
Ant7-SA	14473.9	47440	136
R_{13}-SA	15490.1	41940	142
R_9-SA	14865.3	41940	138
Tat13-SA	15195.7	43430	142
TLM12-SA	14598.9	41940	140
ST	13282.5	41940	127
Ant16-ST	15699.4	52940	145
Ant7-ST	14485.0	47440	136
R_{13}-ST	15501.1	41940	142
R_9-ST	14876.4	41940	138
Tat13-ST	15206.8	43430	142
TLM12-ST	14610.0	41940	140

Table 4-3. Theoretical protein parameters: MWs, εs, and number of amino acids for all recombinant proteins were determined by using the online tool ProtParam at the ExPASy website.

PEPTIDE SYNTHESIS

Apart from *Strep*-tag II (IBA), all peptides (table 4-4) were chemically synthesized at the Peptide Synthesis Core Facility of the German Cancer Research Center (Heidelberg, Germany) using Fmoc

Peptide	Sequence
Strep-tag	SAWRHPQFGG
Strep-tag II	WSHPQFEK
FITC-*Strep*-tag II	FITC-WSHPQFEK
His_6-*Strep*-tag II	HHHHHHSAWSHPQFEK
His_6-PEO_3-biotin	HHHHHH-PEO_3-biotin
Tat13-PEO_3-biotin	YGRKKRRQRRRPPG-PEO_3-biotin
Tat13-*Strep*-tag II	YGRKKRRQRRRPPGSAWSHPQFEK

Table 4-4. Peptide syntheses: Sequences of synthetic peptides, given as single-letter amino acids code

(N-(9-fluorenyl)methoxycarbonyl) chemistry. Crude peptides were purified by employing C_{18} RP-HPLC and further analyzed by electrospray ionization mass spectrometry (ESI-MS). Measured mol peaks were checked for consistency with the expected value. 25 mM peptide stocks in DMSO were stored at - 80 °C and freshly diluted in H_2O.

PREPARATION OF PROTEIN COMPLEXES

SA/ST and SA/ST-HRP proteins in PBS were complexed with Tat13-fused *Strep*-tag II or biotin by incubation for 15 min at RT. PTD-SA/ST proteins in PBS were complexed with *Strep*-tag II- or biotin-fused cargo molecules under identical conditions. The complexes were directly injected into FBS-free DMEM media of cultured cells.

SODIUM DODECYL SULFATE POLYACRYLAMIDE ELECTROPHORESIS

Protein extracts and purified proteins were separated according to their electrophoretic mobility by SDS-PAGE. Samples were mixed with 4x protein sample buffer, boiled at 95 °C for 5 min, and loaded into slots of small precast vertical slab gel units (Gibco BRL). Two 15 % separation gels were composed of 5 mL of 30 % (w/v) polyacrylamide, 1.2 mL of separation gel buffer, 3.6 mL of H_2O, 100 µL of 10 % (w/v) SDS, 100 µL of 10 % (w/v) APS, and 5 µL of TEMED. Two 5 % stacking gels were composed of 830 µL of 30 % (w/v) polyacrylamide, 620 µL of stacking gel buffer, 3.47 mL H_2O, 50 µL of 10 % (w/v) SDS, 50 µL of 10 % (w/v) APS, and 5 µL of TEMED. Electrophoresis was performed at a constant voltage of 65 V (Standard Power Pack P25) for approximately 90 min in running buffer. Gels were stained with Coomassie Blue solution and destained with destaining buffer. Gels were stored in storage buffer, photographed using a Gel Jet Imager (INTAS), and finally dried on 3 mm Whatman filters paper (Schleicher & Schuell, Dassel, Germany) using a model 583 gel dryer (Bio-Rad, Munich, Germany).

Storage solution

7 % (v/v)	acetic acid
2 % (v/v)	glycerol

Staining solution

0.25 % (w/v)	Coomassie Blue R-250
40 % (v/v)	methanol
10 % (v/v)	acetic acid

De-staining solution

40 % (v/v)	methanol
10 % (v/v)	acetic acid

Separation gel buffer

3 M	Tris/HCl (pH 8.8)
0.4 % (w/v)	SDS

Stacking gel buffer

0.47 M	Tris/HCl (pH 6.7)

Running buffer

25 mM	Tris/HCl (pH 8.6)
192 mM	glycine
0.1 % (w/v)	SDS

4.3 BIOPHYSICAL METHODS

MALDI-TOF MASS SPECTROMETRY

MS is an analytical technique which can be used for the determination of the MWs of proteins. Protein samples were desalted using C4 ZipTip pipette tips (Millipore). Briefly, ZipTips were prewashed with 0.1 % TFA / 50 % acetonitrile and equilibrated with 0.1 % TFA by repetitive pipetting steps. After loading of the protein samples, ZipTips were washed three times with 0.1 % TFA to remove salts. For MALDI-TOF MS, 0.3 µL of a saturated solution of sinapinic acid in ethanol were deposited as thin film onto individual spots of a MALDI target plate. Subsequently, proteins were eluted from the ZipTips with 1 µL to 2 µL of a saturated solution of sinapinic acid in 0.1 % TFA / 50 % acetonitrile, directly loaded on top of the thin film spots and allowed to co-crystallize slowly at ambient temperature. MALDI mass spectra were recorded in the positive ion linear mode with delayed extraction on a Reflex II TOF instrument (Bruker-Daltonik) equipped with a SCOUT-26 probe and a 337 nm nitrogen laser. Ion acceleration voltage was set to 20.0 kV and the first extraction plate to 17.1 kV. Mass spectra were obtained by averaging up to 200 individual laser shots. Spectra were calibrated externally by a quadratic fit using the singly protonated average masses of ubiquitin I at m/z 8565.89, cytochrom c at m/z 12361.55, and myoglobin at m/z 16952.55. MH^+(av) values were calculated using the online tool ProteinProspector v 4.27.1 (http://prospector.ucsf.edu/).

EDMAN-SEQUENCING

N-terminal amino acid sequence analyses were performed by Edman-sequencing (GRANT *et al.*, 1997). Aliquots of protein samples were spotted on TFA-treated filters (Applied Biosystems, Darmstadt, Germany), dried under N_2 stream and introduced into a cartridge of an ABI Procise 494 Sequencer (Applied Biosystems) followed by N-terminal Edman sequencing performed with a pulsed-liquid program.

THERMAL TETRAMER STABILITY

3 µg of purified SA protein or its derivatives without or with a 2-fold molar excess of biotin, *Strep*-tag, or *Strep*-tag II were combined with SDS-containing sample buffer and heated at selected temperatures for 5 min, then chilled on ice until SDS-PAGE. Gels were stained with Coomassie Blue solution and de-stained with destaining buffer as described.

CIRCULAR DICHROISM SPECTROSCOPY

CD relies on the differential absorption of left and right circularly polarised radiation by chromophores which either possess intrinsic chirality or are placed in chiral environments. Proteins possess a number of chromophores which can give rise to CD signals (KELLY and PRICE, 2000). In the far-UV region (180 nm to 240 nm), which corresponds to peptide bond absorption, the CD spectrum can be analyzed

to determine the fractions of the secondary structure. CD spectroscopy was carried out using a J-710 spectropolarimeter (JASCO, Gross-Umstadt, Germany) calibrated with a solution of 0.05 % β-androsterone dissolved in dioxane. Sample temperature control during measurement was achieved by using a JASCO PFD-350S peltier thermostat. Samples at a concentration of ~ 100 μg/mL protein in distilled water were scanned in a 1 mm quartz cuvette from 190 nm to 240 nm for secondary structure determination. CD spectra were subtracted from identically scanned and signal-averaged solvent baselines. Final spectra were the result of four-fold signal averaging. CD spectra were normalized for the mean residue weight (MRW) according to equation (3).

$$\Theta_{MRW} = \frac{\Theta_{obs} \cdot M_R}{10 \cdot c \cdot d \cdot N_A} \quad [\deg\, cm^2\ dmol^{-1}] \qquad (3)$$

Θ_{MRW} denoted the molar ellipticity, Θ_{obs} the measured ellipticity, M_R the molecular mass of the protein, c the protein concentration, d the path length of the quartz cuvette, and N_A the number of the amino acids. Spectra were finally plotted with Kaleidagraph (Synergy Software, Reading, PA, USA).

Secondary structure contents were calculated from the far-UV CD spectra. After their conversion to mean residue ellipticity (Θ_{MRW}) and removal of residual noise, the program PEPFIT (a Fast Fourier Transform program specifically designed for the secondary structure analysis of peptides rather than globular proteins) (REED and REED, 1997) was employed for the fitting of the processed spectra.

To determine differences in the thermal stabilities between SA and its derivatives, thermal denaturation spectra were run from 40 °C to 95 °C at a gradient of 1.0 °C per min. It was paid attention to the fact that all relevant parameters were identical for all protein samples measured since such properties as the T_m are not absolute and vary with measurement conditions. Due to the unusual spectral characteristics of SA and its related proteins, the observational wavelength for temperature denaturation was chosen to be 215 nm rather than the standard 222 nm. Raw data were fit by nonlinear regression to an equation for a two-state transition using Kaleidagraph according to equation (4) (BRUMANO *et al.*, 2000).

$$y_{obs} = \frac{\left(m_N \cdot T + b_N\right) + \left(m_U \cdot T + b_U\right)\left\{\exp\left[\frac{\Delta H_m}{R}\left(\frac{1}{T_m} - \frac{1}{T}\right)\right]\right\}}{1 + \exp\left[\frac{\Delta H_m}{R}\left(\frac{1}{T_m} - \frac{1}{T}\right)\right]} \quad [m\deg] \qquad (4)$$

y_{obs} denoted the ellipticity, T was the temperature, R was the gas constant, T_m was the transition temperature, and ΔH_m was the enthalpy of unfolding at T_m (van't Hoff enthalpy). b_N and b_U referred to the y intercepts of the native and unfolded baselines, respectively, while m_N and m_U were the slopes of the baselines. To compare the transitions, each unfolding curve was normalized to the apparent fraction of the unfolded form $f(u)$ according to equation (5) (BRUMANO *et al.*, 2000).

$$f(u) = \frac{\exp\left[\frac{\Delta H_m}{R}\left(\frac{1}{T_m} - \frac{1}{T}\right)\right]}{1 + \exp\left[\frac{\Delta H_m}{R}\left(\frac{1}{T_m} - \frac{1}{T}\right)\right]} \quad (5)$$

4.4 CYTOLOGY METHODS

CELL CULTURES

Human cell lines (table 4-5) were maintained in Dulbecco's minimal essential medium (DMEM), supplemented with 10 % fetal bovine serum (FBS), 1 % Penicillin-Streptomycin sulfate solution and

Cell line	Description	Reference
HeLa	HPV18 cervix epithelial adenocarcinoma	ATCC CCL-2
SiHa	HPV16 cervix squamous cell carcinoma	ATCC HTB-35
U-2 OS	osteosarcoma	ATCC HTB-96

Table 4-5. Human cell lines: Overview of human cell lines and their tissue origin. ATCC (American Type Cell Culture Collection, Rockville, MD, USA) catalogue numbers are given.

1 % of 200 mM L-glutamine solution at 37 °C in 5 % CO_2 atmosphere. For routine passage, cells reaching confluence were split in ratios between 1:5 and 1:20, generally every 3 days, employing trypsin-EDTA solution.

WHOLE CELL EXTRACTS

The cells were washed and re-suspended by trypsination. After threefold washing with PBS, cells were lysed with RIPA buffer supplemented with 1 % P8340 protease inhibitor cocktail and 4 % Pefablock. After 30 min on ice, cell extracts were centrifuged (13200 rpm, 4 °C, 5 min) and the supernatants were collected. Protein extracts were stored at - 80 °C.

RIPA buffer

10 mM	Tris/HCl (pH 7.5)
150 mM	NaCl
1 mM	EDTA
1 % (v/v)	Nonidet P-40
0.5 % (w/v)	sodium deoxycholate
0.1 % (w/v)	SDS

BRADFORD ASSAY AND SAMPLE PREPARATION

Protein concentrations in cell extracts were estimated by the method of Bradford (BRADFORD, 1976). 1 µL of the supernatant was added to 999 µL of Bradford working solution (1:5 dilution of Bio-Rad

reagent in water, Bio-Rad), mixed, and incubated for 2 min. Subsequently, absorbance of the solution at 595 nm was measured with a spectrophotometer (GeneQuant). Absorbance values were converted into protein concentrations on the basis of a BSA calibration curve. Cell extracts were adjusted to a protein concentration of 3 µg/µL by adding appropriate volumes of RIPA buffer and 4x protein sample buffer. Samples were stored at - 80 °C for further analysis.

WESTERN BLOTS

HeLa, SiHa, and U-2 OS cells were plated on 35 mm or 60 mm dishes (Greiner Bio-one) at 60 % to 90 % confluence. Proteins and complexes (tables 4-6 and 4-7) were directly injected into FBS-free media of cultured cells. After a 120 min incubation at 37 °C, 5 % CO_2, the cells were washed, trypsinized, harvested, and lysed. Proteins separated by SDS-PAGE were transferred into a semi-dry blotter system (cti, Idstein, Germany) to 0.45 µm Immobilon-P (polyvinylidene fluoride, PVDF) membranes (Millipore). In brief, membranes were washed in methanol and subsequently equilibrated in

Transporter	Concentration [µM]	Cargo	Concentration [µM]	Ligand	Concentration [µM]
Tat13-ligand	10	SA	20	Biotin	40
Tat13-SA	10	-	-	Biotin	40

Table 4-6. Ligand replacement: PTD-fused ligands: biotin or *Strep*-tag II

Transporter	Concentration [µM]
PTD-SA	1
PTD-ST	1

Table 4-7. Internalization of PTD-SA/ST transporters

EMBL buffer together with the gel and Whatman filters. The gel was placed at the cathode side of the membrane and embedded between Whatman filters. Protein transfer was performed at a current flow of 2.24 mA per cm^2 gel area (Standard Power Pack P25) for 60 min.

EMBL buffer

40 mM	Tris/HCl (pH 9.2)
39 mM	glycine
1.3 mM	SDS
20 % (v/v)	methanol

Blocking buffer

0.2 % (v/v)	Tween 20
5 % (w/v)	non-fat dry milk
	in 1x PBS

Washing buffer

0.2 % (v/v)	Tween 20
	in 1x PBS

ENZYME-LINKED IMMUNODETECTION OF PROTEINS ON WESTERN BLOTS

For immunodetection of proteins, membranes were blocked overnight at 4 °C in blocking buffer and consecutively incubated with the primary antibody (table 4-8) and the appropriate secondary antibody conjugated with HRP (table 4-9) to allow detection by enhanced chemiluminescence (ECL). Incubation steps were intermitted by rinsing in blocking buffer and washing buffer. Immunoprinted and washed

Primary antibodies	Specification	Manufacturer
anti-SA (1:2000)	rabbit polyclonal antibody	Sigma-Aldrich
anti-Tubulin (1:5000)	mouse monoclonal antibody DM1A, CP06	Calbiochem
anti-Actin (1:100000)	mouse monoclonal antibody, AC74	Sigma-Aldrich

Table 4-8. Primary antibodies: List of primary antibodies used for enzyme-linked immunodetection on Western blots

Secondary antibodies	Manufacturer
goat anti-mouse, HRP-conjugate (1:3000)	Promega
goat anti-rabbit, HRP-conjugate (1:3000)	Promega

Table 4-9. Secondary antibodies: List of secondary antibodies used for immunodetection of proteins by ECL

membranes were incubated with a freshly prepared 1:1 mixture of detection reagent 1 and 2 (Amersham) for 1 min and wrapped in cling film. Luminescent light signals were detected by Kodak Biomax MR photographic films (Eastman Kodak, Stuttgart, Germany), which were processed in an Optimax TR X-ray film processor (Protec, Oberstenfeld, Germany).

IMMUNOFLUORESCENCE

HeLa, SiHa, and U-2 OS cells were plated on 35 mm dishes at 40 % to 60 % confluence. Complexes were prepared according to table 4-10 and directly injected into FBS-free media. Endosomes were

Transporter	Concentration [µM]	Cargo	Concentration [µM]
Tat13-ligand	10	SA	10
Tat13-ligand	10	ST	10
Transvidin	10	-	-
Transtactin	10	-	-
Transvidin	10	FITC-ligand	10
Transtactin	10	FITC-ligand	10

Table 4-10. Compilation of the complexes used for immunofluorescence analyses: Ligands: biotin or *Strep*-tag II.

visualized with the fluid-phase marker TRITC-dextran, as described (RINNE *et al.*, 2007). After a 120 min incubation at 37 °C, 5 % CO_2, the cells were washed, trypsinized, and plated on glass cover-slips. After approximately 4 hours, cover-slips were washed with PBS, subsequently fixed with 4 % PFA for 30 to 60 min, washed twice with PBS, and finally stored in 70 % ethanol at - 20 °C until further analysis. For immunofluorescence studies, cover-slips were consecutively incubated at room temperature in a wet incubation chamber with blocking buffer, first antibody dilution (table 4-11), and

second antibody dilution (table 4-12) in PBS, the latter supplemented with DAPI (Roche). Incubation steps were intermitted by washing steps using PBS. For co-localization studies, cover-slips were incubated with DAPI in PBS only. Finally, cover-slips were washed in ethanol, dried, and embedded in

Primary antibody	Specification	Manufacturer
anti-SA (1:500)	rabbit polyclonal antibody against SA	Sigma-Aldrich

Table 4-11. Primary antibody: anti-SA antibody used for immunofluorescence

Secondary antibody	Manufacturer
goat anti-rabbit, Cy3-conjugate (1:400)	Dianova, Hamburg, Germany

Table 4-12. Secondary antibody: Cy3-labeled secondary antibody used for immunofluorescence

VectaShield H-1000 mounting medium (Vector Laboratories, Burlingame, CA USA). Cy3-, FITC-, and TRITC-signals were detected using a Vanox-T AH-2 epifluorescence microscope (Olympus, Hamburg, Germany). Pictures were captured with an F-View camera and analyzed with analySIS^B software (both Soft Imaging System, Olympus).

Blocking buffer

1 % (w/v) BSA
2 % (v/v) FBS
In 1x PBS

First antibody dilution

1 % (w/v) BSA
In 1x PBS

HORSERADISH PEROXIDISE ACTIVITY ASSAY

HeLa cells were plated on 35 mm dishes at 60 % to 90 % confluence. Complexes were prepared according to table 4-13 and directly injected into FBS-free media. Cells were incubated at 37 °C, 5 % CO_2 for 2 hours, then trypsinized, washed with 1x PBS, and lysed with 400 µL 1x RLB (ALBARRAN *et al.*, 2005). Cell lysates were incubated at room temperature for 15 min. After vortexing and pelleting, the supernatants were stored at - 80 °C. 40 µL of the diluted extracts were mixed with 10 µL 1x RLB. At the same time, HRP calibration curves were generated using a series of dilutions of SA/ST-HRP (2 mols HRP per SA tetramer, MW ~ 134 kDa) or SA/ST complexed with linker peptides and Ni-NTA-HRP or HRP-biotin. 10 µL of the proteins or complexes at different dilutions, ranging from 1:2500 to 1:64000000, were mixed with 40 µL of dilutions of untreated HeLa lysates. Colorimetric reactions were initiated by adding 50 µL of 1-Strep Ultra TMB-ELISA substrate solution (Pierce). The reaction was stopped at individual points of time by adding 50 µL of 2 M sulfuric acid and the absorbance was measured at 450 nm (Multiskan fx ELISA reader, Thermo).

Transporter	Concentration [µM]	Cargo	Concentration [µM]
Tat13-ligand	1	SA-HRP	2
Tat13-ligand	1	ST-HRP	2
Transvidin	0.2	HRP-biotin	0.4
Transtactin	1	HRP-biotin	2
Transvidin	0.2	His_6-PEO_3-biotin Ni-NTA-HRP	0.3 0.4
Transtactin	1	His_6-*Strep*-tag II Ni-NTA-HRP	1.5 2

Table 4-13. Compilation of the complexes used for quantification of the PTD-mediated internalization: Ligand: biotin or *Strep*-tag II

Calibration curves of HRP were fitted using the four parameter logistic (4PL) equation in SigmaPlot 10.0 (Systat Software, Erkrath, Germany):

$$A = \min + \frac{(\max - \min)}{1 + \frac{I}{(EC50)^H}} \tag{6}$$

A denoted the absorbance, *I* was the input in ng, *max* and *min* denoted the top and bottom of the curve, *H* was the hillslope and characterized the slope of the curve at its midpoint, and *EC50* was the median effective concentration.

The determined absorbance was recalculated to the amount of PTD-mediated internalized HRP using equation (6). Finally, the efficiencies ($Q_{1/2}$) of PTD-mediated internalization of at least two independent experiments were calculated, firstly, with respect to the theoretical maximum amount of internalized HRP ($HRP_{deployed}$), which equaled the molarity of the transporter (without application of the law of mass action), using equation (7) and, secondly, with respect to both the actual amount of internalized functional HRP and normalized to the amount of total protein using equation (8) (EL-ANDALOUSSI *et al.*, 2007). HRP_{intern} denoted the measured functional amount of internalized enzyme. The total protein concentration *B* was estimated by the method of Bradford.

$$Q_1 = \frac{HRP_{intern} \cdot 100}{HRP_{deployed}} [\%] \tag{7}$$

$$Q_2 = \frac{HRP_{intern} [pmol]}{B [mg]} \tag{8}$$

The amount of theoretically formed complexes consisting of SA/ST-HRP and Tat13-fused ligands was calculated by means of the law of mass action according to equation (9).

$$PL = \frac{L_0 + P_0 + K_D - \sqrt{(L_0 + P_0 + K_D)^2 - 4 \cdot (P_0 \cdot L_0)}}{2} \; [\mu M] \qquad (9)$$

PL denoted the concentration of the formed complexes, L_0 and P_0 were the initial concentrations of the ligand and the protein, whereas K_D was the dissociation constant.

Abbreviations and symbols

Abbreviations and symbols

IUPAC/IUB SYMBOLS

The following one-letter code for amino acids was utilized (table 5-1), as declared by the International Union of Pure and Applied Chemistry (IUPAC) and the International Union of Biochemistry (IUB).

One-letter code	Amino acid
A	Alanine
C	Cysteine
D	Aspartic acid
E	Glutamic acid
F	Phenylalanine
G	Glycine
H	Histidine
I	Isoleucine
K	Lysine
L	Leucine
M	Methionine
N	Asparagine
P	Proline
Q	Glutamine
R	Arginine
S	Serine
T	Threonine
V	Valine
W	Tryptophan
Y	Tyrosine

Table 5-1. List of amino acids and their corresponding one-letter symbols.

IUPAC FORMULAS

The following IUPAC formulas for chemical compounds have been utilized in this work:

H_2O	Water
HCl	Hydrochloric acid
KCl	Potassium chloride
KH_2PO_4	Potassium dihydrogen phosphate
$MgCl_2$	Magnesium chloride
$MgSO_4$	Magnesium sulfate
NaCl	Sodium chloride
Na_2HPO_4	Di-sodium hydrogen phosphate
NaOH	Sodium hydroxide

ABBREVIATIONS

Commonly used abbreviations from the fields of biology, chemistry, and biophysics which have been utilized in this work are listed below in alphabetic order:

4PL	Four parameter logistic
A	Absorbance
A_{280}	Absorption at 280 nm
ADEPT	Ab-directed enzyme prodrug therapy
Amp	Ampicillin
Ant	Antennapedia
AP	Alkaline phosphatase
APS	Ammonium persulfate
ATCC	American Type Cell Culture Collection
ATP	Adenosine 5'-triphosphate
av	Average
B	Amount of total protein estimated by the method of Bradford
$b_{N/U}$	Y intercepts of the native and unfolded baselines
bp	Base pair
BSA	Bovine serum albumine
c	Concentration
CD	Circular dichroism
CIAP	Calf intestinal AP
CO_2	Carbon dioxide
CPP	Cell penetrating peptide
d	Path lenght
Da	Dalton
DAPI	4',6-Diamidino-2-phenylindole dihydrochloride
DMEM	Dulbecco's minimal essential medium
DMSO	Dimethyl sulfoxide
DNA	Deoxyribonucleic acid
dNTP	Deoxynucleotide
ε	Extinction coefficient
EC50	Median effective concentration
ECL	Enhanced chemiluminescence
E. coli	*Escherichia coli*
EDTA	Ethylenediaminetetraacetic acid
ESI	Electrospray ionization
EtBr	Ethidium bromide
FBS	Fetal bovine serum
Fc	Crystallizable fragment
FITC	Fluorescein iso-thiocyanate
Fmoc	N-(9-fluorenyl)methoxycarbonyl
Fv	Variable fragment
H	Enthalpy, hillslope
HA	Hemaglutinin protein

HBV	Hepatitis B virus
HPLC	High-performance liquid chromatography
HPV	Human papillomavirus
HRP	Horseradish peroxidase
I	Input
IPTG	Isopropyl β-D-1-thiogalactopyranoside
IUB	International union of biochemistry
IUPAC	International union of pure and applied chemistry
K_A	Association constant
K_D	Dissociation constant
kDa	Kilo Da
L_0	Initial concentration of the ligand
lac	Lactose
LB	Luria-Bertani
M	Monomer, mol/L
mA	Milliampere
MALDI	Matrix-assisted-laser desorption/ionization
MH^+	Mass-to-charge ratio
min	Minutes
$m_{N/U}$	Slopes of the baselines
MPP	Membrane permeable peptide
M_R	Molecular mass
mRNA	Messenger RNA
MRW	Mean residue weight
MS	Mass spectrometry
MW	Molecular weight
m/z	Mass-to-charge ratio
N_2	Nitrogen
N_A	Number of amino acids
ND	Not determined
Ni-NTA	Nickel-nitrilotriacetic acid
NLS	Nuclear localization signal
NMR	Nuclear magnetic resonance
NP-40	Nonidet P-40
obs	Observed
OD	Optical density
P_0	Initial concentration of the protein
PAGE	Polyacrylamide gel electrophoresis
PBS	Phosphate-buffered saline
PCR	Polymerase chain reaction
PDB	Protein data bank
PEG	Poly(ethylene glycol)
PEO	Poly(ethylene oxide)
PFA	Paraformaldehyde fixation
PL	Concentration of the protein/ligand complex
PNK	Polynucleotide kinase

PPAA	Poly(propyl-acrylic acid)
PTD	Protein transduction domain
PTD-SA	Transvidin
PTD-ST	Transtactin
R	Gas constant
RE	Restriction endonucleases
RIPA	Radioimmunoprecipitation assay
RLB	Reporter lysis puffer
RNA	Ribonucleic acid
RNAi	RNA interference
RP	Reversed phase
rpm	Rounds per min
RT	Room temperature
SA	Streptavidin
SDS	Sodium dodecyl sulfate
siRNA	Small interfering RNA
ST	*Strep*-Tactin
SV	Simian virus
T	Temperature, tetramer, transporter
TAE	Tris-acetate-EDTA
Tat	Trans-activator
TE	Tris EDTA
TEMED	Tetramethylendiamin
TFA	Trifluoroacetic acid
TLM	Translocation motif
T_m	Melting temperature
TMB	3,3',5,5'-Tetramethylbenzidine
TOF	Time-of-flight
Tris	Tris(hydroxymethyl)-aminomethan
TRITC	Tetramethyl rhodamine iso-thiocyanate
U	Unit
UV	Ultraviolet
V	Volt
Vis	Visible

References

References

ADAMS GP and WEINER LM (2005). "Monoclonal antibody therapy of cancer." Nat Biotechnol **23**(9): 1147-57.

ALBARRAN B, TO R and STAYTON PS (2005). "A TAT-streptavidin fusion protein directs uptake of biotinylated cargo into mammalian cells." Protein Eng Des Sel **18**(3): 147-52.

ALLEN TM (2002). "Ligand-targeted therapeutics in anticancer therapy." Nat Rev Cancer **2**(10): 750-63.

ARGARANA CE, KUNTZ ID, BIRKEN S, AXEL R and CANTOR CR (1986). "Molecular cloning and nucleotide sequence of the streptavidin gene." Nucleic Acids Res **14**(4): 1871-82.

BAGHERI S and KASHANI-SABET M (2004). "Ribozymes in the age of molecular therapeutics." Curr Mol Med **4**(5): 489-506.

BAYER EA, BEN-HUR H, HILLER Y and WILCHEK M (1989). "Postsecretory modifications of streptavidin." Biochem J **259**(2): 369-76.

BAYER EA, EHRLICH-ROGOZINSKI S and WILCHEK M (1996). "Sodium dodecyl sulfate-polyacrylamide gel electrophoretic method for assessing the quaternary state and comparative thermostability of avidin and streptavidin." Electrophoresis **17**(8): 1319-24.

BINZ HK, AMSTUTZ P and PLUCKTHUN A (2005). "Engineering novel binding proteins from nonimmunoglobulin domains." Nat Biotechnol **23**(10): 1257-68.

BORGHOUTS C, KUNZ C, DELIS N and GRONER B (2008). "Monomeric recombinant peptide aptamers are required for efficient intracellular uptake and target inhibition." Mol Cancer Res **6**(2): 267-81.

BORGHOUTS C, KUNZ C and GRONER B (2005). "Current strategies for the development of peptide-based anti-cancer therapeutics." J Pept Sci **11**(11): 713-26.

BRADFORD MM (1976). "A rapid and sensitive method for the quantitation of microgram quantities of protein utilizing the principle of protein-dye binding." Anal Biochem **72**: 248-54.

BREITZ HB, WEIDEN PL, BEAUMIER PL, AXWORTHY DB, SEILER C, SU FM, GRAVES S, BRYAN K and RENO JM (2000). "Clinical optimization of pretargeted radioimmunotherapy with antibody-streptavidin conjugate and 90Y-DOTA-biotin." J Nucl Med **41**(1): 131-40.

BROOKS H, LEBLEU B and VIVES E (2005). "Tat peptide-mediated cellular delivery: back to basics." Adv Drug Deliv Rev **57**(4): 559-77.

BRUMANO MH, ROGANA E and SWAISGOOD HE (2000). "Thermodynamics of unfolding of beta-trypsin at pH 2.8." Arch Biochem Biophys **382**(1): 57-62.

BUTZ K, DENK C, ULLMANN A, SCHEFFNER M and HOPPE-SEYLER F (2000). "Induction of apoptosis in human papillomaviruspositive cancer cells by peptide aptamers targeting the viral E6 oncoprotein." Proc Natl Acad Sci U S A **97**(12): 6693-7.

CARON DE FROMENTEL C, GRUEL N, VENOT C, DEBUSSCHE L, CONSEILLER E, DUREUIL C, TEILLAUD JL, TOCQUE B and BRACCO L (1999). "Restoration of transcriptional activity of p53 mutants in human tumour cells by intracellular expression of anti-p53 single chain Fv fragments." Oncogene **18**(2): 551-7.

CARTIER R and RESZKA R (2002). "Utilization of synthetic peptides containing nuclear localization signals for nonviral gene transfer systems." Gene Ther **9**(3): 157-67.

CHAIET L, MILLER TW, TAUSIG F and WOLF FJ (1963). "Antibiotic Msd-235. Ii. Separation and Purification of Synergistic Components." Antimicrob Agents Chemother (Bethesda) **161**: 28-32.

CHAIET L and WOLF FJ (1964). "The Properties of Streptavidin, a Biotin-Binding Protein Produced by Streptomycetes." Arch Biochem Biophys **106**: 1-5.

CHEN EY and SEEBURG PH (1985). "Supercoil sequencing: a fast and simple method for sequencing plasmid DNA." DNA **4**(2): 165-70.

CHILKOTI A, TAN PH and STAYTON PS (1995). "Site-directed mutagenesis studies of the high-affinity streptavidin-biotin complex: contributions of tryptophan residues 79, 108, and 120." Proc Natl Acad Sci U S A **92**(5): 1754-8.

CHU TC, TWU KY, ELLINGTON AD and LEVY M (2006). "Aptamer mediated siRNA delivery." Nucleic Acids Res **34**(10): e73.

COLAS P (2000). "Combinatorial protein reagents to manipulate protein function." Curr Opin Chem Biol **4**(1): 54-9.

CROOKE ST (2004). "Antisense strategies." Curr Mol Med **4**(5): 465-87.

DEROSSI D, JOLIOT AH, CHASSAING G and PROCHIANTZ A (1994). "The third helix of the Antennapedia homeodomain translocates through biological membranes." J Biol Chem **269**(14): 10444-50.

DIETZ GP and BAHR M (2004). "Delivery of bioactive molecules into the cell: the Trojan horse approach." Mol Cell Neurosci **27**(2): 85-131.

DOWNWARD J (2003). "Targeting RAS signalling pathways in cancer therapy." Nat Rev Cancer **3**(1): 11-22.

DYMALLA S, SCHEFFNER M, WEBER E, SEHR P, LOHREY C, HOPPE-SEYLER F and HOPPE-SEYLER K (2008). "A novel peptide motif binding to and blocking the intracellular activity of the human papillomavirus E6 oncoprotein." J Mol Med.

EL-ANDALOUSSI S, JARVER P, JOHANSSON HJ and LANGEL U (2007). "Cargo dependent cytotoxicity and delivery efficacy of cell-penetrating peptides: a comparative study." Biochem J.

ESCRIOU V, CARRIERE M, SCHERMAN D and WILS P (2003). "NLS bioconjugates for targeting therapeutic genes to the nucleus." Adv Drug Deliv Rev **55**(2): 295-306.

FAWELL S, SEERY J, DAIKH Y, MOORE C, CHEN LL, PEPINSKY B and BARSOUM J (1994). "Tat-mediated delivery of heterologous proteins into cells." Proc Natl Acad Sci U S A **91**(2): 664-8.

FEENER EP, SHEN WC and RYSER HJ (1990). "Cleavage of disulfide bonds in endocytosed macromolecules. A processing not associated with lysosomes or endosomes." J Biol Chem **265**(31): 18780-5.

FISCHER PM, KRAUSZ E and LANE DP (2001). "Cellular delivery of impermeable effector molecules in the form of conjugates with peptides capable of mediating membrane translocation." Bioconjug Chem **12**(6): 825-41.

FRANKEL AD and PABO CO (1988). "Cellular uptake of the tat protein from human immunodeficiency virus." Cell **55**(6): 1189-93.

FUCHS SM and RAINES RT (2005). "Polyarginine as a multifunctional fusion tag." Protein Sci **14**(6): 1538-44.

FUCHS U, DAMM-WELK C and BORKHARDT A (2004). "Silencing of disease-related genes by small interfering RNAs." Curr Mol Med **4**(5): 507-17.

FUTAKI S, NIWA M, NAKASE I, TADOKORO A, ZHANG Y, NAGAOKA M, WAKAKO N and SUGIURA Y (2004). "Arginine carrier peptide bearing Ni(II) chelator to promote cellular uptake of histidine-tagged proteins." Bioconjug Chem **15**(3): 475-81.

FUTAKI S, SUZUKI T, OHASHI W, YAGAMI T, TANAKA S, UEDA K and SUGIURA Y (2001). "Arginine-rich peptides. An abundant source of membrane-permeable peptides having potential as carriers for intracellular protein delivery." J Biol Chem **276**(8): 5836-40.

GONZALEZ M, ARGARANA CE and FIDELIO GD (1999). "Extremely high thermal stability of streptavidin and avidin upon biotin binding." Biomol Eng **16**(1-4): 67-72.

GRANT GA, CRANKSHAW MW and GORKA J (1997). "Edman sequencing as tool for characterization of synthetic peptides." Methods Enzymol **289**: 395-419.

GREEN M and LOEWENSTEIN PM (1988). "Autonomous functional domains of chemically synthesized human immunodeficiency virus tat trans-activator protein." Cell **55**(6): 1179-88.

GREEN NM (1975). "Avidin." Adv Protein Chem **29**: 85-133.

GREEN NM and MELAMED MD (1966). "Optical rotatory dispersion, circular dichroism and far-ultraviolet spectra of avidin and streptavidin." Biochem J **100**(3): 614-21.

GRIFFIN H, ELSTON R, JACKSON D, ANSELL K, COLEMAN M, WINTER G and DOORBAR J (2006). "Inhibition of papillomavirus protein function in cervical cancer cells by intrabody targeting." J Mol Biol **355**(3): 360-78.

GRISHINA IB and WOODY RW (1994). "Contributions of tryptophan side chains to the circular dichroism of globular proteins: exciton couplets and coupled oscillators." Faraday Discuss(99): 245-62.

GRONER B, HARTMANN C and WELS W (2004). "Therapeutic antibodies." Curr Mol Med **4**(5): 539-47.

GROS E, DESHAYES S, MORRIS MC, ALDRIAN-HERRADA G, DEPOLLIER J, HEITZ F and DIVITA G (2006). "A non-covalent peptide-based strategy for protein and peptide nucleic acid transduction." Biochim Biophys Acta **1758**(3): 384-93.

GUMP JM and DOWDY SF (2007). "TAT transduction: the molecular mechanism and therapeutic prospects." Trends Mol Med **13**(10): 443-8.

HANAHAN D (1983). "Studies on transformation of Escherichia coli with plasmids." J Mol Biol **166**(4): 557-80.

HANAHAN D (1985). "Techniques for transformation of E. coli. published in " DNA cloning: A Practical Approach, IRL Press, Oxford, United Kingdom **1**: 109-135.

HANAHAN D and WEINBERG RA (2000). "The hallmarks of cancer." Cell **100**(1): 57-70.

HNATOWICH DJ, VIRZI F and RUSCKOWSKI M (1987). "Investigations of avidin and biotin for imaging applications." J Nucl Med **28**(8): 1294-302.

HOFMANN K, WOOD SW, BRINTON CC, MONTIBELLER JA and FINN FM (1980). "Iminobiotin affinity columns and their application to retrieval of streptavidin." Proc Natl Acad Sci U S A **77**(8): 4666-8.

HOLLIGER P and HUDSON PJ (2005). "Engineered antibody fragments and the rise of single domains." Nat Biotechnol **23**(9): 1126-36.

HONDA A, MOOSMEIER MA and DOSTMANN WR (2005). "Membrane-permeable cygnets: rapid cellular internalization of fluorescent cGMP-indicators." Front Biosci **10**: 1290-301.

HOPPE-SEYLER F, CRNKOVIC-MERTENS I, TOMAI E and BUTZ K (2004). "Peptide aptamers: specific inhibitors of protein function." Curr Mol Med **4**(5): 529-38.

HOWARTH M, CHINNAPEN DJ, GERROW K, DORRESTEIN PC, GRANDY MR, KELLEHER NL, EL-HUSSEINI A and TING AY (2006). "A monovalent streptavidin with a single femtomolar biotin binding site." Nat Methods **3**(4): 267-73.

HUMBERT N, ZOCCHI A and WARD TR (2005). "Electrophoretic behavior of streptavidin complexed to a biotinylated probe: a functional screening assay for biotin-binding proteins." Electrophoresis **26**(1): 47-52.

HYRE DE, LE TRONG I, MERRITT EA, ECCLESTON JF, GREEN NM, STENKAMP RE and STAYTON PS (2006). "Cooperative hydrogen bond interactions in the streptavidin-biotin system." Protein Sci **15**(3): 459-67.

IGOUCHEVA O, ALEXEEV V and YOON K (2004). "Oligonucleotide-directed mutagenesis and targeted gene correction: a mechanistic point of view." Curr Mol Med **4**(5): 445-63.

IKEMURA T (1981). "Correlation between the abundance of Escherichia coli transfer RNAs and the occurrence of the respective codons in its protein genes." J Mol Biol **146**(1): 1-21.

INOUE H, NOJIMA H and OKAYAMA H (1990). "High efficiency transformation of Escherichia coli with plasmids." Gene **96**(1): 23-8.

JIANG T, OLSON ES, NGUYEN QT, ROY M, JENNINGS PA and TSIEN RY (2004). "Tumor imaging by means of proteolytic activation of cell-penetrating peptides." Proc Natl Acad Sci U S A **101**(51): 17867-72.

JIN LH, BAHN JH, EUM WS, KWON HY, JANG SH, HAN KH, KANG TC, WON MH, KANG JH, CHO SW, PARK J and CHOI SY (2001). "Transduction of human catalase mediated by an HIV-1 TAT protein basic domain and arginine-rich peptides into mammalian cells." Free Radic Biol Med **31**(11): 1509-19.

KEEFE AD, WILSON DS, SEELIG B and SZOSTAK JW (2001). "One-step purification of recombinant proteins using a nanomolar-affinity streptavidin-binding peptide, the SBP-Tag." Protein Expr Purif **23**(3): 440-6.

KELLER J, HEISLER I, TAUBER R and FUCHS H (2001). "Development of a novel molecular adapter for the optimization of immunotoxins." J Control Release **74**(1-3): 259-61.

KELLY SM and PRICE NC (2000). "The use of circular dichroism in the investigation of protein structure and function." Curr Protein Pept Sci **1**(4): 349-84.

KOMINE Y, ADACHI T, INOKUCHI H and OZEKI H (1990). "Genomic organization and physical mapping of the transfer RNA genes in Escherichia coli K12." J Mol Biol **212**(4): 579-98.

KORNDORFER IP and SKERRA A (2002). "Improved affinity of engineered streptavidin for the Strep-tag II peptide is due to a fixed open conformation of the lid-like loop at the binding site." Protein Sci **11**(4): 883-93.

LAGRANGE M, BOULADE-LADAME C, MAILLY L, WEISS E, ORFANOUDAKIS G and DERYCKERE F (2007). "Intracellular scFvs against the viral E6 oncoprotein provoke apoptosis in human papillomavirus-positive cancer cells." Biochem Biophys Res Commun **361**(2): 487-92.

LAITINEN OH, HYTONEN VP, NORDLUND HR and KULOMAA MS (2006). "Genetically engineered avidins and streptavidins." Cell Mol Life Sci **63**(24): 2992-3017.

LAMLA T and ERDMANN VA (2004). "The Nano-tag, a streptavidin-binding peptide for the purification and detection of recombinant proteins." Protein Expr Purif **33**(1): 39-47.

LAVALLIE ER, DIBLASIO EA, KOVACIC S, GRANT KL, SCHENDEL PF and MCCOY JM (1993). "A thioredoxin gene fusion expression system that circumvents inclusion body formation in the E. coli cytoplasm." Biotechnology (N Y) **11**(2): 187-93.

LAZAR Z (2007). Protein-Engineering eines Anticalins mit Bindungsspezifität zur Hexahistidin-Sequenz. Lehrstuhl für Biologische Chemie. Freising, Technischen Universität München.

LEA NC, BUGGINS AG, ORR SJ, MUFTI GJ and THOMAS NS (2003). "High efficiency protein transduction of quiescent and proliferating primary hematopoietic cells." J Biochem Biophys Methods **55**(3): 251-8.

LEADER B, BACA QJ and GOLAN DE (2008). "Protein therapeutics: a summary and pharmacological classification." Nat Rev Drug Discov **7**(1): 21-39.

LIVNAH O, BAYER EA, WILCHEK M and SUSSMAN JL (1993). "Three-dimensional structures of avidin and the avidin-biotin complex." Proc Natl Acad Sci U S A **90**(11): 5076-80.

MAI JC, SHEN H, WATKINS SC, CHENG T and ROBBINS PD (2002). "Efficiency of protein transduction is cell type-dependent and is enhanced by dextran sulfate." J Biol Chem **277**(33): 30208-18.

MANDAL K, BOSE SK, CHAKRABARTI B and SIEZEN RJ (1985). "Structure and stability of gamma-crystallins. I. Spectroscopic evaluation of secondary and tertiary structure in solution." Biochim Biophys Acta **832**(2): 156-64.

MANIATIS T, FRITSCH EF and SAMBROOK J (1982). Molecular Cloning: A Laboratory Manual. Cold Spring Habor, NY, Cold Spring Harbor Laboratory Press.

MASUDA K, RICHTER M, SONG X, BEREZOV A, MASUDA K, MURALI R, GREENE MI and ZHANG H (2006). "AHNP-streptavidin: a tetrameric bacterially produced antibody surrogate fusion protein against p185her2/neu." Oncogene **25**(59): 7740-6.

MCMAHAN SA and BURGESS RR (1996). "Single-step synthesis and characterization of biotinylated nitrilotriacetic acid, a unique reagent for the detection of histidine-tagged proteins immobilized on nitrocellulose." Anal Biochem **236**(1): 101-6.

MEADE BR and DOWDY SF (2007). "Exogenous siRNA delivery using peptide transduction domains/cell penetrating peptides." Adv Drug Deliv Rev **59**(2-3): 134-40.

MEYER DL, SCHULTZ J, LIN Y, HENRY A, SANDERSON J, JACKSON JM, GOSHORN S, REES AR and GRAVES SS (2001). "Reduced antibody response to streptavidin through site-directed mutagenesis." Protein Sci **10**(3): 491-503.

MIE M, MORI K, FUNABASHI H and KOBATAKE E (2006). "Delivery of antibody-captured proteins into living cells using PTD-fused protein A." Biotechnol Lett **28**(15): 1209-14.

MIE M, TAKAHASHI F, FUNABASHI H, YANAGIDA Y, AIZAWA M and KOBATAKE E (2003). "Intracellular delivery of antibodies using TAT fusion protein A." Biochem Biophys Res Commun **310**(3): 730-4.

MITCHELL DJ, KIM DT, STEINMAN L, FATHMAN CG and ROTHBARD JB (2000). "Polyarginine enters cells more efficiently than other polycationic homopolymers." J Pept Res **56**(5): 318-25.

MOGK A, SCHMIDT R and BUKAU B (2007). "The N-end rule pathway for regulated proteolysis: prokaryotic and eukaryotic strategies." Trends Cell Biol **17**(4): 165-72.

NITIN N, SANTANGELO PJ, KIM G, NIE S and BAO G (2004). "Peptide-linked molecular beacons for efficient delivery and rapid mRNA detection in living cells." Nucleic Acids Res **32**(6): e58.

O'SHANNESSY DJ, O'DONNELL KC, MARTIN J and BRIGHAM-BURKE M (1995). "Detection and quantitation of hexa-histidine-tagged recombinant proteins on western blots and by a surface plasmon resonance biosensor technique." Anal Biochem **229**(1): 119-24.

OESS S and HILDT E (2000). "Novel cell permeable motif derived from the PreS2-domain of hepatitis-B virus surface antigens." Gene Ther **7**(9): 750-8.

PAHLER A, HENDRICKSON WA, KOLKS MA, ARGARANA CE and CANTOR CR (1987). "Characterization and crystallization of core streptavidin." J Biol Chem **262**(29): 13933-7.

PARK J, RYU J, JIN LH, BAHN JH, KIM JA, YOON CS, KIM DW, HAN KH, EUM WS, KWON HY, KANG TC, WON MH, KANG JH, CHO SW and CHOI SY (2002). "9-polylysine protein transduction domain: enhanced penetration efficiency of superoxide dismutase into mammalian cells and skin." Mol Cells **13**(2): 202-8.

POIRIER MC (2004). "Chemical-induced DNA damage and human cancer risk." Nat Rev Cancer **4**(8): 630-7.

PRASAD PD and GANAPATHY V (2000). "Structure and function of mammalian sodium-dependent multivitamin transporter." Curr Opin Clin Nutr Metab Care **3**(4): 263-6.

PRIVE GG and MELNICK A (2006). "Specific peptides for the therapeutic targeting of oncogenes." Curr Opin Genet Dev **16**(1): 71-7.

QIAN ZM, LI H, SUN H and HO K (2002). "Targeted drug delivery via the transferrin receptor-mediated endocytosis pathway." Pharmacol Rev **54**(4): 561-87.

REED J and REED TA (1997). "A set of constructed type spectra for the practical estimation of peptide secondary structure from circular dichroism." Anal Biochem **254**(1): 36-40.

REICHEL A, SCHAIBLE D, AL FUROUKH N, COHEN M, SCHREIBER G and PIEHLER J (2007). "Noncovalent, site-specific biotinylation of histidine-tagged proteins." Anal Chem **79**(22): 8590-600.

RICHARD JP, MELIKOV K, VIVES E, RAMOS C, VERBEURE B, GAIT MJ, CHERNOMORDIK LV and LEBLEU B (2003). "Cell-penetrating peptides. A reevaluation of the mechanism of cellular uptake." J Biol Chem **278**(1): 585-90.

RINNE J, ALBARRAN B, JYLHAVA J, IHALAINEN TO, KANKAANPAA P, HYTONEN VP, STAYTON PS, KULOMAA MS and VIHINEN-RANTA M (2007). "Internalization of novel non-viral vector TAT-streptavidin into human cells." BMC Biotechnol **7**: 1.

ROTHBARD JB, GARLINGTON S, LIN Q, KIRSCHBERG T, KREIDER E, MCGRANE PL, WENDER PA and KHAVARI PA (2000). "Conjugation of arginine oligomers to cyclosporin A facilitates topical delivery and inhibition of inflammation." Nat Med **6**(11): 1253-7.

SAMBROOK J and RUSSELL DW (2001). Molecular Cloning - A Laboratory Manual. New York City, NY USA, Cold Spring Harbor Laboratory Press.

SANGER F, NICKLEN S and COULSON AR (1977). "DNA sequencing with chain-terminating inhibitors." Proc Natl Acad Sci U S A **74**(12): 5463-7.

SANO T and CANTOR CR (1990). "Expression of a cloned streptavidin gene in Escherichia coli." Proc Natl Acad Sci U S A **87**(1): 142-6.

SANO T and CANTOR CR (1995). "Intersubunit contacts made by tryptophan 120 with biotin are essential for both strong biotin binding and biotin-induced tighter subunit association of streptavidin." Proc Natl Acad Sci U S A **92**(8): 3180-4.

SAWYER CL, HONDA A and DOSTMANN WR (2003). "Cygnets: spatial and temporal analysis of intracellular cGMP." Proc West Pharmacol Soc **46**: 28-31.

SCHLEHUBER S and SKERRA A (2005). "Anticalins as an alternative to antibody technology." Expert Opin Biol Ther **5**(11): 1453-62.

SCHMIDT TG, KOEPKE J, FRANK R and SKERRA A (1996). "Molecular interaction between the Strep-tag affinity peptide and its cognate target, streptavidin." J Mol Biol **255**(5): 753-66.

SCHMIDT TG and SKERRA A (1993). "The random peptide library-assisted engineering of a C-terminal affinity peptide, useful for the detection and purification of a functional Ig Fv fragment." Protein Eng **6**(1): 109-22.

SCHMIDT TG and SKERRA A (1994). "One-step affinity purification of bacterially produced proteins by means of the "Strep tag" and immobilized recombinant core streptavidin." J Chromatogr A **676**(2): 337-45.

SCHMIDT TG and SKERRA A (2007). "The Strep-tag system for one-step purification and high-affinity detection or capturing of proteins." Nat Protoc **2**(6): 1528-35.

SELIVANOVA G and WIMAN KG (2007). "Reactivation of mutant p53: molecular mechanisms and therapeutic potential." Oncogene **26**(15): 2243-54.

SKERRA A (2000). "Lipocalins as a scaffold." Biochim Biophys Acta **1482**(1-2): 337-50.

SKERRA A (2007). "Anticalins as alternative binding proteins for therapeutic use." Curr Opin Mol Ther **9**(4): 336-44.

SKERRA A (2008). "Alternative binding proteins: Anticalins - harnessing the structural plasticity of the lipocalin ligand pocket to engineer novel binding activities." Febs J.

SKERRA A and SCHMIDT TG (1999). "Applications of a peptide ligand for streptavidin: the Strep-tag." Biomol Eng **16**(1-4): 79-86.

STOECKL L, FUNK A, KOPITZKI A, BRANDENBURG B, OESS S, WILL H, SIRMA H and HILDT E (2006). "Identification of a structural motif crucial for infectivity of hepatitis B viruses." Proc Natl Acad Sci U S A **103**(17): 6730-4.

TAUSIG F and WOLF FJ (1964). "Streptavidin--a substance with avidin-like properties produced by microorganisms." Biochem Biophys Res Commun **14**: 205-9.

THOMAS CE, EHRHARDT A and KAY MA (2003). "Progress and problems with the use of viral vectors for gene therapy." Nat Rev Genet **4**(5): 346-58.

THOMPSON LD and WEBER PC (1993). "Construction and expression of a synthetic streptavidin-encoding gene in Escherichia coli." Gene **136**(1-2): 243-6.

TREHIN R and MERKLE HP (2004). "Chances and pitfalls of cell penetrating peptides for cellular drug delivery." Eur J Pharm Biopharm **58**(2): 209-23.

TUNNEMANN G, MARTIN RM, HAUPT S, PATSCH C, EDENHOFER F and CARDOSO MC (2006). "Cargo-dependent mode of uptake and bioavailability of TAT-containing proteins and peptides in living cells." Faseb J **20**(11): 1775-84.

VIVES E, BRODIN P and LEBLEU B (1997). "A truncated HIV-1 Tat protein basic domain rapidly translocates through the plasma membrane and accumulates in the cell nucleus." J Biol Chem **272**(25): 16010-7.

VIVES E, SCHMIDT J and PELEGRIN A (2008). "Cell-penetrating and cell-targeting peptides in drug delivery." Biochim Biophys Acta **1786**(2): 126-38.

VOSS S and SKERRA A (1997). "Mutagenesis of a flexible loop in streptavidin leads to higher affinity for the Strep-tag II peptide and improved performance in recombinant protein purification." Protein Eng **10**(8): 975-82.

WADIA JS, STAN RV and DOWDY SF (2004). "Transducible TAT-HA fusogenic peptide enhances escape of TAT-fusion proteins after lipid raft macropinocytosis." Nat Med **10**(3): 310-5.

WANER MJ, NAVROTSKAYA I, BAIN A, OLDHAM ED and MASCOTTI DP (2004). "Thermal and sodium dodecylsulfate induced transitions of streptavidin." Biophys J **87**(4): 2701-13.

WANG Y, NAKAMURA K, LIU X, KITAMURA N, KUBO A and HNATOWICH DJ (2007). "Simplified Preparation via Streptavidin of Antisense Oligomers/Carriers Nanoparticles Showing Improved Cellular Delivery in Culture." Bioconjug Chem.

WEBER PC, OHLENDORF DH, WENDOLOSKI JJ and SALEMME FR (1989). "Structural origins of high-affinity biotin binding to streptavidin." Science **243**(4887): 85-8.

WHIBLEY C, PHAROAH PD and HOLLSTEIN M (2009). "p53 polymorphisms: cancer implications." Nat Rev Cancer **9**(2): 95-107.

WILEMAN T, HARDING C and STAHL P (1985). "Receptor-mediated endocytosis." Biochem J **232**(1): 1-14.

XU CW and LUO Z (2002). "Inactivation of Ras function by allele-specific peptide aptamers." Oncogene **21**(37): 5753-7.

ZUR HAUSEN H (2002). "Papillomaviruses and cancer: from basic studies to clinical application." Nat Rev Cancer **2**(5): 342-50.

DISSERTATION

submitted to the
Combined Faculties for the Natural Sciences
and for Mathematics
of the Ruperto-Carola-University Heidelberg, Germany,
for the degree of
Doctor of Natural Sciences

presented by
Markus Andreas Moosmeier, M.Sc.
born in Landshut, Germany
Date of oral examination: 2009/07/23